

**GAZIANTEP UNIVERSITY GRADUATE  
SCHOOL OF NATURAL & APPLIED SCIENCES**

**EFFECT OF WATER INJECTION ON THE  
PERFORMANCE OF LPG FUELLED SPARK  
IGNITION ENGINE**

**PH.D THESIS  
IN  
MECHANICAL ENGINEERING**

**BY  
HAKAN ÖZCAN  
OCTOBER 2005**

**Effect of Water Injection on the Performance of LPG Fuelled  
Spark Ignition Engine**

**PhD Thesis**  
**In**  
**Mechanical Engineering**  
**University of Gaziantep**

**Supervisor**  
Assoc. Prof. Dr. M. Sait SÖYLEMEZ

**by**  
**Hakan ÖZCAN**  
**October 2005**

Approval of the Graduate School of Natural and Applied Sciences

---

Prof. Dr. Sadettin ÖZYAZICI  
Director

I certify that this thesis satisfies all the requirements as a thesis for the degree of Ph.D. of Science.

---

Prof. Dr. Melda ÇARPINLIOĞLU  
Head of Department

This is to certify that we have read this thesis and that in our opinion it is fully adequate, in scope and quality, as a thesis for the degree of Ph.D. of Science.

---

Assoc. Prof. Dr. M. Sait SÖYLEMEZ  
Supervisor

Examining Committee Members:

Prof. Dr. Kadir AYDIN

---

Prof. Dr. Melda ÇARPINLIOĞLU

---

Prof. Dr. A. Rıza TEKİN

---

Assoc. Prof. Dr. M. Sait SÖYLEMEZ

---

Assoc. Prof. Dr. Mehmet KANOĞLU

---

## ABSTRACT

# EFFECT OF WATER INJECTION ON THE PERFORMANCE OF LPG FUELLED SPARK IGNITION ENGINE

ÖZCAN, Hakan

PhD in Mechanical Engineering

Supervisor: Assoc. Prof. Dr. M. Sait SÖYLEMEZ

October 2005, 171 pages

The effect of water injection on LPG fuelled SI engine performance, fuel economy, combustion characteristics, and exhaust gas emissions were investigated in this thesis. In addition, an exergy and energy analysis based on experimental results was also investigated.

Investigation presented in this thesis was realized in two main stages. In the first stage; an experimental set up was designed and constructed. A data acquisition system composed of all of data acquisition, accumulation, and processing components was installed to carry a fully computer aided experimental study from the test engine. In the second stage: an experimental study was conducted to determine the effects of the water injection.

Experimental results showed that several combustion variables were affected by water injection. Results showed that, at  $m_w/m_f=0.5$ , energy analysis indicated that only 37.9% of the fuel energy could be utilized as an indicated power, where 62.1% of fuel energy was not available for conversion to useful work. Exergy analysis showed that 52.1% of fuel energy could be utilized as useful work (35.7% as an indicated power, 12% from the exhaust and only 4.4% from the cooling water) and the available energy unaccounted for represented 47.9% of the total available energy for the same condition. It was also found that water injection increased the combustion irreversibility significantly. Water addition provided a 35% reduction in peak  $\text{NO}_x$  emissions without any significant change in CO and HC emissions. In addition, greater ignition advance was obtained. The average increase in the brake thermal efficiency for a water to fuel mass ratio of 0.5 was approximately 2.7% over the use of LPG alone.

**Keywords:** Internal Combustion Engine, Water injection, Data Acquisition, LPG, Exergy, Thermal balance

## ÖZET

# SU ENJEKSİYONUNUN LPG İLE ÇALIŞAN BİR MOTORUN PERFORMANSI ÜZERİNE ETKİLERİ

ÖZCAN, Hakan

Doktora Tezi, Makine Mühendisliği Bölümü  
Tez Yöneticisi: Doç. Dr. M. Sait SÖYLEMEZ  
Ekim 2005, 171 sayfa

Bu çalışmada, su enjeksiyonunun LPG ile çalışan buji ateşlemeli bir motorun performansı, yakıt tüketimi, yanma karakteristikleri ve eksoz gazı emisyonu üzerine etkileri incelenmiştir. Ayrıca deney sonuçlarına dayalı olarak energy ve ekserji analizi bu çalışmada incelenmiştir.

Bu tezde sunulan çalışma iki ana safhada gerçekleştirilmiştir. Birinci safhada, bir deney düzeneği tasarlanmış ve yapılmıştır. Motor üzerinde tamamen bilgisayar destekli deneysel bir çalışma yürütmek için, veri iletme, toplama ve işleme sistemlerinden oluşan bir iletim sistemi kurulmuştur. İkinci aşamada, su enjeksiyonunun etkilerini ortaya koyacak incelemeler yapılmıştır.

Sonuçlar, su enjeksiyonunun birçok yanma parametresini etkilediğini göstermektedir. Kütleli olarak 0.5 su yakıt oranında, enerji analizi yakıttan elde edilen enerjinin %37.9'unun indike güce dönüştüğünü, %62.1'inin ise kaybedildiğini göstermektedir. Ekserji analizi ise yakıttan elde edilen enerjinin %52.1'inin faydalı işe çevrilebildiğini (%35.7'si indike güç, %12'si eksoz ve yalnızca %4.4'ü soğutma suyuna geçen enerji olarak), %47.9'unun ise kaybedildiğini göstermektedir. Bununla birlikte su enjeksiyonunun yanma tersinemezliğini önemli oranda artırdığı görülmüştür. Sonuçlar, su enjeksiyonunun azot oksit emisyonunda %35 azalmaya neden olduğunu, CO ve HC emisyonlarında ise önemli oranda değişikliğe sebep olmadığını göstermektedir. Ayrıca su enjeksiyonu, daha fazla ateşleme avansı sağlamaktadır. Kütleli olarak 0.5 su/yakıt oranında, ortalama fren termik verim; yaklaşık %2.7 artmaktadır.

**Anahtar Kelimeler:** İçten Yanmalı Motorlar, Su enjeksiyonu, Veri analizi, LPG, Ekserji, Isı Bilânçosu

## **ACKNOWLEDGEMENTS**

I would like to thank my advisor, Assoc. Prof. Dr. M. Sait SÖYLEMEZ, for his guidance, technical advice, and support during my research. I would also like to thank Prof. Dr. Kadir AYDIN for sharing his technical expertise and for taking time from his schedule to join my committee. Additional thanks are extended to Prof. Dr. Melda ÇARPINLIOĞLU and the rest of the Mechanical engineering department staff, who provided crucial support to my research efforts.

The financial support from the research fund of University has been essential, so thanks to all Turkish taxpayers.

I also thank my family for their support during this difficult achievement, particularly my parents who instilled an intellectual curiosity in me from my youth, which has guided me through my academic career.

I would also like to thank everyone who helped make during my research so special for me.

## TABLE OF CONTENTS

APPROVAL OF EXAMINING COMMITTEE.....	ii
ABSTRACT.....	iii
ÖZET.....	iv
ACKNOWLEDGMENTS.....	v
TABLE OF CONTENTS.....	vi
LIST OF TABLES .....	x
LIST OF FIGURES.....	xi
LIST OF SYMBOLS. ....	xvi
<b>CHAPTER 1: INTRODUCTION.....</b>	<b>1</b>
<b>CHAPTER 2: LITERATURE SURVEY.....</b>	<b>8</b>
2.1 Introduction.....	8
2.2 Previous Studies on LPG as an Internal Combustion Engine fuel....	8
2.3 First Studies on the Water Injection Concept.....	9
2.4 Previous Studies on the Effect of Water Addition on the Internal Combustion Engine Performance.....	10
2.5 Previous Studies on the Effect of Water Addition on the Exhaust Emissions.....	11
2.6 Previous Studies on the Water/Fuel Emulsion.....	13
2.7 Previous Studies on the Engine Energy Balance.....	14
2.8 Previous Studies on the Exergy Analysis for Internal Combustion Engines.....	15
2.9 Conclusions.....	17
<b>CHAPTER 3: EXPERIMENTAL SET-UP AND MEASUREMENT</b>	
<b>DEVICES.....</b>	<b>20</b>
3.1 Introduction.....	20
3.2 Hardware.....	20

3.2.1	Engine.....	21
3.2.2	Pressure Transducers.....	23
3.2.3	Optical Shaft Encoder.....	25
3.2.4	Cylinder Pressure vs. Crank Angle.....	26
3.2.5	Readout or Recording Device.....	28
3.2.6	Dynamometer.....	31
3.2.7	Air Flow Measurements.....	32
3.2.8	Exhaust Emission Reading Apparatus.....	33
3.2.9	Temperature Measurements.....	33
3.2.10	Fuel and Water Flow Measurements.....	35
3.2.11	Ignition Timing.....	36
3.2.12	Measurement of Engine Speed.....	36
3.2.13	Acceleration of the Engine.....	37
3.2.14	Adjustment of Water Injection.....	37
3.3.	Software.....	39
3.3.1	Data Collection Software.....	39
3.3.2	Data Analysis Software.....	41
3.4	Calibrations of the Measurement Systems.....	49

#### **CHAPTER 4: EVALUATION OF DATA AND EXPERIMENTAL**

	<b>PROCEDURE.....</b>	<b>51</b>
4.1	Introduction.....	51
4.2	Geometrical Properties of Reciprocating Engines.....	51
4.3	Brake Power.....	53
4.4	Corrected Brake Power.....	53
4.5	Corrected Engine Torque.....	54
4.6	Indicated Power.....	54
4.7	Actual Air Flow Rate.....	55
4.8	Brake Thermal Efficiency.....	56
4.9	Brake Specific Fuel Consumption .....	57
4.10	Mean Effective Pressure.....	58
4.11	Actual Air-Fuel Ratio and Air Fuel Equivalence Ratio.....	59
4.12	Volumetric Efficiency.....	60
4.13	Energy Analysis.....	61



4.14	Second Law Analysis.....	63
4.15	Experimental Procedures.....	68
4.16	Error Analysis.....	70
<b>CHAPTER 5: EXPERIMENTAL AND THEORETICAL RESULTS.....</b>		<b>74</b>
5.1	Introduction.....	74
5.2	Thermal Balance of an LPG Fuelled, Four Stroke SI Engine with Water Addition.....	74
5.3	Experimental Investigation of Effects of Water Addition on the Exhaust Emissions.....	80
5.4	Effect of Water Addition on the Performance of Four Cylinder, LPG Fuelled Spark Ignition Engine.....	87
5.5	Effect of Water Addition on the Combustion.....	92
5.6	Energy and Exergy Analysis of Water Addition.....	95
	5.6.1 Energy Analysis.....	95
	5.6.2 Exergy Analysis.....	100
5.7	Effect of Water Addition on the Exergy Balances .....	104
5.8	Effect of Steam Water Injection .....	110
5.9	Effect of Water Injection on the Engine Parts.....	118
5.10	Theoretical Calculations.....	118
5.11	Conclusions.....	128
<b>CHAPTER 6: SUGGESTIONS AND RECOMMENDATIONS FOR FUTURE STUDIES.....</b>		<b>134</b>
<b>REFERENCES.....</b>		<b>136</b>
<b>APPENDICES.....</b>		<b>147</b>
A-1:	Technical Specifications of the Test Engine.....	148
A-2:	Technical Specifications of the Pressure Transducers.....	149
A-3:	Technical Specifications of the Charge Amplifier.....	152
A-4:	Technical Specifications of the Shaft Encoder.....	153
A-5:	Technical Specifications of the Used Readout and Recording Devices.....	154
A-6:	Technical Specifications of the Dynamometer.....	157
A-7:	Technical Specifications of the Air-flow-meter.....	158

A-8: Technical Specifications of the Exhaust Emissions	
Testing Apparatus.....	159
A-9: Technical Specifications of the Used Electronic	
Balances for Flow Rate Measurements.....	160
A-10: Technical Specifications of the Other Sensors	
Used in the Thesis.....	161
A-11: Programs Used in the Thesis.....	162
<b>PUBLICATIONS</b> .....	169
<b>VITA</b> .....	171

## LIST OF TABLES

Table 3.1: Test Engine Specifications.....	22
Table 3.2: Tested Fuel Specifications.....	22
Table 3.3: Minimum Pressure Measurement of ADCs in Pascal.....	28
Table 3.4: Types of Thermocouples and Their Point of Use.....	34
Table 4.1: General Availability Equations for Various Processes.....	65
Table 4.2: The Preset Conditions of the Tests.....	68
Table 4.3: Maximum Estimated Experimental Uncertainties.....	72
Table 4.4: Accuracy of Instrumentation.....	72
Table 5.1: Data of the Thermal Balance and Performance Parameters for LPG Fuel Only.....	75
Table 5.2: Data of the Thermal Balance and Performance Parameters with $m_w/m_f=0.125$ .....	75
Table 5.3: Data of the Thermal Balance and Performance Parameters with $m_w/m_f=0.25$ .....	75
Table 5.4: Data of the Thermal Balance and Performance Parameters with $m_w/m_f=0.33$ .....	76
Table 5.5: Data of the Thermal Balance and Performance Parameters with $m_w/m_f=0.5$ .....	77
Table 5.6: Engine Performance Parameters for the Different Fuel to Water Mass Ratio at Constant Spark Timing.....	94
Table 5.7: Theoretical Calculations.....	123
Table 5.8: Calculated NO Formation Rate and $T_{fl}$ .....	125

## LIST OF FIGURES

Figure 3.1: The Complete Test Engine Hardware System.....	21
Figure 3.2: Test Engine.....	22
Figure 3.3: Replacement of the Piezo-electric Pressure Transducer on the Engine Block.....	23
Figure 3.4: Measurement of Cylinder Pressure vs. Crank Angle System.....	27
Figure 3.5: Multi-port Serial Adaptor.....	29
Figure 3.6: The Prosig Model P-5600 Data Acquisition System.....	29
Figure 3.7: The Data Logger.....	30
Figure 3.8: Water Brake Dynamometer.....	31
Figure 3.9: Airflow Meter.....	32
Figure 3.10: The Fuel Flow Measuring System.....	35
Figure 3.11. Schematic View of the Acceleration System of the Engine.....	37
Figure 3.12: Water Injection System.....	38
Figure 3.13: Steam Injection to Intake Manifold.....	39
Figure 3.14: Measured Parameters by Hilton Data Logger.....	40
Figure 3.15: RS-232 Port Reader Program.....	40
Figure 3.16: A Pressure versus Volume Plot Produced by Analysis.m.....	44
Figure 3.17: Output of the Home-made Software for the Combustion Analysis.....	46
Figure 3.18: Input Data of the Home-made Software Named as Mass-burned for the Combustion Analysis.....	47
Figure 3.19: Output of the home-made software named as Mass-burned.....	47
Figure 3.20: Mass Fraction Burned Curve Determined from Measured Cylinder Data.....	48
Figure 3.21: Log P-log V Plot.....	49
Figure 4.1: Basic Geometry of the Reciprocating	

Internal Combustion Engine.....	52
Figure 4.2: Typical Engine System.....	61
Figure 4.3: Engine Availability Streams.....	64
Figure 5.1: Thermal Balance of Engine Operating with LPG only and Various Water/fuel Mass Ratio of Water Injection.....	78
Figure 5.2: Brake Thermal Efficiency Variations with Engine Speed for Various Water/fuel Mass Ratio of Water Injection.....	79
Figure 5.3: Brake Specific Fuel Consumption Variations with Engine Speed for Various Water/fuel Mass Ratio of Water Injection.....	80
Figure 5.4: Effect of Water Addition on NO <sub>x</sub> as a Function of F/A Equivalence Ratio.....	81
Figure 5.5: Effect of Water Addition on HC Emissions as a Function of F/A Equivalence Ratio.....	82
Figure 5.6: Effect of Water Addition on CO Concentration.....	83
Figure 5.7: The Effect of Water Addition on Exhaust Temperature.....	84
Figure 5.8: The Effect of Water Addition on MBT Timing.....	85
Figure 5.9: The Effect of Water Addition on Knocking and Misfire.....	85
Figure 5.10: The effect of Water Addition on Engine Thermal Efficiency.....	86
Figure 5.11: Effect of Water Injection on Engine Torque Output versus Engine Speed.....	88
Figure 5.12: Effect of Water Injection on Engine Power Output versus Engine Speed.....	89
Figure 5.13: Effect of Water Injection on Brake Specific Fuel Consumption versus Engine Speed.....	90
Figure 5.14: Effect of Water Injection on Brake Thermal Efficiency versus Engine Speed.....	91
Figure 5.15: Effect of Water Injection on Gases Exhaust Temperatures versus Engine Speed.....	91
Figure 5.16: Combustion Duration as a Function of Engine Speed and Water Injection Rate.....	92
Figure 5.17: Ignition Delay as a Function of Engine Speed and Water Injection Rate.....	93
Figure 5.18: A P-θ Diagram for the Cylinder.....	94

Figure 5.19: Schematic Presentation of Carnot Heat Engine.....	96
Figure 5.20: Change of Percent Available Energy with Water Injection Rate...	96
Figure 5.21: Energy Balance for Lean Mixture with Increasing Amount of Water Addition.....	97
Figure 5.22: Energy Balance for Rich Mixture with Increasing Amount of Water Addition.....	98
Figure 5.23: Unaccounted Energy for Lean and Rich Mixture with Amount of Water Addition.....	99
Figure 5.24: Energy distribution for water to fuel ratio 0.5 at lean region and $Q_{in} = 24.62$ kW.....	99
Figure 5.25: Effect of Water Addition on the First Law Efficiency.....	100
Figure 5.26: Availability versus Water Addition for Lean Mixture.....	101
Figure 5.27: Availability versus Water Addition for Rich Mixture.....	101
Figure 5.28: Exhaust Availability versus Water Addition for Rich and Lean Mixture.....	102
Figure 5.29: Unaccounted Availability versus Water Addition for Lean Mixture.....	102
Figure 5.30: Availability Distribution for Water to Fuel Mass Ratio 0.5 at Lean Region and $Q_{in} = 24.62$ kW.....	103
Figure 5.31: Reversible Power versus Water Addition.....	103
Figure 5.32: Effect of Water Addition on Second Law Efficiency.....	104
Figure 5.33: Effect of Water Injection over Pressure Traces.....	105
Figure 5.34: Effect of Water Injection on the Mass Fraction Burned.....	106
Figure 5.35: Effect of Water Injection on the Availability Transfer by Work...	107
Figure 5.36: Effect of Water Injection on the Availability Transfer by Heat Transfer.....	107
Figure 5.37: Total System Availability as a Function of Crank Angle.....	108
Figure 5.38: Effect of Water Injection on the Availability Destruction vs. Crank Angle.....	109
Figure 5.39: Terms of Availability Balance for No Water Injection Case and $m_w/m_f = 0.5$ Case.....	110
Figure 5.40: Effect of Water Injection as Steam and Liquid Water on $NO_x$ Emission.....	111

Figure 5.41: Effect of Water Injection as Steam and Liquid Water on HC Emission.....	112
Figure 5.42: Effect of Water Injection as Steam and Liquid Water on CO Emission.....	112
Figure 5.43: Effect of Water Injection as Steam and Liquid Water on Exhaust Temperature.....	113
Figure 5.44: Effect of Water Injection as Steam and Liquid Water on Combustion Duration.....	114
Figure 5.45: Effect of Water Injection as Steam and Liquid Water on Ignition Delay.....	115
Figure 5.46: Effect of Water Injection as Steam and Liquid Water on Brake Thermal Efficiency.....	116
Figure 5.47: Effect of Water Injection as Steam and Liquid Water on Brake Specific Fuel Consumption.....	116
Figure 5.48: Effect of Water Injection as Steam and Liquid Water on Volumetric Efficiency.....	118
Figure 5.49: Percent Reduction in Output Power due to Evaporation of the Water.....	120
Figure 5.50: Percent Increase in Output Power due to Reduction in Inlet Temperature.....	120
Figure 5.51: Net Change in Output Power due to Water Addition.....	121
Figure 5.52: Percent Reduction in Output Power due to Evaporation of Water for 1/3 Water to Fuel Mass Ratio as a Function of F/A Equivalence ratio.....	121
Figure 5.53: Percent Increase in Output Power due to Reduction in Inlet Temperature for 1/3 Water to Fuel Mass Ratio as a Function of F/A Equivalence Ratio.....	122
Figure 5.54: Percent Net Change in Output Power due to Water Addition for 1/3 Water to Fuel Mass Ratio as a Function of F/A Equivalence Ratio.....	122
Figure 5.55: Theoretical Results of Water Addition Effect on $T_1$ , $T_2$ , AFT and Temperature Drop of Inlet Air.....	125
Figure 5.56: The Calculated the Relative NO Formation Rate at the Diffusion	

	Flame Surface with Different Amount of Water Injection.....	126
Figure 5.57:	Effect of Water Injection on Second Law Efficiency of the Otto Cycle.....	127
Figure 5.58:	Effect of Water Injection on Maximum Work, Actual Work and Lost Work of Combustion Process for an Otto Cycle.....	127



## LIST OF SYMBOLS

### Abbreviations and Symbols

$a$	Specific Availability
$A$	Availability
$BP$	Brake power
$bsfc$	Brake Specific Fuel Consumption
$C$	Number of Carbon Atoms in Fuel's Structure
$C_p$	Specific Heat at Constant Pressure
$EGR$	Exhaust Gas Recycle
$F/A$	Fuel-Air Ratio
$FP$	Friction Power
$h$	Specific enthalpy
$H$	Number of Hydrogen Atoms
$h_f$	Enthalpy of Formation
$IC$	Internal Combustion.
$IP$	Indicated Power
$imep$	Indicated Mean Effective Pressure
$isfc$	Indicated Specific Fuel Consumption
$P$	Pressure
$R$	Gas Constant
$s$	Specific Entropy
$LHV$	Lower Heating Value
$LPG$	Liquefied Petroleum Gas
$m$	Mass Flow Rate
$MW$	Molecular Weight
$MBT$	Maximum Brake Torque.

$n_1$	BDC Induction Crank Angle
$n_2$	BDC Exhaust Crank Angle
$N$	Engine Speed
$P-V$	Pressure versus Volume
$R$	Crank Length
$rpm$	Revolutions per Minute
$T$	Temperature
$T_f$	Fuel Droplet Surface Temperature.
$TDC$	Top Dead Center
$U$	Specific Internal Energy
$v$	Specific Volume
$x$	Cylinder Travel

#### Greek Symbols

$\eta_I$	First Law Efficiency
$\eta_{II}$	Second Law Efficiency
$\phi$	Fuel/Air Equivalence Ratio
$\theta$	Crank Angle in Radians

#### Subscripts

$b$	Brake
$i$	Indicated
$con$	Convective
$s$	Sensible
$cv$	Control Volume
$cw$	Cooling Water
$d$	Destroyed
$e$	Exhaust
$F$	Fuel
$a$	Air
$H$	High

<i>ic</i>	Incomplete Combustion
<i>in</i>	Inlet to Engine
<i>O</i>	Environment
<i>K</i>	Kinetic
<i>L</i>	Low
<i>out</i>	Outlet of the Engine
<i>max</i>	Maximum
<i>rev</i>	Reversible
<i>un</i>	Unaccounted
<i>P</i>	Products
<i>R</i>	Reactants
<i>r</i>	Reservoir

# **CHAPTER 1**

## **INTRODUCTION**

The purpose of internal combustion engines is to produce mechanical power from the chemical energy contained in the fuel. The two main types of internal combustion engine are: spark ignition (SI) engines and compression ignition (CI) engines. The Otto engine often runs on gasoline fuel, which is injected into the intake port. The fuel mixes with the air that is sucked into the engine, and as a result, the cylinder is filled with a charge which is close to homogeneous mixture. When the charge has been compressed up close to Top Dead Center (TDC), the spark ignites the air/fuel mixture. In compression ignition engines, air alone is inducted into the cylinder. The fuel is injected directly into combustion chamber in the cylinder just before the combustion process is required to start. The compression ignition engine is generally called as the diesel or oil engine. Since the development of the first commercially successful steam engine in 1769 by James Watt, engineers and scientists have studied the intra-cylinder phenomena of reciprocating engines to understand their principles of operation in order to develop new methods of optimizing the performance of these versatile power sources (Cummins, 1989).

For most of the 20<sup>th</sup> century, the two main fuels that have been used in internal combustion engines have been gasoline (SI engines) and fuel oil (diesel oil for CI engines). The energy crisis and the limitation of oil resources dictated a growing demand for using alternative fuels. The number of motor vehicle has been increasing with the development of technology. Consequently the fuel sources have been consumed rapidly. This also leads to search alternative energy sources and fuels. Most alternate fuels are very costly at present time. This often because of the quantity used. Many of these fuels will cost much less if the amount of their usage gets to the same order of magnitude as gasoline. The cost of manufacturing,

distribution, and marketing all would be less. Another problem with alternate fuels is the lack of distribution points where the fuels is available to the public. Attempts to use many types of fuel have been tried throughout the history of IC engines. Alcohol has been used as a fuel for auto-engines since 19th century; however, it is not widely used because of its high price in comparison with the gasoline. Hydrogen is projected as a possible major fuel of the future to replace the eventual dwindling of gasoline supplies. Fuel storage and refueling for an automobile are the two greatest problems that must be solved to make this a viable vehicle fuel.

LPG has been widely used in automobiles recently as an alternate to petroleum fuels due to its low price. The utilization of LPG as an automotive fuel varied very widely from one country to another. LPG can be produced from natural gas and crude oil. Although this fuel mainly consists of propane and butane, it may also include different hydrocarbons such as propane, iso-butane and n-butane in various proportions (Thring, 1983). When environmental impacts of LPG are taken into consideration as compared to that for petroleum, LPG provides a decrease in hydrocarbon emission as 55 per cent and in carbon dioxide emission as 95 per cent because it has lower carbon content and ease of evaporation before combustion. The biggest disadvantage of the LPG has more NO<sub>x</sub> emissions as compared to petroleum. Performance and drivability of propane vehicles is essentially the same as for gasoline vehicles. For LPG, the gas displacement effect is 4%, it means that the displacement of air by LPG causes reduction in power in the order of 4% (volumetric efficiency decrease) from a requirement gasoline counterpart. On the other hand, evaporative cooling of gasoline increases the intake air density and the engine power. Test results showed that 6% less power was obtained by using LPG than that for gasoline (The Clean Fuels Report, 1992). LPG contains about 5% more energy per unit mass however the density is approximately 32% less. The net result is that a liter LPG at 5 atm pressure contains 28% less energy than a liter of gasoline. Assuming that an engine is operated on LPG and gasoline with equal efficiency, more liters of propane will be consumed to provide equivalent performance. Fortunately, engines generally operate on LPG with greater efficiency than that for gasoline so that the increase in fuel volume is not as great as the energy comparison suggests. LPG fueled vehicles can achieve the same driving range as a gasoline vehicle by installing

a slightly larger tank. LPG consumes approximately 5% more fuel for equivalent performance but it costs 15% less than gasoline.

A large number of researches have been directed towards the reduction in fuel consumption and exhaust emissions. The exhaust of automobiles is the one of the major contribution to the world's air pollution problem. In addition, oil reserves all over the world is depleting at an alarming rate. As the fuel is vaporized during intake and start of compression, evaporative cooling lowers the intake temperature and raises intake density. This increases the volumetric efficiency of the engine. Fuels with high latent heat of evaporation, such as water, have greater evaporative cooling and generally make for cooler engine operation. The concept of injecting water into the internal combustion engine has been around for over 50 years since this idea was used in some World War-II aircraft engines. The water addition to diesel and gasoline automobile engines has been investigated and reported in the published papers which are available in the literature extensively. In recent years, the technology of adding water to the intake systems of engines has been used again. This is done in both automobile engines, in large ships and stationary engines. Several different combustion variables are affected by water injection. It depends on the location of the water injection and the position at where the evaporation takes place, etc. The water in the form of vapor, liquid or steam can be admitted to engine. There are several practical means of inducing water into the engine. Water can be added by one of the following three methods: (1) injection of water into the incoming air, either in intake system or directly into the combustion chamber; (2) emulsifying water with fuel; or (3) using high humidity inlet air.

Water addition will have different effects depending upon how it is introduced. As the water evaporates, it increases evaporative cooling, which then increases power because of higher volumetric efficiency. However, part (or all) of this effect can be lost if the water evaporates off of a solid surface instead of in the air stream. If charge cooling occurs in the intake manifold before intake valves close, it cools the air but also displaces it with water vapor. Therefore water injection may cause a net reduction or increase in air density. At this point, the amount of water injection is also the most important parameter.

The vaporization of the injected water at the start of the compression stroke will cool the gas and consequently less work will be required for the compression stroke in the engine. It is a well-known fact that water does not burn, but it is an efficient coolant, so it makes good sense to use it to reduce peak combustion and inlet air temperatures. It can therefore be used to control induction temperatures for high performance naturally aspirated and turbocharged engines. Also water injection can be used to increase the density of air making the air cooler. If one adds more air into the engine he can gain more power. Water injection can lead to increase the amount of air drawn into the engine as cooling the air and so to make it denser similar to supercharging effect. A simple way of testing this theory can be done by measuring acceleration of an engine for two days with opposite weather conditions. First try it on a hot, dry day when the air is warm and thin, then compare it with a cold wet winter's day and you will see that the car will be faster on the cold wet day, because the cold, wet air is denser (more of it) than the warm air and as most simple fuel metering devices can detect dense air the fuel is increased to match.

In addition to increasing volumetric efficiency and power, water injection process was also done to decrease the generation of  $\text{NO}_x$  by reducing the cycle temperatures (Harrington, 1982). Another application for water injection is to reduce or prevent detonation by reducing the combustion temperature. If an engine starts to detonate, injecting water into the inlet tract will stop detonation. With this in mind, it is possible to reduce advance angle i.e. ignition timing to achieve more power (which would normally put the engine at risk of detonation), and to prevent engine failure by injecting water into the engine. A test was carried out on a normally aspirated engine, which proved the ignition timing could be advanced by 6 degrees more than normal position and low octane unleaded fuel used instead of gasoline when a water injection system was fitted. Water injection may yield to an improved fuel economy by running with leaner mixtures. Saab Automobile company has searched water injection to improve fuel economy at high speed and fast acceleration. Water injection is also slows flame front speed and improving the complete combustion by improving the oxidation of CO. When the water changes its state from liquid to gas in the heat of combustion, it is able to supply the piston with significant expansion work. Water vapor, with its high ratio of expansion, is particularly suited for this purpose.

In addition, by adding a water injection system to a SI engine it keeps the pistons, valves and plugs clean. Water injection also helps to prevent pinging by cleaning away carbon deposits during the combustion process, which reduces oxides of nitrogen by reducing the combustion temperature. Additionally, the cooling effect acts as a strong knock inhibitor. Water injection also prolongs engine life by controlling the excess heat. Because of its huge specific- and latent- heat capacity, water is the perfect liquid for regulating excess heat under certain engine-operating conditions.

Many researchers' results shows that the water emulsions have a positive effect on the combustion process through the micro-vaporization of the fuel drops. This vaporization occurs due to the "explosion" of the small water droplets in the fuel during combustion, yielding to a better mixing of the fuel and the air. The water in the combustion chamber will also increase the specific heat capacity of the charge, resulting in lower combustion temperatures. In practical application, emulsification achieves about 20% NO<sub>x</sub> reduction because the water content is limited by reliability considerations. Water to fuel emulsion is used generally for the diesel engines.

The present study was planned as the first sophisticated experimental study on the subject in Turkey. A test engine and necessary measuring devices for experimental investigation on the subject was the basic difficulty of this investigation at the starting stage. The main difficulty is to obtain reliable experimental results and analysis of these. In this thesis, the effect of water and steam injection on LPG fueled SI engine performance, fuel economy, combustion characteristics, and exhaust gas emissions were investigated by various methods of introducing water into the combustion chamber. These methods were manifold injection and manifold induction. Previously, there were many theoretical and/or experimental studies separately on the effect of water addition to the internal combustion engines. But, there was no cited experimental study on the effect of water addition to LPG fuelled, conventional spark ignition engine. Energy is supplied to the engine as the chemical energy of the fuel and leaves as energy in the exhaust, cooling water, brake power and heat transfer. Heat losses must be decreased to improve the engine efficiency. Therefore, it is very important to know about the fraction of the heat absorbers. This is the aim of the thermal balance experiments. Experiments with internal combustion



engines very often involve a thermal balance on the engine. It was apparent that a little information was available on the thermal balance of LPG fueled spark ignition engines including water addition effects. Therefore, effect of water addition on the thermal balance of the test engine was investigated.

The engine system is analyzed by using two methods based on the two main laws of thermodynamics. First law of thermodynamics depends upon energy conservation. It states that the energy can be neither created nor destroyed, but only transformed. Availability is based on second law of thermodynamics and it is not a conserved property since it can be lost by irreversibility. Engine developers determine the performance of the system normally by using the first law analysis. Otherwise, the second law analysis serves as a supplement to the former to enhance the investigation of losses in the system. Such analysis can also be useful in appraising various design concepts of systems. Energy and availability analysis have been used for internal combustion engine for a long time. The effect of water injection on the calculated exergy terms using measured energy terms was investigated in the present study. The exergy changes as a function of crank angle with added water was also investigated. The results of the second-law analysis of engine operation with water addition case were compared with the results of a similar analysis for cases where no water addition took place. This was an original feature since the second law analysis was not available for this case.

In the second chapter of this thesis, an extensive available literature survey on the theoretical and experimental studies about the water addition concept are presented in a detailed manner. For the present experimental study, an experimental set-up consisting of an engine, a dynamometer, an air meter, a fuel and a water meter, a fuel tank, and the necessary piping for discharging the combustion products were prepared firstly. In the second stage; measuring and processing systems to obtain a fully computer aided experimental study on the prepared set-up was installed. This experimental set-up is presented in Chapter 3. Different computer programs were used for reading data by the computer and the analysis of the experimental data. Detailed information about all of these programs is presented in this chapter. The calibrations of the used measurement devices are also outlined in this chapter.

The formulations used during the investigation are presented in Chapter 4. The procedures of experiments are also given in this chapter. The experimental set-up used in present study was made up of several different transducers and data acquisition systems. The information supplied by these systems was used for the generalized analyses in this thesis. Since it was desirable to know the accuracy of these parameters, an error analysis is conducted for the measuring system in this chapter. The results of the experiments are discussed in view of the available literature in Chapter 5. The conclusions derived as results of comparative discussions are also given in this chapter. In Chapter 6, suggestions for further complementary works are given.

The experimental study presented in this thesis was financially supported by the Research Fund of the University of the Gaziantep under the project no: MF 01-06.

## **CHAPTER 2**

### **LITERATURE SURVEY**

#### **2.1 INTRODUCTION**

In this chapter; a summary of the related literature based on theoretical and experimental investigations conducted on the effect of water addition into the IC engines are presented.

#### **2.2 PREVIOUS STUDIES ON LPG AS AN INTERNAL COMBUSTION ENGINE FUEL**

Liquefied petroleum gas (LPG) has been well known as a clean alternative fuel for internal combustion engines and widely used in commercial vehicles. Promising results with LPG have been obtained from the fuel economy and exhaust emissions points of view (Beer et al., 2002; Selim, 2004; Bayraktar and Durgun, 1998). Several researchers (Thring, 1983; Ulrich and Wallace, 1987) have worked with LPG as alternative fuel for both compression ignition and spark ignition engines. When environmental effects of LPG are taken into consideration compared with liquid fuels, significant improvements in exhaust emissions can be achieved (Bayraktar and Durgun, 2005). LPG fuelled spark ignition engines produce virtually zero emissions of particulate matter, very little carbon monoxide and moderate hydrocarbon emissions (Bass, Bailey, and Jaeger, 1993). A major disadvantage of the LPG was NO<sub>x</sub> emission which was greater than that for liquid fuels (Murillo et al., 2005). Murillo et al. (2005) researched into the use of LPG in spark-ignition outboard engines. They showed that the use of LPG instead of conventional gasoline a great reduction in low power outboard engine fuel consumption and pollutant

emission. Yamin and Badran (2002) presented a discussion on the parameters that affect the engine's heat losses mainly during power stroke, with suggestions to minimize it from a LPG powered four-stroke spark ignition engine. Wallace (1989) showed that by offsetting the heat in the inlet manifold; a gain of up to 8% in volumetric efficiency that for LPG with respect to gasoline was achieved, accompanied by an increase in engine power output levels equal to that of gasoline.

### **2.3 FIRST STUDIES ON THE WATER INJECTION CONCEPT**

The concept of injecting water into the internal combustion engine is not new, but nowadays it is considered carefully for the benefits that it allows. The use of water, as a separate liquid or emulsion with fuels has been considered repeatedly since the early development of internal combustion engines.

Kuhring (1938) carried out a series of tests to determine the effect of water injection on the operation of a full-scale aircraft engine. Colwell, Cummings and Anderson (1945) investigated the usage of the alcohol water injection in both aircraft and ground-vehicle engines, where it can give more and smooth operation, with a fuel of about 12 octane numbers less than the normal engine requirements. Rowe and Lodd (1946) illustrated the results or effects of water-alcohol injection on aircraft engine performance. Eaton (1946) carried out a cost analysis for increasing airplane performance by water injection. Obert (1948) summarized the following discussion related with water injection. Firstly, Injection of water into on unheated manifold in conjunction with high speeds of the engine will not have sufficient time to vaporize the water during the compression stroke. Secondly, complete vaporization of the internal coolant is probably not secured until the combustion period is under way. Thirdly, the mechanism whereby water suppress detonation is secured by slowing the combustion time and also by cooling the end portion of the charge by vaporizing water contained in the end portion.

## 2.4 PREVIOUS STUDIES ON THE EFFECT OF WATER ADDITION ON THE INTERNAL COMBUSTION ENGINE PERFORMANCE

Water has been added as an internal coolant, as a knock suppressant and a means to control emissions. Observations generally regarded water effects on engine performance, knock and emissions.

Obert (1948) showed that the injection of water decreased the knock and increased the power output until essentially the same power was obtained from either the 65- or 85- octane fuel. Obert (1948) and Zeilinger (1971) have showed that water addition to the reactant mixture slowed the combustion process in S.I. engines. In addition to the possible engine efficiency gain brought about by raising the compression ratio, water addition could also have a beneficial effect on the efficiency at a given compression ratio due to changes in the thermodynamics of the cycle (Modak and Caretto, 1970; Nicholls, El-messiri and Newhall, 1969). Unfortunately, in despite of the expectations of improved efficiency, the reported gains were generally small and sometimes negative (Weiss and Rudd, 1959; Obert, 1948; Weatherford and Quillian, 1970). Lestz, Melton and Rambie (1975) concluded that total cooling of diesel engines by direct water injection could be accomplished with increased power and better BSFC. Evaporative cooling of the metal surfaces was a more efficient process and produces beneficial effects in the cycle. Also, they noted that the fuel consumption improved from 0.65 to 0.54 lb/Bhp.hr for the best water injection condition (N=1800 rpm). Peters and Stebar (1976) observed in volumetric efficiency changes ranging from 1% loss to a 3% gain were computed using a sample of the water addition data. Obert (1948) observed a 2% loss with a 50% water addition (i.e. mass of water/mass of fuel is 0.5) level. It was observed that water input caused a slight but sustained increase (2-3%) in volumetric efficiency, increases occur due to change and engine metal cooling, while decrease one due to the formation of steam on the intake stroke (Lestz, Melton and Rambie, 1975). Peters and Stebar (1976) purposed to evaluate the potential of water-gasoline fuels in spark ignition engines in light of contemporary engine constraints. They generated information from laboratory engine tests engine cycle calculation, and vehicle tests. Thus to maintain MBT spark settings, the timing must be advanced when using

water-gasoline fuels. They also showed that the exhaust temperature did not significantly change for rich mixture conditions when water was added to the fuel. However, for lean mixture conditions exhaust temperatures decreased somewhat. Water-gasoline-fuel allows higher knock limited compression ratios. Indicated efficiencies measured using direct manifold water addition from 11 to 48% by weight at  $\phi=0.91$  only varied between 0.37 to 0.38, values that fall almost exactly on the emulsified  $N=1200$  rpm. No significant improvement in indicated engine efficiencies was observed with water addition either directly to the manifold or via emulsified.

Harrington (1982) tested a single cylinder engine to determine basic combustion, emission and performance characteristics of water-gasoline mixtures, with water introduced to the intake manifold as a liquid or a vapor. Harrington (1982) concluded that engines could be calibrated to operate with small amounts of water addition to gasoline, and so knock could be suppressed, and fuel and so energy consumption would be increased. Jost (1995) operated the water injection system at full-throttle acceleration and at high speed for gasoline fuelled Saab V6 ecopower concept engine. To avoid the need for an additional water source, fluid was taken from the windshield washer reservoir. Antifreeze solution and washer additives did not seem to harm the engine. High-speed fuel consumption has been reduced by 20-30%. This consumption reduction for the LPG fuelled engines was searched in the present study. Lanzafame (1999) investigated the effects of water injection in the intake pipe from both a theoretical and experimental viewpoints. His results showed that water injection to intake pipe really represented a new way to avoid detonation, to reduce compression work and to control  $NO_x$  production in spark ignition engines.

## **2.5 PREVIOUS STUDIES ON THE EFFECT OF WATER ADDITION ON THE EXHAUST EMISSIONS**

Water injection affected the exhaust emissions significantly. Water injection is well known to be capable of reducing the oxides of nitrogen. Obert (1948) explained that the ability of water addition to slow down the burning rate and to reduce the gas temperature in the cylinder probably suppressed detonation. Nicholls,

El-messiri and Newhall (1969) showed nitric oxide concentration reductions of over 50% with a water-fuel mass ratio of one. Conversely, water addition probably increased hydrocarbon emissions (Quader, 1971). Wilson, Muir and Pelliciotti (1974) showed that the introduction of one part water for every two parts fuel into the intake air caused  $\text{NO}_x$  concentration to drop about 50%. They concluded that the water injection seems to have a greater potential for reduction at high speeds and low-to-medium loads. Secondly, when water was injected into the air intake and hence throughout the cylinder, some water was wasted; by contrast, the potential for  $\text{NO}_x$  reductions for fuel/water emulsions appeared to be greater. Finally, with respect to carbon monoxide emissions, Kummer (1975) stated that, the effect of water addition on CO emissions would be remained. The hydrocarbon emissions increased rapidly with water addition to the engine caused a small drop in carbon monoxide emission concentrations. The effect was only noticeable at rich conditions where carbon monoxide levels were relatively high (Peters and Stebar, 1976). Peters and Stebar (1976) investigated the effect of water-gasoline fuels on spark ignition engine emissions and performance. They showed that 40% of water addition by weight to the fuel produced about a 40% drop in the peak nitric oxide emission level. Conversely, direct manifold water injection in amounts equal to the fuel flow caused about a 50% increase in HC emissions. In addition, their results showed that the effect of water addition on carbon monoxide emissions was small. Nicholls et al. (1969) reported that dramatic reductions of about 50% occurred in nitric oxide emissions by the effect of water addition at a water-fuel mass ratio of unity. It was found that 10% water in gasoline caused 10-20% reductions in nitrogen oxides. Lestz et al. (1975) showed that  $\text{NO}_x$  concentration decreased while HC and CO emissions increased with water injection for diesel engine.

Harrington (1982) tested a single cylinder engine, and concluded that engines could be calibrated to operate with small amounts of water to gasoline, and, by doing this knock could be suppressed, hydrocarbon emissions slightly increased,  $\text{NO}_x$  emissions decreased, CO did not change significantly. The effect of the water addition on the burned gas temperature and  $\text{NO}_x$  emissions was simulated (Ishida and Chen, 1994). Their simulation introduced a negative effect of water addition at water vapor contents in the working gas more than usual. Water addition had caused an

increase in the specific heat and molecular weight of the burned gas accounted for a decrease in burned gas temperature. Ishida et al. (1997) investigated the effect of port water injection on NO<sub>x</sub> formation theoretically as well as experimentally. Their results showed that the exhaust NO<sub>x</sub> reduced significantly by port water injection, and about 50% reduction in NO<sub>x</sub> concentration was attained under various engine operation conditions by injecting the amount of water of 0.03 kg per unit kg of dry air. Dodge et al. (1996) developed a PC-based model for predicting the NO<sub>x</sub> reduction in diesel engines. Bedford et al. (2000) described the water injection as a practical NO<sub>x</sub> reduction technology for DI Diesel engines. Their calculations showed that the main mechanism behind the NO<sub>x</sub> and soot reduction was lower peak temperatures in the combustion region provided by the vaporization of liquid water, which caused an increase in specific heat of the gas around the flame. They used a CFD program to simulate the effect of added water droplets into the Lagrangian diesel spray model. Their model study put forth water injection as a practical NO<sub>x</sub> reduction technology due to the higher heat capacity of the water, which resulted in longer evaporation times and thus longer liquid injection lengths.

Several different methods of water addition have been developed for diesel engine (Kohketsu S. et al., 1996; Kegl B. and Pehan S., 2001). For example, Kahketsu et al. (1996) investigated the direct injection of water with a new designed stratified fuel water injection system. They applied this new system to an automotive diesel engine. Their results showed that NO<sub>x</sub> were reduced by 50% in comparison with original. Kegl and Pehan (2001) discussed some aspects of injecting or adding water either into the intake air or to the fuel of a diesel engine in order to reduce harmful emissions. These studies have showed that further reduction of harmful emissions was still possible

## **2.6 PREVIOUS STUDIES ON THE WATER / FUEL EMULSION**

Several authors investigated the water-emulsified diesel and water-emulsified fuel in gasoline engines. Emulsified fuel-water blends can be used as an alternative fuel and to reduce NO<sub>x</sub> and particulate matter (PM) emissions. The main



disadvantage of water emulsified fuels was the difficulties to supply uniform mixture.

Bignardi et al. (1981) computed the composition, temperature, internal energy and nitric oxides content of the exhaust gas, under influence of water added to fuel. Satpov and Lusho (1982) reported the effects of water presence in fuel on SI engines. They indicated that the NO<sub>x</sub> content in exhaust gas dropped by 1.3% for 1% addition of water to emulsified fuel. Park et al. (2001) showed that water-emulsified diesel reduced NO<sub>x</sub> and smoke at the same brake specific fuel consumption at high speeds after their experiments. Tsukahara and Yoshimoto (1992) reported the reduction of NO<sub>x</sub> with water emulsified diesel fuel for a low compression ratio diesel engine. Abu-Zaid (2003) investigated the effect of water emulsification on the performance and exhaust gas temperature of a single cylinder diesel engine. His results indicated that the exhaust gas temperature decreased as the percentage of water in the emulsion increased. Gross (1991) investigated the different methods for reducing Diesel Engine NO<sub>x</sub> emissions such as retarding the fuel injection timing, lowering the intake temperature, water injection, water emulsified in the fuel or introduced to the combustion space with the air or through a separate nozzle, EGR, lower compression ratio, etc.

## **2.7 PREVIOUS STUDIES ON THE ENGINE ENERGY BALANCE**

Experiments with internal combustion engines very often involve an overall first law energy balance on the engine. It provides useful information on the disposition of the initial fuel energy.

Ament et al. (1977) investigated the energy balance for a six-cylinders SI engine. They analyzed that the brake power, coolant load, sensible exhaust enthalpy, and miscellaneous energy transfers as percent of input fuel energy for SI engines at road-load operating conditions. Their results showed that the coolant heat transfer rate is 2 to 3 times of the brake power at low speeds and loads. Yüksel and Ceviz (2003) investigated the effects of adding constant quantity hydrogen to gasoline–air mixture on SI engine thermal balance and performance. Ajav et al. (1999) reported

the thermal balance of a constant speed medium size compression ignition engine operating on ethanol-diesel blends and fumigated ethanol as fuels. Taymaz et al. (2003) evaluated the heat losses at different engine loads and speeds with and without ceramic-coated diesel engine.

## **2.8 PREVIOUS STUDIES ON THE EXERGY ANALYSIS FOR INTERNAL COMBUSTION ENGINES**

Investigations on the detailed use of the second law of thermodynamics to study internal combustion engines have been published for over 40 years. These previous investigations, in which the second law of thermodynamics or availability analyses used, were identified. The second law of thermodynamics is a rich and powerful statement of related physical observations that has a wide range of implications with respect to engineering design and operation of thermal systems. For example, the second law can be used to determine the direction of processes, to establish the conditions of equilibrium, to specify the maximum possible performance of thermal systems, and to identify those aspects of processes that are detrimental to overall performance. The second law analysis also provides an explanation to why and where available energy is lost or destroyed in the engine system. A review of such studies relating to internal combustion engines is available elsewhere, like that of Caton (2000a).

Traupel (1957) was the one of first investigator on availability analysis for internal combustion engine. He completed calculations to determine the availability values based on measurements of the principal energy terms. Most authors have been studied the concept of the use of the second law or availability concept for internal combustion engine. These studies were based on comprehensive model of all processes (Primus, 1986; Gallo, 1992; Rakopoulos, 1993; Caton, 1999; Caton, 2000b; so on); comprehensive model of all processes included experimental measurements (Lipkea, 1989; Bozza, et al., 1991; Rakopoulos, C. D and Giakoumis, 1997; and so on) and calculated availability with experimental measurements of energy terms (Alkidas, 1988; Alkidas, 1989; Rakopoulos, C. D., and Andritsakis, 1993; Alasfour, 1997; and so on). Alkidas (1988 and 1989) studied the application of

a second law analysis for a typical diesel engine. Alkidas (1988) examined the application of availability for a single cylinder diesel engine and he calculated the availability values by using experimental measurements on the energy rejection to the coolant and lubricating oil, the brake power, and the air and fuel flow rates. Alkidas (1989) used water-cooled and un-cooled single cylinder diesel engine for investigating the application of a second law analysis experimentally. His results showed that the first-law and second-law efficiencies of the un-cooled engine were significantly higher than the water-cooled engine.

Rakopoulos and Andritsakis (1993) used the second law of thermodynamics for analyzing irreversibility rates. They used direct injection (DI) and indirect-injection engine (IDI). Rakopoulos et al. (1993) used a high-speed direct injection and naturally aspirated diesel engine to determine the fuel reaction rates, and the computed irreversibility production rate at the valve-closed period. Alasfour (1997) experimentally investigated the availability analysis of a single cylinder spark ignition engine by using a butanol-gasoline-blend. He examined the effect of use of a butanol-gasoline blend in a spark-ignition engine on the first and the second law efficiencies. His results showed that an increase in both of the first and the second law efficiencies in the lean region for both fuels. Van Gerpen and Shapiro (1990) also used a second law analysis including the “chemical component” of the availability with a standard cycle simulation for a diesel engine. Shapiro and van Gerpen (1989) reported their results on the application of the ‘two-zone model’ including an analysis based on the second law of thermodynamics with chemical availability considerations for both compression-ignition and spark ignition engines with no residuals. Their work considered only the compression and expansion strokes, but not the intake or exhaust flows. They showed that the combustion irreversibility increased by increasing combustion period. Caton (1999–2001) reported on the use of the second law of thermodynamics to study a spark-ignition engine. His work was based on the use of a comprehensive thermodynamic cycle simulation, and examined the effects of engine load and speed on a number of performance, energy and availability terms. Caton (2002) extended his earlier works to performance, energy and availability results using multiple zones for combustion process.

## 2.9 CONCLUSIONS

According to literature on water injection, different conclusions exist because authors investigated the effect of water injection, which is tested different engine with different engine load and speed. On the other hand, though analyzed by a few researches, the observations of water injection in spark ignition engines does not yield homogeneous results, owing to various typologies of engines used for experiments.

Different conclusions can be done according to literature. The following main conclusion can be drawn from the analysis.

- 1) Water injection can increase power, not the fuel consumption.
- 2) It does not increase volumetric efficiency. Actually, obtaining more energy from the charge allowing lower throttle settings and engine speed for a given output power. It improves the completeness of combustion. In other words there is less un-burnt fuel in the exhaust gases.
- 3) In addition, it can be basically used as an anti-detonant. It can supply better fuel economy by increasing the basic compression ratio of the given engine or run more boost-instead of using higher-octane fuel grade.
- 4) If water can reduce temperature of the intake within the sweeping volume during the induction stroke, then in theory, it can supply to pack more air inside the combustion chamber, provided the air speed in the inlet tract is constant, hence volume efficiency of the induction stroke is increased. In addition, theoretically, when a liquid and gas are compressed, vaporization of the liquid will cool the gas and less work will be required for the compression.

Water emulsion seems to have a positive effect on the combustion process through the micro-vaporization of the fuel drops. This vaporization occurs due to the “explosion” of the small water droplets in the fuel during combustion, giving better mixing between the fuel and the air. The water in the combustion chamber will also increase the specific heat capacity of the charge, resulting in lower combustion

temperatures. The  $\text{NO}_x$  reduction effect of water emulsion is the highest at high loads, because water emulsion gives increased ignition delays at part load. Long ignition delays imply increased amount of fuel in the cylinder before the charge ignites, which result in high peak temperatures and high  $\text{NO}_x$  formation. In practical application, emulsification achieves about 20%  $\text{NO}_x$  reduction because the water content is limited by reliability considerations.

As a result of these conclusions, the purpose of this thesis is to evaluate the effects of water addition on combustion in a SI engine. The method of water addition (manifold injection and manifold induction), antiknock characteristics with water addition, MBT spark requirement, engine efficiency, engine cooling requirement, exhaust emissions, volumetric efficiency, bsfc, engine power and exhaust temperature were examined at different engine speeds and load conditions by using a LPG fueled SI engine with four cylinder. The unexpected results (i.e. volumetric efficiency, fuel economy etc.) of most authors were considered about water injection due to tested single cylinder test engine and low speed operation. The best results were expected as high ratio of injected water to fuel mass at high speed in the present study. Because, gasoline is vaporized during intake and start of compression, evaporative cooling lowers the intake temperature and raises intake density. Therefore, gasoline fueled engine has a better volumetric efficiency than LPG fueled engine. The temperature of the LPG air mixture also rapidly increases, than the gasoline air mixture during the intake and compression stroke. This study was presented that the concept of supplementing LPG as a spark ignition engine fuel with water is beneficial in some respects and deleterious in others. In this thesis, water injection and steam injection systems were designed. In addition, the important parameter of water injection was obtained as the size of water droplets. For this purpose, in the experiments two different nozzles were used. There were many reports about the energy balance for the engine. However, it was apparent that a little information was available on thermal balance of the effect of water addition for spark ignition engines operating on LPG as fuel. The study reported in this thesis is to establish the thermal balance of such a conventional spark ignition engine. Investigations of engine operations based on the second law of thermodynamics have been reported since the 1950's. Many engineering systems have been studied using

analyses based on the second law, but effect of water addition on the engine analysis including second-law analysis was not reported. In this thesis, effect of water addition on the second-law was investigated and reported.

## **CHAPTER 3**

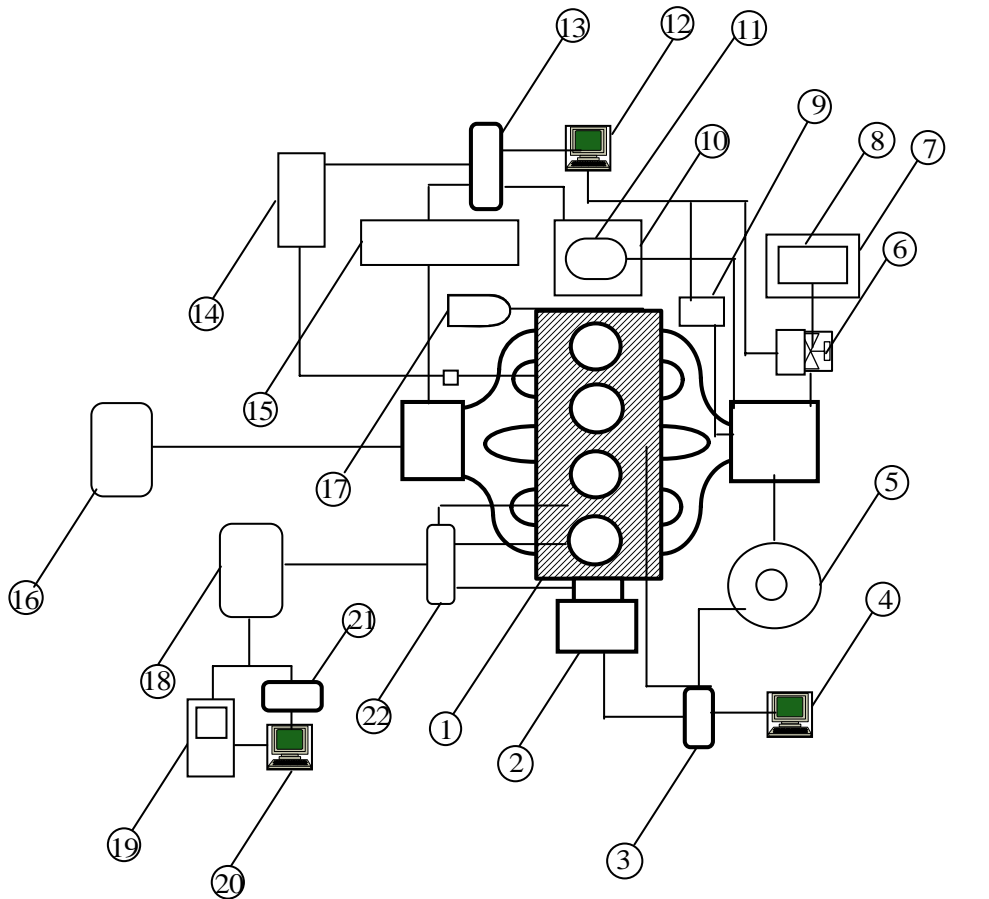
### **EXPERIMENTAL SET-UP AND MEASUREMENT DEVICES**

#### **3.1 INTRODUCTION**

In this chapter, the configuration of the experimental set-up, specifications of the components, measurement and control devices and the measurement techniques are presented. In addition, the calibration information of the devices used in the measurements is given.

#### **3.2 HARDWARE**

In this study, the first approach with the aim of improving the combustion characteristics of LPG, which will be reflected in improving the engine performance. Water injection method was chosen in this study to improve LPG combustion qualities. The requirements for the test system are that it must be rugged, reliable, accurate, and user friendly. To meet these requirements, the key components were carefully selected and assembled with precision. These key components include an engine, dynamometer, airflow meter, pressure transducers, an optical shaft encoder, thermocouples, a fuel and water flow monitoring system, and data acquisition systems. The parts of the system were given in the following sections. The complete hardware system can be seen in Figure 3.1. The specifications of components of the hardware system were given in Appendix 1 to Appendix 10.



- |                                     |                                      |
|-------------------------------------|--------------------------------------|
| 1.Engine block                      | 12.Computer 2                        |
| 2.Dynamometer stand                 | 13.Multiport Serial adapter          |
| 3.Data acquisition & control unit 1 | 14.RPM measurement unit              |
| 4.Computer 1                        | 15.Exhaust gas analysis system       |
| 5.Air-flow meter                    | 16.Exhaust gas calorimeter           |
| 6.Water flowrate control unit       | 17.Cooling water flowmeter           |
| 7.Water- flow balance               | 18.Signal conditioner                |
| 8.Water supply                      | 19.DSO                               |
| 9.Speed control unit                | 20.Computer 3                        |
| 10.Fuel-flow balance                | 21.Data acquisition & control unit 2 |
| 11.Fuel Tank                        | 22.Interface unit                    |

Figure 3.1: The Complete Test Engine Hardware System

### 3.2.1 Engine

The engine chosen as a test engine for the water injection tests was a spark ignition engine as shown in Figure 3.2. It has an overhead valve design and is water-cooled.





Figure 3.2: Test Engine

A fully instrumented SI engine was mounted on a hydraulic dynamometer. The specifications of test engine were listed in Table 3.1. In addition, the detailed specifications of the engine used in experiments were given in Appendix 1.

Table 3.1: Test Engine Specifications

Type	4 cycle, 4 cylinder
Bore	76 mm
Stroke	71.5 mm
Swept Volume	1297 cm <sup>3</sup>
Compression Ratio	7.8

The specification of an ordinary LPG fuel used as the test fuel was shown in Table 3.2.

Table 3.2: Tested Fuel Specifications

Gas fuel name	Liquefied Petroleum Gas
Propane	30% by Volume
Butane	70% by Volume

### 3.2.2 Pressure Transducers

An electronic pressure transducer produces an electrical signal proportional to the pressure. Many different types of electronic pressure transducers have been developed, each operating on a different scientific principle. Two pressure transducers were utilized for acquiring the cylinder pressure versus crank angle. The first transducer is a piezo-electric pressure transducer. It is mounted directly into the cylinder head to the combustion space (see in figure 3.3) and is used to monitor the cylinder pressure throughout the engine cycle.

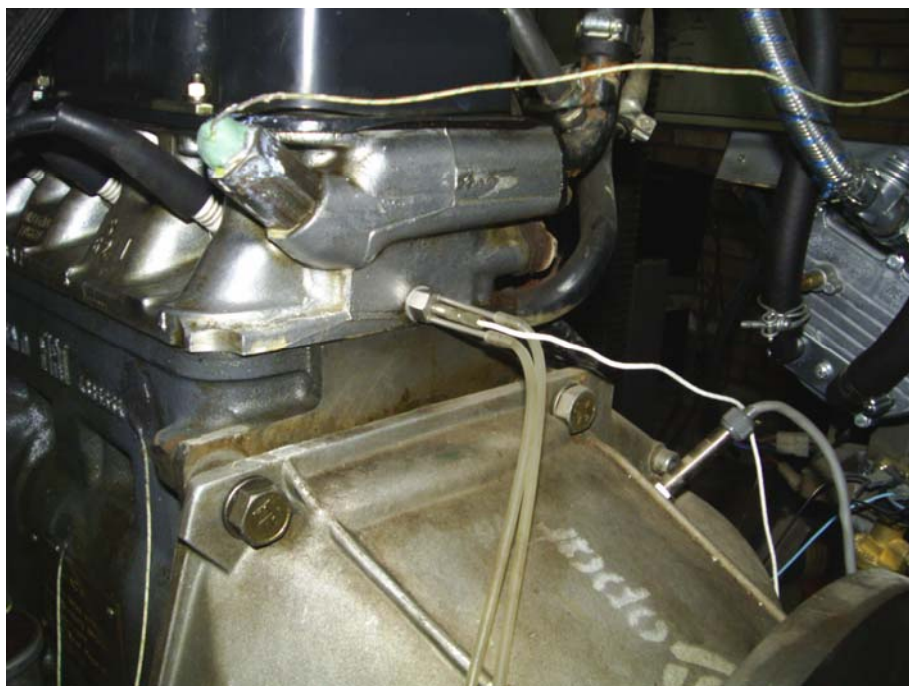


Figure 3.3: Replacement of the Piezo-electric Pressure Transducer on the Engine Block

Piezoelectric pressure transducers are the most commonly used form of pressure transducer for the purpose of acquiring in-cylinder pressure data. They however have several disadvantages, these include sensitivity to thermal shock, long and short-term drift, sensitivity to temperature and that the output has to be referenced to an absolute pressure. Transducer drift increases the measured cyclic variability. As the pressure applied to the unit changes, the piezoelectric properties of the quartz produce a static charge that is linearly proportional to the change in pressure. This charge can then be amplified and recorded to obtain an accurate record

of the changes in the pressure applied to the unit. The main shortcoming of the piezoelectric charge mode pressure transducer is that it measures the changes in pressure rather than measuring the absolute pressure. Consequently, an accurate baseline for the pressure data must be determined. Correcting absolute cylinder pressure on a cycle-by-cycle basis is also necessary due to drift of the piezoelectric pressure transducers. Absolute pressure correction can be carried out by using one of three processes:

1. Fixed pressure value at fixed crank angle: This is the simplest method available although it has the disadvantage that it is difficult to describe such a value or a suitable crank angle to apply a fixed value. Therefore this method, although available, is not recommended.
2. Equating manifold pressure to in-cylinder pressure at fixed crank angle: Whilst this method may seem to be the best method available there is difficulty in determining what crank angle to equate inlet manifold and in-cylinder pressure. Due to the inertia effects of charge entering the cylinder the pressure at the end of the induction stroke can be above that of the inlet manifold. Also, the inlet manifold pressure can fluctuate at higher engine speeds with the effects of resonating pressure waves in the inlet tracts.
3. Fitting the recorded compression pressure to a polytropic process: many researchers favor this method. It has the benefit that no additional data need to be recorded with the cylinder pressure data. However, it has the drawback that it can be difficult to select a polytropic index and which crank angle period to fit.

As stated previously, when using a piezoelectric charge mode transducer it is necessary to determine an accurate baseline to establish the absolute values for the points on the pressure trace. The simplest method to accomplish this is to assume that the pressure at the completion of the intake stroke is equal to the average intake manifold pressure, which can be measured with a transducer or manometer. It has been suggested that one accurate method of doing this is to set the pressure at BDC on the intake stroke equal to the average intake manifold pressure (Randolph, 1990). For this purpose, the second pressure transducer was mounted in the intake manifold and was used to acquire the baseline necessary to establish the absolute values for the pressure curve produced by the cylinder head transducer.

$$P_{int\ ake} = 40.95V - 105.45 \quad (3.1)$$

where V is the signal from the transducer in volts. The detailed specifications of the pressure transducers that are used in experiments were given in Appendix 2.

### 3.2.3 Optical Shaft Encoder

One of the greatest obstacles that had to be overcome during the development of electronic indicator systems was the problem of acquiring accurate data concerning the piston position and synchronizing that data with the cylinder pressure data. Several schemes for accomplishing this task have been devised. One early method involved the mounting of a number of AC generators to the crankshaft and using their output to generate engine position data (Alyea, 1969). Another technique, which was employed by Caterpillar Tractor Company researchers, involved using a photocell to measure the intensity of light shining through a slot that was partially blocked by a cam driven by the crankshaft (Brown, 1973).

As mentioned above, one of the major problems in the development of an electrical indicator system is developing a method of acquiring accurate data concerning the piston position and synchronizing that data with the cylinder pressure data. To accomplish this, a flexible mounts incremental encoder to be directly coupled to the crankshaft. By this way, crank angle information can be obtained from either high-resolution shaft encoder or from a tooth wheel input via electronic indicating system. Optical shaft encoder gives more accurate and high-resolution crank angle measurement than the crank angle information from two magnetic pick up of the electronic indicating system. This shaft encoder produces 1000 pulses per revolution, allowing the shaft angle to be determined to within 0.36 degrees. In addition, there is a reference channel that displays only one pulse per revolution. The detailed specifications of the encoder that was used in the present work were given in Appendix 3. The encoder was installed so that the occurrence of the reference signal corresponds to the piston being at top dead center in the cylinder. This was accomplished by first positioning the engine crank so that the piston was at exactly top dead center. Lancaster et al. (1975) notes that since physical dimensions of the engine can be determined quite accurately, the accuracy of the total volume

calculation is limited by the accuracy of both the clearance volume measurement and the determination of crank angle. TDC must be determined within 0.1 degrees in order to accurately calculate work (imep) and can generally be determined using a dial-gauge during engine construction or by determination of the line of symmetry of motored engine pressure data.

The exact top dead center of the engine was then determined using the procedure described in the ASME test codes for the measurement of indicated power (ASME, 1970). This position was determined by mounting a dial indicator in such a way that its shaft went through the spark plug mounting hole and made contact with the piston. First, the engine was turned clockwise to a position that was approximately twenty degrees before top dead center. Using the pointer, this position was marked on the flywheel and the dial indicator was settled to zero. Next, the engine was turned clockwise until the dial indicator passed top dead center and passed the zero reading. The engine was then turned counter clockwise until the dial indicator returned to the zero reading. This position was also marked using the pointer. Bisecting the angle between these two marks allowed an accurate mark indicating top dead center to be produced. This mark was lined up with the pointer, and the encoder was rotated until the reference signal point was reached. The encoder was then firmly coupled to the crankshaft. With the encoder synchronized with top dead center, it is possible to use the reference pulse to trigger the data acquisition system to begin taking data at top dead center.

#### **3.2.4 Cylinder pressure vs Crank Angle**

One of the most effective means of quantifying the performance of a given engine is to develop a plot of cylinder pressure verses volume. By integrating this curve, indicated power can be determined. Over the years, various means have been devised to produce this plot. In the thesis, an electronic indicating system was used for this purpose. The various parameters of interest, i.e. cylinder pressure, spark event were monitored by transducers fitted to the engine, their outputs being conditioned by their associated electronic channels for output to data acquisition or display system. Electronic indicators have been designed using a wide variety of hardware, but they all share the same general components, namely a power supply, a

motion transducer, a pressure transducer, and a readout or recording device. The measurement of cylinder pressure vs crank angle system used in this study was shown in Figure 3.4.

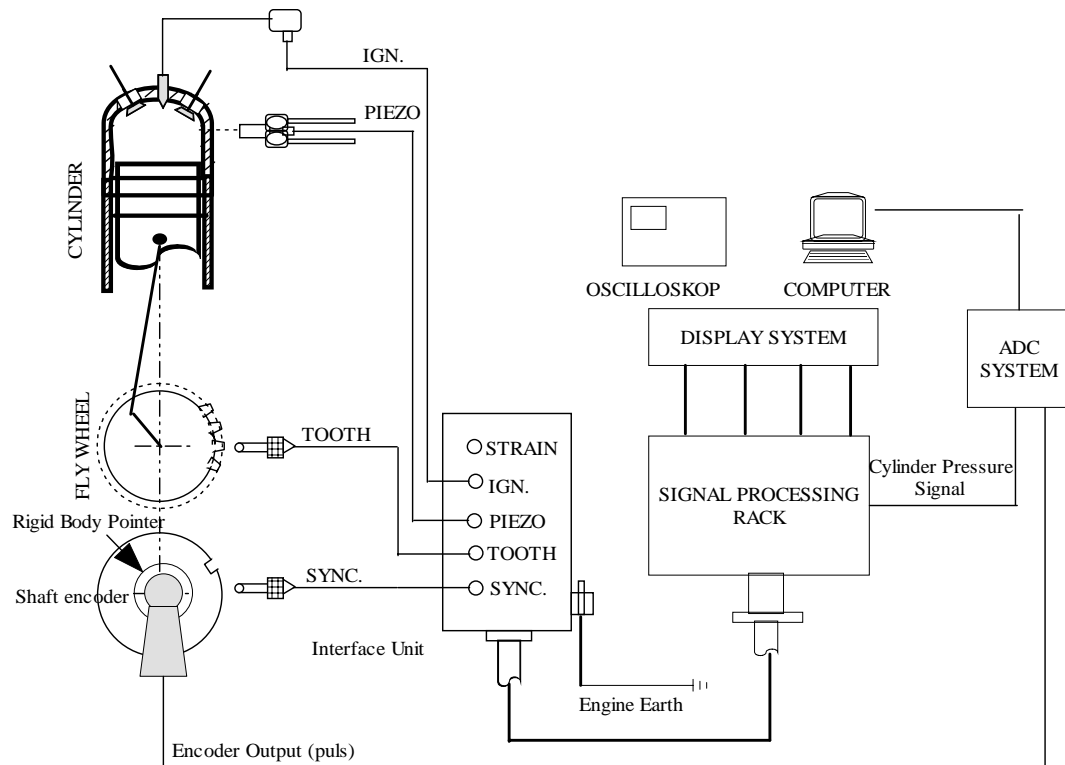


Figure 3.4: Measurement of Cylinder Pressure vs Crank Angle System

The system shown in Figure 3.4 consists of an electronic indicating system, a shaft encoder and display system. A DSO (digital-storage-oscilloscope) and a data acquisition system exist in display system. DSO was used to monitor the cylinder pressure versus crank angle and to observe any engine instability. Data acquisition system was used for acquiring the outputs of transducer fitted to the engine. These outputs were used for the analysis of the engine parameters such as mass fraction burned, imep, and indicated power and so on. The specification of Pressure transducer and shaft encoder used in this study were given in Appendix 2 and Appendix 4.

### 3.2.5 Readout or recording device

Early researchers utilized oscilloscopes and oscillographs as readout and recording devices. However, due to the availability of economical high-speed microcomputers, these methods are virtually absolute. A variety of manufacturers produce data acquisition boards that interface with personal computers, allowing the researcher to monitor a number of analog signals at millions of samples per second. Various computer software packages can then be used to compile and analyze the stored experimental data. The analogue to digital converter (ADC) resolution determines the minimum amount of pressure change that can be recorded. The actual minimum value of pressure is given by:

$$\Delta p = \frac{\Delta P}{2^k} \quad (3.2)$$

Where  $\Delta P$  is the total pressure range (typically 100 bar) and  $k$  is the bit resolution of the ADC. Minimum resolutions for typical pressure ranges are given in Table 3.3.

Table 3.3: Minimum pressure measurement of ADCs in Pascals

Resolution (bits)	50 bar range	100 bar range
8	195.32 Pa	390.63 Pa
10	48.43 Pa	97.66 Pa
12	12.21 Pa	24.41 Pa
14	3.05 Pa	6.10 Pa
16	0.77 Pa	1.53 Pa

All measurement parameters were logged on personal computers. Three personal computers and two different data acquisition system were used in this thesis. Analog voltages representing temperatures, airflow and engine torque were conducted through a data logger. A proper software was used to store the acquired data and for their analysis. A multi-port serial card, see in figure 3.5, was used with its software for continuous measurements of fuel and water consumption rates, rpm (revolution per minute) and different gas composition in the exhaust. This software included the correction for exhaust emission readings. A high-speed data acquisition

system was used to display and store the cylinder pressures, crankshaft positions and spark event data. Different homemade programs were used for the analysis of the acquired data.



Figure 3.5: Multi-port Serial Adaptor

Data acquisition system was used for high-speed data acquisition that can be seen in Figure 3.6.



Figure 3.6: The Prosig Model P-5600 Data Acquisition System

Basically the P5600 will measure an input voltage on the of  $\pm 10V$  to  $\pm 10mV$  depending on the gain. This data acquisition system is connected to a computer that is used to acquire and compile the engine data. The various transducers are then connected to this data acquisition system, allowing the transducers to interface and communicate with the computer. This system is capable of monitoring 8 differential analog input channels with 16-bit resolution. It is also capable of sampling at rates up



to 100,000 samples per second for multi-channel scanning. This data acquisition system is used for the transducers used in-cylinder measurements. In excess of 100000 samples/second/channel simultaneously which corresponds to a maximum speed of:

1500 rev/min at 0.1-degree resolution

4000 rev/min at 0.25-degree resolution

6000 rev/min at 0.36-degree resolution

8000 rev/min at 0.5-degree resolution

Data acquisition system can be stored about different engine revolutions at different degree resolution.

Second data acquisition system was the Hilton D 102 Data Logger System that can be seen in figure 3.7.



Figure 3.7: The Data Logger.

The Hilton Data Logger (D102) is an industrially proven 35 channel interface with 15 thermocouple/differential voltage inputs ( $\pm 80\text{mV dc}$ ), 8 single ended dc voltage inputs ( $\pm 8\text{V}$ ), 8 logic or frequency inputs, 3 AC current inputs one mains voltage input and 8 current sinking output channels. In addition there are on board 12V DC,  $\pm 5\text{V DC}$  and  $\pm 15\text{V DC}$  power supplies for most commercially available transducers. Hilton Data logger (D102) is connected using the cable supplied to a standard RS232 port on the computer. Temperature measuring points were more than temperature measurements channel of Data Logger. Therefore, some voltage channels were used

for temperature measurements by the help of 5B40 plug-in signal conditioners. The specifications of the Readout or recording device used in this study were given in Appendix 5.

### 3.2.6 Dynamometer

Dynamometers are used to measure torque and power over the engine operating ranges of speed and load. They do this by using various methods to absorb the energy output of the engine, all of which eventually ends up as in the form of heat. Some of dynamometers absorb energy in a mechanical friction brake (prony brake). These are the simplest dynamometers but are not as flexible and accurate as others at higher energy levels. Fluid or hydraulic dynamometers absorb engine energy in water or oil which are pumped through orifices or dissipated with viscous losses in a rotor-stator combination. Large amounts of energy can be absorbed in this manner, making this an attractive type of dynamometer for the largest engines. Eddy current dynamometers use a disk, driven by the engine being tested, rotating in a magnetic field of controlled strength. One of the best types of dynamometer is the electric dynamometer, which absorbs energy with electrical output from a connected generator (Pulkrabek, 1997).

The test engine was loaded with the help of dynamometer shown in figure 3.8. This dynamometer uses a turbulent action water brake retarder to convert the rotating torque of the test engine to a stationary torque that can be measured.

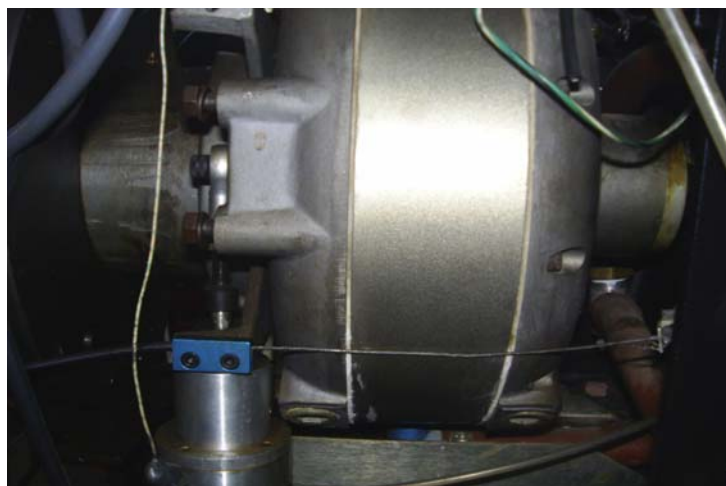


Figure 3.8: Water Brake Dynamometer

The maximum allowable speed of the dynamometer is defined as 7400 rpm, however, in the experiments; only 4500 rpm was used as maximum speed. The dynamometer utilized load onto the engine by pressurized water around the rotor of the shaft that was connected to the engine's flywheel. The opposing torque occurred as soon as the rotational speed of the shaft reaches to 400 rpm. Setting the position of the stator like assembly closer to the blades increased the load. A pressure transducer was mounted to the load cells to measure tension loads in axial direction. The output of this pressure transducer was measured and stored by the data logger. Loads should be introduced as close as possible to in the direction of measurement. Torsional and bending moments cause measurement errors and are likely to damage the load cell. The specifications of the dynamometer used in this study were given in Appendix 6.

### 3.2.7 Air Flow Measurements

The air flow was measured with the help of airflow meter as shown in Figure 3.9. The air stream that was drawn into the engine passes through a pulse-damping drum and then exits through a flexible hose before arriving to the intake manifold. Moreover, the filter cap filled with oil filters the air that will go into the intake manifold. The flow rate was measured by means of the pressure difference across the nozzle. A pressure transducer was used for the measurement of this pressure difference. The output of this pressure transducer was sent to data logger using voltage channel.



Figure 3.9: Airflow Meter

The equations of the charts used in calculations were found by best-polynomial curve fitting to the original charts. The polynomials that were fitted to the data are also supplied on the charts. The detailed formulation for the airflow rate and the corrections for temperature (measured with a thermometer in °C) and pressure (measured with a barometer in mm-Hg) were given in chapter 4. The specifications of the air-flow meter were given in Appendix 7.

### **3.2.8 Exhaust Emission Reading Apparatus**

The spark-ignition engine exhaust emission measurement is carried out using exhaust gas analyzer. Different sensors have been used for reading the exhaust gas compositions in the set up. Exhaust gas analyzer using Non-dispersive Infrared Detection (NDIR) for determining emissions of Hydrocarbon (HC). The analyzer provided an O<sub>2</sub>, CO and NO measurements realized by the charging of electro-chemical cells. Measured exhaust parameters were the exhaust pressure, soot, O<sub>2</sub>, CO, NO and HC. Heat losses, Combustion efficiency, excess Air, carbon dioxide and CO, NO value corrected to 0% Oxygen are important parameters for the measurement at the end of a combustion process. Calculations are based on the formulas according to the ASME standard method. The specifications of the exhaust emission reading apparatus used in this study were given in Appendix 8.

### **3.2.9 Temperature Measurements**

There are a number of devices available that can accurately measure such temperatures, the most common of which is thermocouple. The thermocouple is the most versatile of the temperature measuring devices. It is observed that when two wires made of dissimilar metals are joined at both ends and one end is heated, there is a continuous current that flows in the thermoelectric circuit. To take the data as electrical output to a PC, thermocouples of applicable type were used in this study. The relationship between thermocouple voltage output and junction temperature is nonlinear, but it can be accurately modeled by a higher order polynomial function. This somewhat complicates the use of thermocouples as temperature monitoring devices, but these polynomial equations are readily available for the thermocouples and are easily programmed into personal computers for data acquisition applications.

Depending on the type of metals used, thermocouples are available that can measure temperatures up to 1815 °C with an error of less than 2 °C (Temperature Handbook, 1995). Often, it is necessary to monitor certain operating temperatures of an engine.

The engine temperatures at various points were measured using a data logger. Temperature measuring points by using thermocouples types were presented in Table 3.4. Two types of thermocouples were utilized in the instrumentation of the test engine.

Table 3.4: Types of Thermocouples and Their Point of Use

S.No	Designation	Type	Point of use
1	T1	Cu-Cons <sup>a</sup>	Inlet water to engine
2	T2	Cu-Cons	Outlet water from engine
3	T3	Cu-Cons	Cylinder block (left side)
4	T4	Cu-Cons	Cylinder block(left side)
5	T5	Cu-Cons	Cylinder block (left side)
6	T6	Cu-Cons	Cylinder block (left side)
7	T7	Cu-Cons	Cylinder block (right port)
8	T8	Cu-Cons	Cylinder block (right side)
9	T9	Cu-Cons	Cylinder block (right side)
10	T10	Cu-Cons	Cylinder block (right side)
11	T11	Cu-Cons	Inlet air
12	T12	Cr-Al <sup>b</sup>	Exhaust gases

a Cu±Cons: Copper±Constantan (type T).

b Cr±Al: Cromel±Alumel (type K).

These thermocouples were type K and type T, which means that they were capable of measuring temperatures from –200 °C to 1250 °C and –60 °C to 200 °C, respectively with a maximum error of 0.75% of the measured temperature value (Temperature Handbook, 1995). These two types of thermocouples were chosen because the temperatures to be measured were predicted to fall into this range. The polynomials of the thermocouples used in this thesis that were fitted to the data are also supplied by Beckman thermometer. The signals produced from thermocouples sent to input

ports of the data logger. In manifold temperature measurements and water temperature measurements, T type thermocouples have been used. The specifications of the thermocouples were tabulated in Appendix 10.

### 3.2.10 Fuel and Water Flow Measurements

Two electronic scales with 0.1 g resolution were used for the measurement of water and fuel mass flow rate. The measurements were displayed and stored by computer. For fuel measuring a weight measuring electronic signal output system was used. The entire fuel flow system can be seen in Figure 3.10.



Figure 3.10: The Fuel Flow Measuring System

In order to calculate the indicated specific fuel consumption, it is necessary to determine accurately the mass of fuel that is consumed by the engine per unit time under the given operating conditions. To accomplish this, the engine fuel was supplied with fuel from a small tank. The tank rests on a digital scale that was calibrated in grams. This allows the mass of fuel used by the engine over a given length of time to be measured, so the mass fuel consumption per unit time can be calculated. One of the most important features of the fuel monitoring system is the

fuel line support stand. This stand is a tripod structure that straddles the scale supporting the fuel line so that it does not rest on the beaker, which would cause an error in the fuel mass measurements. This digital scale was mounted to the computer by using RS-232 port. Home-made software was used for reading and saving the outputs of the digital scale.

Water flow rate measuring system was similar with the fuel measuring system. The specifications of the electronic balances used in this study were given in Appendix 9.

### **3.2.11 Ignition timing**

The ignition timing was monitored and measured as a function of crank angle by capacitive coupling pickups with the high voltage pulse associated with the spark event. The ignition system was provided with a magnetic trigger pick up mounted adjacent to a special grinded flywheel that enables the ignition timing to be varied and measured over (-70) to (20) crank angle before top dead center. In addition, the ignition timing was monitored and measured by display systems in the test set-up. The specifications of the sensor were given in Appendix 10.

### **3.2.12 Measurement of engine speed**

Engine speed, rpm, can be measured by an inductive pick-up clamp on ignition secondary cables, by capacitive pick-up on a primary wire or an injector wire, or via a direct connection to a square wave from the engine management system. This way one can be able to measure rpm with 1 rpm resolution on conventional, wasted spark and direct ignition systems. In this thesis, engine speeds were measured by this method and displayed on computer screen by using a multi-port RS 232 reader. Homemade software was used for the measurement from the RS 232 port as mentioned in part 3.3. The specifications of the rpm sensor used in this study were given in Appendix 10.

### 3.2.13 Acceleration of the Engine

Figure 3.11 showed the schematic view of the acceleration system of the engine. Throttle valve was adjusted for each speed with a linkage, actuated by a stepper motor. This stepper motor was driven with the computer through its parallel port and via software. Test engine could be also accelerated by hand with a small increment by means of this mechanism.

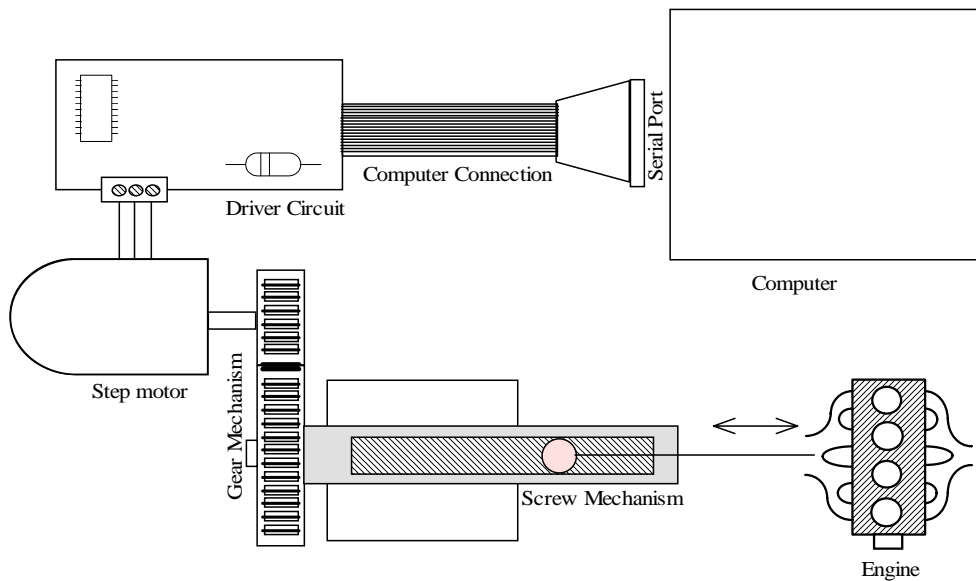


Figure 3.11: Schematic View of the Acceleration System of the Engine

### 3.2.14 Adjustment of Water Injection

Water is introduced into engine by different ways. Figure 3.12 shows the water addition to intake manifold method used in this thesis. Two different nozzles were used in the thesis. Firstly, water could be injected into suction port using a gasoline injector. The amount of water injection was controlled by varying water supply pressure and/or by an adjustable valve controlled via a step motor by using computer parallel port. Secondly, water was also introduced into the intake manifold upstream of the intake valve using a capillary tube with a 0.35 mm of bore diameter. Control over water flow rate to the engine was obtained by varying water supply pressure and/or by needle valve adjustments. Water addition rate was controllable



either automatically by the parallel port of computer, via the help of a proper software or manually.

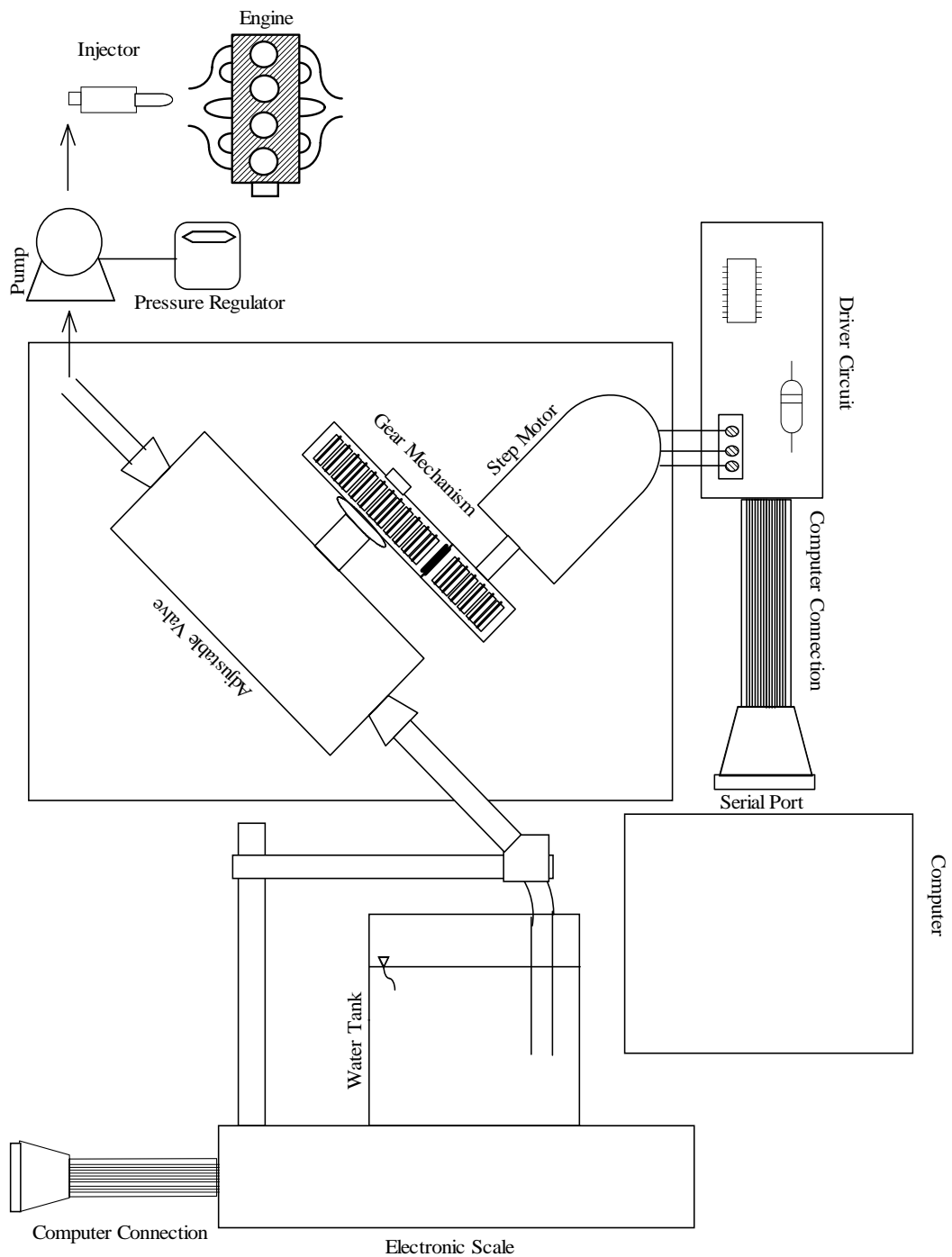


Figure 3.12: Water Injection System

Figure 3.13 shows the steam injection system into intake manifold. Both of the nozzles used for the liquid water injection could be used for the steam injection.

The amount of steam could be controlled with the method given above for liquid water injection.

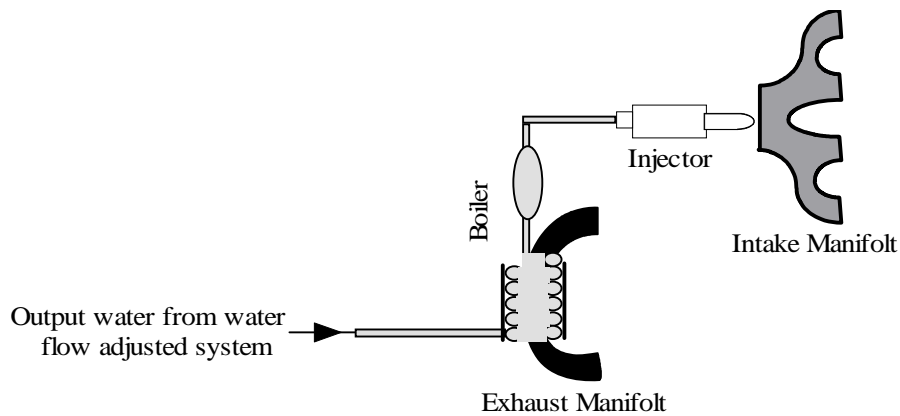


Figure 3.13: Steam Injection to Intake Manifold

### 3.3. Software

The numerous transducers were used in the test engine. In order to collect and compile this information, a number of software packages were utilized. Two homemade softwares were used for the analysis of collected data. An RS 232 reader program for the display of output of transducers such as engine speed, water and fuel flow rate and exhaust emissions were prepared. Last, two homemade software were used for the control of the step motor mounted on water injection and acceleration systems. In addition, programs of data logger and high-speed data acquisition system were used to collect the outputs of the transducer. Detailed features and flow charts of software were given in Appendix 11.

#### 3.3.1 Data Collection Software

The complete D102 Data Logger System consists of the Computer Interface Data Acquisition and Control Software. This software allows transducers to be easily and quickly configured to return data in the engineering units selected by the operator and for these configurations to be simply stored using a standard Windows format. Data files are easily exported to Excel or another spreadsheet format. This Data logger (D102) has re-configurable Windows compatible software shown in

Figure 3.14. DATS software of the high-speed data acquisition system was used to acquiring cylinder pressure and spark events vs crank angle data.

Channel	Label	Value	Unit	Channel	Label	Value	Unit
1	RT-INLET	0.221E+02	°C	23	WETBULB	0.210E+02	C
2	RT-OUTLET	0.221E+02	°C				
3	IMT-AW-I	0.226E+02	°C				
4	IMT-BW-I	0.221E+02	°C				
5	ET-C1R	0.225E+02	°C				
6	ET-C2R	0.221E+02	°C				
7	ET-C3R	0.221E+02	°C				
8	ET-C4R	0.221E+02	°C				
9	ET-C1L	0.221E+02	°C				
10	ET-C2L	0.225E+02	°C				
11	ET-C3L	0.221E+02	°C				
12	ET-C4L	0.221E+02	°C				
13	OILTEMP.1	0.219E+02	°C				
14	OILTEMP.2	0.216E+02	°C				
17	TORQUE	0.300E+00	FT-IN				
18	Airflow rate	-.120E-01	inc.wat.				
19	In. Vacuum	0.216E+00	kPa				
20	WATER-TEMP.	0.210E+02	C				
21	AIRTANK-TEMP	0.215E+02	C				
22	AMBIENT-TEMP	0.210E+02	C				

Figure 3.14: Measured Parameters by Hilton Data Logger

The output of the Exhaust gas analyzer, electronic scales and engine speed were collected by home-made software. This software was used to display and collect data from the RS-232 port in Visual basic. This program could be seen in Figure 3.15.

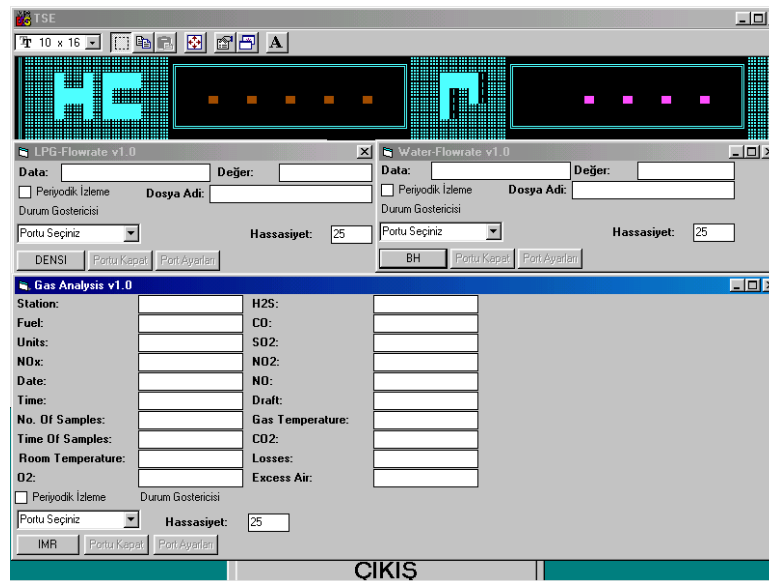


Figure 3.15: RS-232 Port Reader Program

For the control of the step motors mounted on water injection and acceleration systems, two-control program with same codes were prepared. These programs run the step motor in clockwise or in reverse direction with a small increment.

### **3.3.2 Data Analysis Software**

The codes (Chambers, 1998) were modified and an analysis program was re-written. This program was used to generate cylinder pressure vs volume, graphically. In addition, it was computed the parameters such as mean effective pressure, indicated power etc. using Microsoft Excel and Matlab.

The in-cylinder data for this test engine application was created to allow digital triggering of the data acquisition. Digital triggering was necessary to allow the optical shaft encoder reference signal to trigger the start of data acquisition, thus beginning data acquisition at top dead center. In addition, the data acquisition system employs an external counter clock. This feature allows the signal from the encoder to be used to trigger the acquisition of each data point. Therefore, the exact piston position at the time of data acquisition is known. Data acquisition system also allows the acquired data to be saved to a user specified file in a comma-delimited format, allowing the data to be transferred to a spreadsheet program for analysis.

The number of scans to acquire determines the amount of data to be collected before data acquisition is terminated. The software which is developed to analyze recorded cylinder pressure data is programmed in Matlab and provides processing and analysis functions that are required for combustion analysis. After data has been secured from the engine transducers by the software of data acquisition system, it is transferred to an Excel spreadsheet. The data analysis was made to perform these tasks in Excel and Matlab for the ease of data manipulation that they provide. Once the data is transferred, a set of custom macros that were created using Excel's macro recording feature is applied to the data files. The macro is used to compile the engine pressure, intake pressure and position data. It first applies a five point moving average to the data set. This reduces the amount of noise that is found in the data signal. Next, the macro repositions the information into the first 8000 rows of the spreadsheet. This is necessary to allow the next step of the macro, which is saving

the file to the Matlab directory in a “filename.wk1” format. This format allows the file to be opened by Matlab. Once the engine data has been processed through the spreadsheet macros, the Matlab program Analysis.m is executed. This program first asks the user to input the fuel consumption of the engine in grams per minute under the current operating conditions. This information is obtained by using the digital scale to monitor fuel flow during testing. Next, the program opens the data file and arranges the data points into the proper arrays. Then, the program uses the other data recorded to determine the intake manifold air pressure. The next stage of the program is concerned with the beginning the analysis at top dead center (TDC) on the intake stroke. To determine this point, the program looks at the pressure data for the first two TDC points. It then picks the one with the lowest pressure and marks it as TDC1. The remaining TDC points are then located and labeled by adding 1000 to the previous TDC value. This technique works because the encoder pulses that trigger the acquisition of each data point have a resolution of 1000 pulses per revolution. Once the TDC values have been labeled, the program proceeds to convert the pressure data into units of pressure and shift these pressure curves so that the pressure at the completion of the intake stroke is equal to the average manifold air pressure (Randolph, 1990). To accomplish this, first five data points are at the end of the intake stroke by adding 496...500 to the respective intake TDC values. The output of the pressure transducer for these data points is then averaged to obtain a “zeroing” value. That is a value that when subtracted from the entire pressure curve will shift that curve so that the end of the intake stroke lies on the x-axis. Using the average of five data points for this “zeroing” value protects the true pressure trace from being corrupted by noise in the signal. Once the pressure trace is “zeroed,” then the intake manifold air pressure can be added to the curve. The next stage of the program creates an array of crank angles from 0 to  $4\pi$  radians in increments of  $2\pi/1000$  for each engine cycle. Each crank angle value then corresponds to a pressure data point since the pressure data acquisition was triggered by the optical encoder every  $2\pi/1000$  radians. Once the crank angle arrays have been created, then if the physical parameters of the engine are known, they can be transformed into cylinder volume arrays. (Heywood, 1988; Stone, 1999) have all published formulae for obtaining cylinder volume from crank angle for a slider-crank mechanism.

$$V = V_c + \frac{\pi B^2}{4} \left( 1 + r - r \cos \theta - \sqrt{l^2 - r^2 \sin^2 \theta} \right) \quad (3.3)$$

where

$$V_c = \frac{\pi B^2}{4} \frac{2r}{CR} \quad (3.4)$$

The pressure and volume arrays for each cycle are then divided into separate arrays for the intake, compression, expansion, and exhaust strokes. From Equation 3.5, it is known that the integral, or area under the pressure versus volume curve, can be used to determine the indicated horsepower.

$$W_i = \int P dV \quad (3.5)$$

This area is calculated by using the TRAPZ function in Matlab. This function utilizes trapezoidal numerical integration to determine the area under each curve. Gross indicated power is defined as work delivered to the piston over the compression and expansion strokes only. The program then calculates the gross indicated work for the cylinder by subtracting the area under the compression stroke from the area under the expansion stroke. This results in the total area enclosed by the power loop, which is equal to the gross indicated power. The program also calculates the net indicated power, which is the area enclosed by the pumping loop subtracted from the gross indicated power. Since this work is primarily concerned with gross engine parameters, the program does not currently utilize this quantity; however, its availability allows the program to be easily modified to analyze net engine parameters. With the gross indicated work for each cycle calculated, the program then calculates the gross indicated power for each cycle by using Equation 3.6.

$$IP = \dot{W}_i = k \left( \int_{comp. - expn.} P dV \right) \frac{N [rev/sec]}{2 [rev/cycle]} \quad (3.6)$$

Mean effective pressure was calculated from the cylinder pressure values by this program. The program could also calculate the indicated fuel consumption for each cycle. This program then displayed the calculated values to the user, and through a

graphical user interface and allowed the user to request a pressure versus volume plot, such as the one shown in Figure 3.16, for any of the cycles.

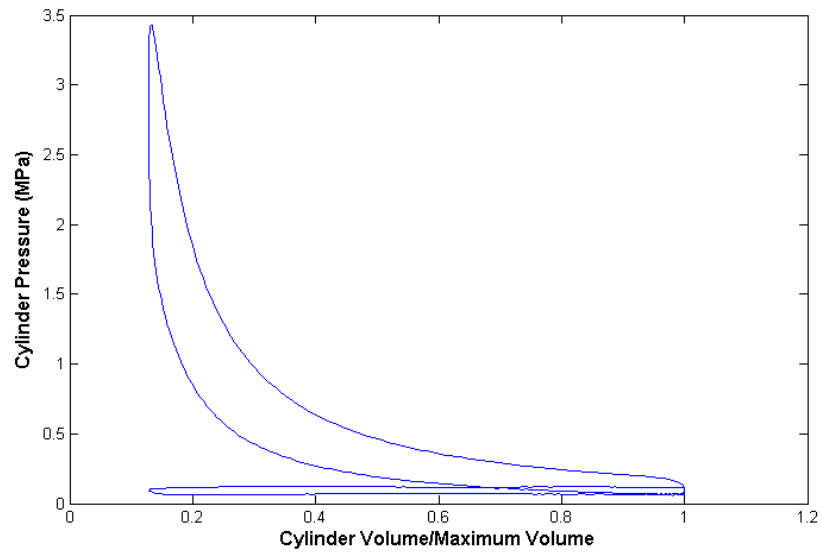


Figure 3.16: A Pressure versus Volume Plot Produced by Analysis.m.

In this thesis, engine in-cylinder pressure data were analyzed for mass burned fractions with respect to crank angle (CA). The heat release analysis of a carefully measured cylinder pressure time-history has long been used as a diagnostic of the combustion process for determining the mass fraction of the charge burned in spark-ignition (SI) engines. The method proposed by (Rassweiler and Withrow, 1938) to obtain combustion information from cylinder pressure data has still recently been used for calculating the mass fraction burned in SI engines. They developed a model that predicts the mass fraction of burnt fuel as a function of cylinder pressure. It is based on the assumption that the difference between the measured cylinder pressure and the pressure predicted from polytropic compression or expansion scales with the mass burned. The difference is the work output, which leads to the mass fraction burnt. This method, however, assumes complete combustion and can therefore only be considered as a relative mass fraction burned.

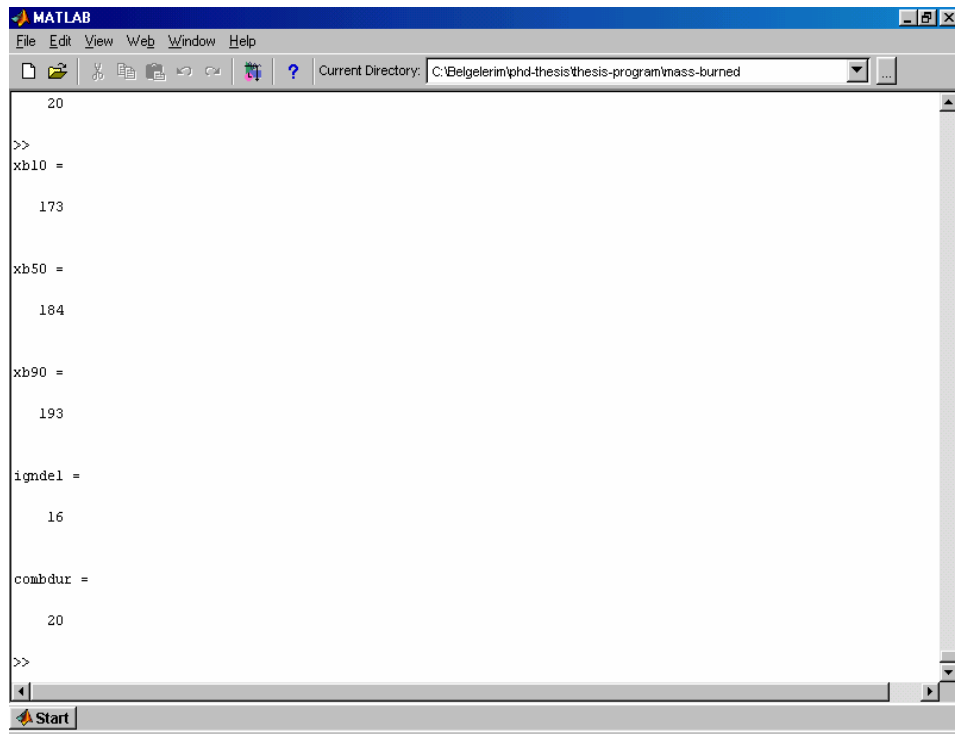
The curve of mass-burned fraction with respect to CA allowed for identification of ignition delay, the fully developed combustion period and the combustion tail. Further, it gave information about how much fuel was unburned at

any point in the combustion cycle. Pressure data were collected for all speed and load combinations. The engine was run at the specified speeds and loads for a minimum of 6 min and data were collected during the last 2 min of operation. Engine cycle data were collected over 40 cycles at each point and averaged for analysis by an excel macro. The start of combustion is required for burn rates and heat release analysis. For a spark ignition engine this is the ignition timing. The start of combustion is determined from a recorded channel, either low or high-tension coil current for spark ignition engines. The estimated end of combustion is required for determining the normalizing value for mass fraction burned and for heat release analysis. For the purpose of cycle-to-cycle analysis, the crank angle at which burn rate percentages of 1%, 2%, 5%, 10%, 50%, 90%, 95% and 99% by mass are determined. Additionally, the ignition delay and combustion duration are determined from mass fraction burned curves. The ignition delay is the crank angle between start of combustion and typically 1,5 or 10% mfb. Combustion duration is calculated as the crank angle between the end of the ignition delay and typically 90, 95 or 99% mfb. Determining small or large percentages such as 1 or 99% can be difficult due to the susceptibility of the calculation to the effects of noise with small pressure changes.

A single-zone heat release analysis procedure was used in the thesis. A refined heat release model has been proposed and applied to the in-cylinder pressure data reduction for investigation of SI engine combustion parameters. A complete engine cycle analysis was conducted to analyze in-cylinder pressure data to estimate the rate of heat release and mass-burned fraction with respect to the crank angle. Ignition delay and burning period were determined from mass burned fraction data. The mass burned fraction was obtained by integrating the rate of heat release. A homemade analysis code in Matlab was used to calculate the mass fraction burned. This software reads the pressure data file and calculates things like heat release rate etc. Pressure data file is actually angle-averaged value of consecutive about 50 cycles. Mass fraction burned can be found from angle-averaged rate of heat release by simply accumulating and normalizing it. Output of this software are the plots of heat release, log p-log V and values of mass fraction burned. Figures 3-17 to 3.21 shows the outputs of this software. The methodology using analysis is described (Heywood, 1988).



Different percent mass fraction burned can be selected for determining the ignition delay and combustion period in program. Figure 3.17 shows the output of the program named mass-burned.m at computer screen. This example output shows the ignition delay (0 to 10% burn) and combustion intervals (10 to 90% mfb) were selected.



```
MATLAB
File Edit View Web Window Help
Current Directory: C:\Belgeler\imphd-thesis\thesis-program\mass-burned

20
>>
x_b10 =

    173

x_b50 =

    184

x_b90 =

    193

igmdel =

    16

combdur =

    20

>>
```

Figure 3.17: Output of the Home-made Software for the Combustion Analysis

Figure 3.18 shows the cylinder pressure versus crank angle data. Mass fraction burned curve was determined from measured cylinder data. As stated above, this cylinder pressure versus crank angle data were obtained by using another home-made software. This software reads the cylinder pressure versus crank angle data in a file generated by data acquisition system.

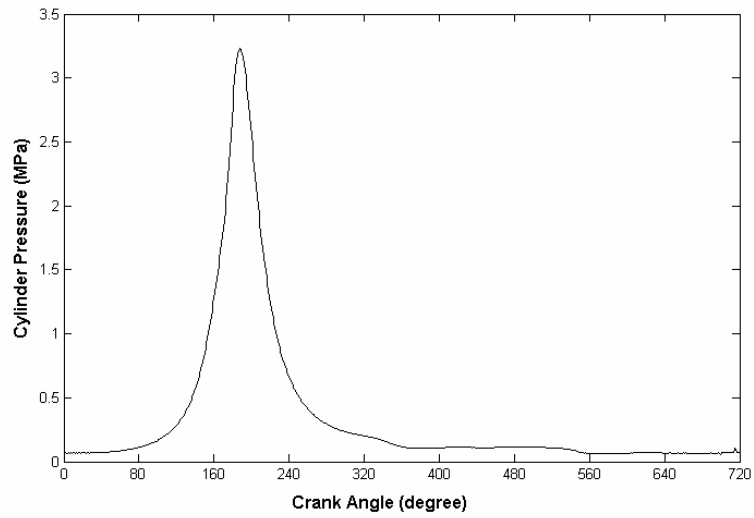


Figure 3.18: Input Data of the Home-made Software Named as Mass-burned for the Combustion Analysis

Figure 3.19 shows the results from the analysis such as the estimated rate of heat release by burning fuel, cumulative heat loss and work production throughout one thermodynamic cycle.

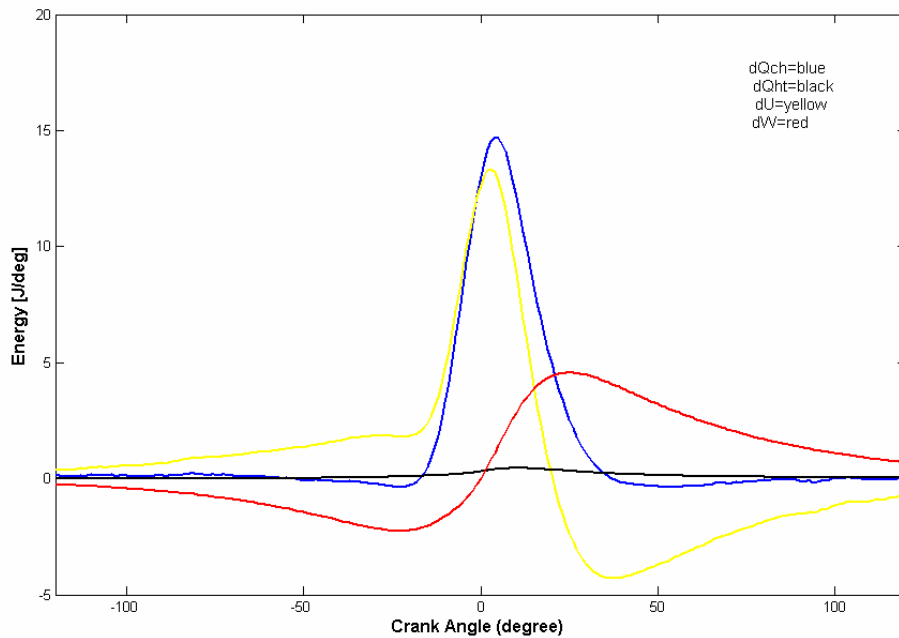


Figure 3.19: Output of the Home-made Software Named as Mass-burned

Figure 3.20 shows a typical mass fraction burned curve determined from the measured cylinder data using homemade software named as mass-burned.m. The curves were actually angle-averaged value of consecutive about 50 cycles. With accurate pressure versus crank angle records, values of final mass fraction burned should be close to but lower than unity, usually in the range 0.93 to 0.98: the difference from unity is the combustion inefficiency for lean mixtures and incomplete oxygen utilization for rich mixtures.

Figure 3.21 shows the Log P-log V plot. Log P-log V plots can be used to check the quality of cylinder pressure data. In addition, these plots approximately define the start and end of combustion, but do not provide a mass fraction burned profile. The 10, 50, and 90% mfb were also marked on the log P-log V curves. On the log P-log V diagram the compression process is a nearly straight line. The start of combustion can be identified by the departure of the curve from the straight line. The end of combustion can be located approximately in similar fashion; the expansion stroke following combustion is essentially linear.

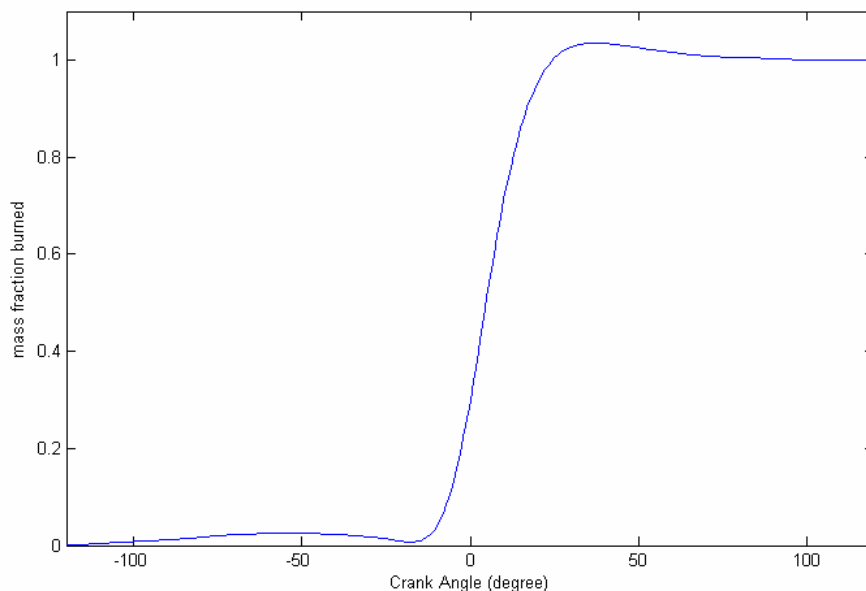


Figure 3.20: Mass Fraction Burned Curve Determined from Measured Cylinder Data

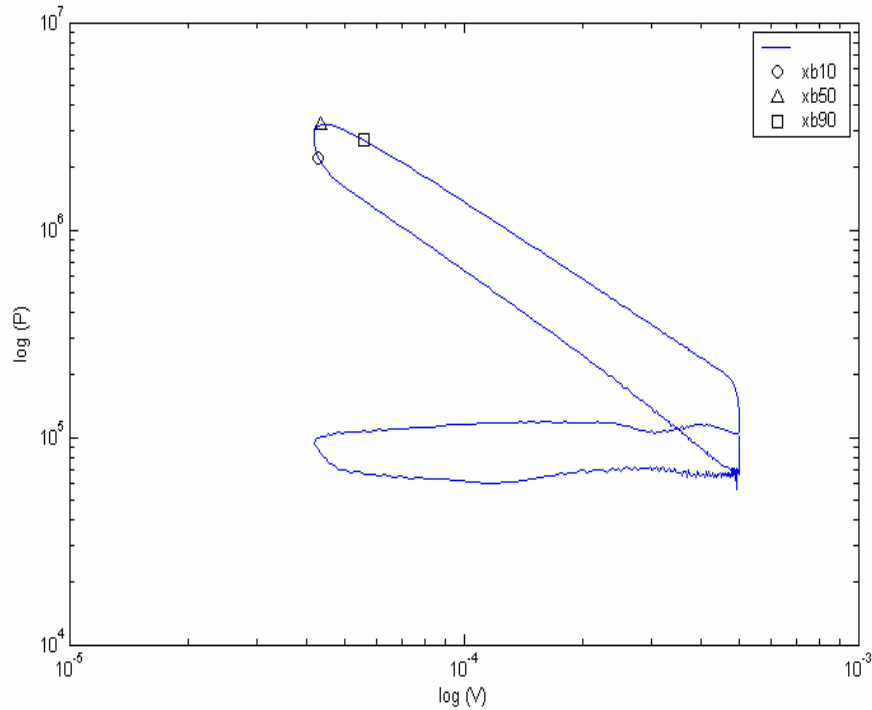


Figure 3.21: Log P-log V Plot

### 3.4 CALIBRATIONS OF THE MEASUREMENT SYSTEMS

In the case of high precision measurements, it was recommended to calibrate the devices periodically. Overall calibration checks were made a minimum of two times during each 12-hour running period. In addition, instruments zero calibration checks must be made before and after each successful measurement. Where the sensitivity of the transducer is not accurately known, an overall system calibration can be achieved by applying known pressures to the transducer using a suitable dead weight tester. The pressure transducers were calibrated or tested by means of a dead-weight tester. The pressures that were read by data logger must be exactly same with the pressures produced by the weights loaded in the dead weight tester. This was checked before the experiments.

An internal calibration system was used for the calibration of the charge amplifier. This calibration system was provided by the injection of an internally generated voltage into the input capacitance of the charge amplifier thus allowing calibration to be obtained in terms of output voltage per unit charge where the charge

was calculated from the product of the injected voltage and the charge amplifier output capacitance. For the calibration of the thermocouples probe; temperature of the air stream was measured with calibrated mercury thermometer and a digital thermometer. These measured values were compared with the value measured by the Data Logger.

To check the calibration of the load cell in the dynamometer, a basket of appropriate weight was used for the torque range to be tested. One may added the effective weight stamped on the calibration arm to twice the combined weight of the basket and weights. For example, if the effective weight of the arm was 4.4 lbs, and the weight of the basket was 12 lbs, then with additional weight of 25 lbs the formula would be  $4.4+2(12+25)=$ a pressure transducer reading of 73.4 lbs. For the best results, average of two reading must be taken with the same weight. The first, or ascending, reading should be taken after lifting up the arm and releasing it slowly. The second, or descending, reading should be taken after pressing down to arm and releasing it slowly. In addition, the output signals of the dynamometer were calibrated by plotting the analogue voltage output measured by the data logger. To check the calibration of the scales, the standard weights are used.

Exhaust gas analyzer has self-calibration option. The gas-sampling probe of the exhaust gas analyzer has to be in ambient air during the zero calibration. The calibration is taken about 3-minute for zero calibration and 30-second for re-calibration. All toxic sensors are adjustable. The calibration of the exhaust gas analyzer was recommended checking the calibration once a year by manufacturer firm. Calibration gas is needed for each toxic sensor. If it is known what the measurement concentration will be, then the concentration of the calibration gas can be changed to meet the requirements of the expected measurement range. All the toxic calibration gases are needed to adjust the analyzer to the known concentration of the calibration gas. The Oxygen gas is also needed to check the O<sub>2</sub> sensor and its performance.

## CHAPTER 4

### EVALUATION OF DATA AND EXPERIMENTAL PROCEDURE

#### 4.1 INTRODUCTION

In this chapter, some basic geometrical relationships and the parameters commonly used in calculations in this thesis are given. These are the mechanical output parameters of work, torque, and power; the input requirements of air, fuel, and combustion; efficiencies; and emission measurements of engine exhaust. In addition, application of the exergy-balance equation to engine subsystems on a CA basis is also present in this chapter. The equations are available for calculating the terms of energy quantities: brake work, friction work, heat transfer to the coolant, energy lost to the exhaust, and unaccounted energy losses. The equations used to obtain the present results for determining the related second law quantities are also given. The experimental procedure used in the present investigation is presented at the end of this chapter.

#### 4.2 GEOMETRICAL PROPERTIES OF RECIPROCATING ENGINES

The following parameters define the basic geometry of a reciprocating engine as shown in Figure 4.1.

Compression ratio  $r_c$ :

$$r_c = \frac{\text{maximum cylinder volume}}{\text{minimum cylinder volume}} = \frac{V_d + V_c}{V_c} \quad (4.1)$$

Ratio of cylinder bore to piston stroke:

$$R_{bs} = \frac{B}{S} \quad (4.2)$$

The ratio of bore to stroke for small engines is usually from 0.8 to 1.2.

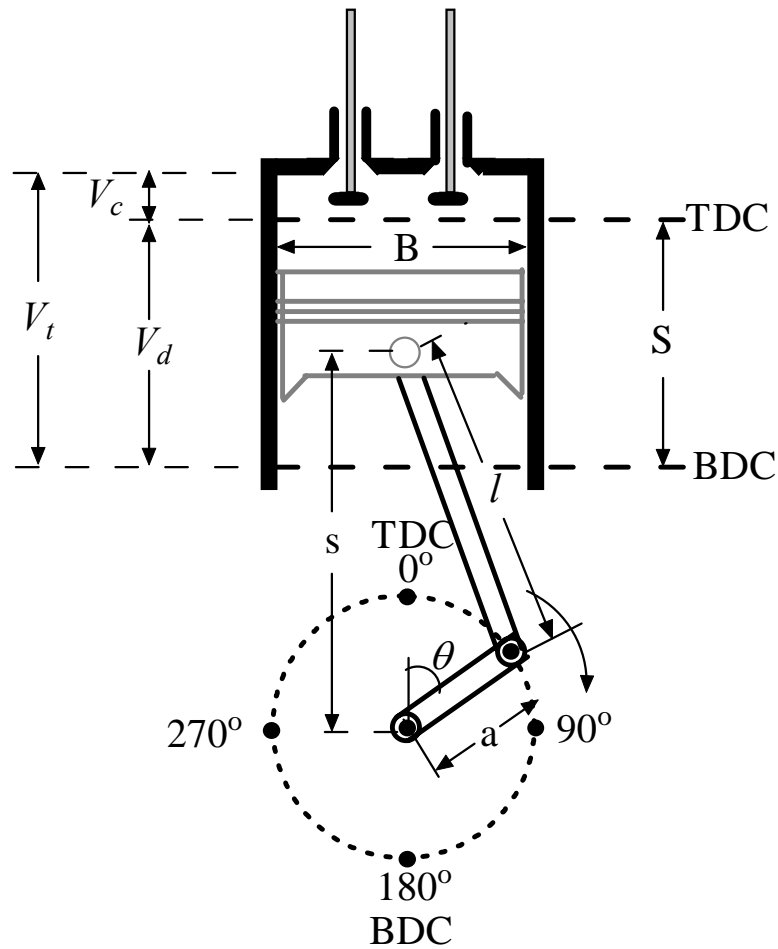


Figure 4.1 Basic Geometry of the Reciprocating Internal Combustion Engine

Ratio of connecting rod length to crank radius:

$$R = \frac{l}{a} \quad (4.3)$$

$R$  usually has values of 3 to 4 for small engines, increasing to 5 to 10 for the larger engines. In addition, the stroke depends upon the crank radius by the following:

$$L = 2a \quad (4.4)$$

The cylinder volume  $V$  at any crank angle position  $\theta$  is

$$V = V_c + \frac{\pi B^2}{4}(l + a - s) \quad (4.5)$$

where  $s$  is the distance between the crank axis and the piston pin axis and is given by

$$s = a \cos \theta + (l^2 - a^2 \sin^2 \theta)^{1/2} \quad (4.6)$$

Displacement, or displacement volume,  $V_d$ , is the volume displaced by the piston as it travels from BDC to TDC:

$$V_d = V_{\text{BDC}} - V_{\text{TDC}} \quad (4.7)$$

Displacement volume can be given for the entire engine.

$$V_d = N_c \left(\frac{\pi}{4}\right) B^2 S \quad (4.8)$$

where  $N_c$  is the number of engine cylinders.

### 4.3 BRAKE POWER

The mechanical brake power of the engine will be a product of the torque on the crankshaft and the rotational speed of the crankshaft. Torque,  $T$  is measured from the engine dynamometer itself. Brake power can be calculated using the following formula;

$$P_b = 2\pi NT \quad (4.9)$$

### 4.4 CORRECTED BRAKE POWER

Test results must always refer to a known datum so that comparisons between different engines or the effect of modifications. All of the measurements should ideally be corrected to standard atmospheric conditions. To find the corrected brake horsepower, the measured value is multiplied by a correction factor: The horsepower measured by the dynamometer is the true horsepower under the test conditions.



However the density of the air changes significantly with atmospheric temperature, pressure, and humidity and these changes affect the horsepower output of engines. It is often desirable to know what the horsepower of the engine would have been if the engine had been tested under other conditions. Equation 4.10 and Equation 4.11 are used for determining the factors for correcting the test horsepower to what the horsepower would have been for dry air at 15.5 °C and 760 mm of mercury barometric pressure (sea level pressure). This is known as Standard Temperature and Pressure (STP). The horsepower correction factor is the result of multiplication of the individual correction factors for temperature, pressure, and humidity times each other.

$$\text{Correction Factor} = \text{Temp. Correction} \times \text{Press. Correction} \times \text{Humidity Correction} \quad (4.10)$$

$$C_b = \left(\frac{99}{P_d}\right)^{1.2} \left(\frac{T}{298}\right)^{0.6} \quad (4.11)$$

Where  $T$  is the absolute temperature, in Kelvins, at the engine air inlet.  $P_d$  is the dry atmospheric pressure, in kilopascals, i.e. the total barometric pressure minus water vapor pressure. This formula applies to spark ignition engines.

#### 4.5 CORRECTED ENGINE TORQUE

Engine torque is the twisting or turning effort that the engine applies through the crankshaft. Engine torque can be found from the following relation:

$$T = \frac{P_{b\text{-corrected}}}{\omega} \quad (4.12)$$

where  $T$  is the Engine torque in N·m,  $P_{b\text{-corrected}}$  is the corrected engine brake power in Watts and  $\omega$  is the Engine angular speed in rad/sec.

#### 4.6 INDICATED POWER

The indicated power developed by one combustion cycle can be determined from the in-cylinder pressure volume plot.

$$W_i = \int PdV \quad (4.13)$$

where  $P$  is the pressure of the working fluid and  $V$  is the volume that is occupied by this fluid. Thus, it can be inferred that the work transferred from the working fluid to the piston for one engine cycle is equal to the area enclosed by the trace of pressure versus volume, supplied by the indicator (Heywood, 1988). This value is known as indicated work and can be used to quantify an engine's performance. This work is assumed to be the gross work. This definition of work represents only the work done during the compression and expansion strokes and ignores any pumping work. This choice was made due to the fact that the research at hand is primarily concerned with the performance of the engine during the compression and expansion strokes. In addition, it is possible to perform tests using a dynamometer to determine values for the brake and frictional works whose summation should approximate the gross indicated work, thereby allowing the validation of the techniques used to determine indicated work (Heywood, 1988). Knowing the work, it is possible to determine the indicated power for the given cylinder. The indicated power output,  $P_i$ , is the power output. It can be calculated from a  $P$ - $V$  indicator diagram. It is based on the gross cycle work done during the compression and expansion strokes.

$$P_i = \frac{W_i N}{2} \quad (4.14)$$

where  $N$  is the angular speed of the engine.

#### 4.7 ACTUAL AIR FLOW RATE

The air mass flow rate can be found by using the equation below. This equation is obtained from original calibration curves.

$$\dot{m}_a \text{ (kg/hr)} = 9.57 + 280.8x - 316.12x^2 + 249.8x^3 - 111.4x^4 + 25.7x^5 - 2.382x^6 \quad (4.15)$$

where  $x$  is the pressure drop across 44 mm nozzle in mm H<sub>2</sub>O. Measuring the pressure drop as voltage and the calibration of the device is:

$$x=0.992V-1.25 \quad (4.16)$$

where  $V$  is the output voltage of the transducer.

The air mass flow rate calculated by this equation is a theoretical value and it should be corrected for the temperature, pressure and humidity of the laboratory to obtain its actual value. The formulations used for corrections are stated in TS 1231 standards. The formulas for corrections, namely; pressure, temperature and humidity factors are as follows, respectively:

$$f_P = 0.0019 P_{amb.} - 0.4477 \quad (4.17)$$

where  $P_{amb.}$  is ambient pressure in mmHg.

$$f_T = 7 \cdot 10^{-6} T_{amb.}^2 - 0.003 T_{amb.} + 1.044 \quad (4.18)$$

where  $T_{amb}$  is ambient temperature in  $^{\circ}C$ .

$$f_H = \frac{0.73 - \omega}{0.73} \quad (4.19)$$

where

$$\omega = \frac{0.622 \phi 1.3 \cdot 10^{-3}}{P_{amb.} - \phi 0.013} \quad (4.20)$$

In Eqn (4.20),  $\phi$  is the relative humidity (%) and  $P_{amb.}$  is ambient pressure (kPa).

Finally, air mass flow rate can be calculated.

#### 4.8 BRAKE THERMAL EFFICIENCY

The thermal efficiency is the ratio of the power the engine delivers at the crankshaft to the power available in the fuel to the power the engine delivers at the crankshaft. Thermal efficiency ( $\eta_{th}$ ) is generally between 15% and 30%. The thermal efficiency of an engine varies with engine speed and throttle setting. An engine can achieve maximum thermal efficiency at only one operation point.

$$\eta_{th} = \frac{P_b}{\dot{m}_f Q_{in}} \quad (4.21)$$

#### 4.9 SPECIFIC FUEL CONSUMPTION (sfc)

In engine tests, the fuel consumption is measured as the mass flow of fuel per unit time. A more useful parameter is the specific fuel consumption. The specific fuel consumption is a measure of efficiency that indicates the amount of fuel an engine consumes for the unit work it produces.

$$\text{sfc} = \frac{\dot{m}_f}{P} \quad (4.22)$$

Specific fuel consumption is generally given in units of g/kW·hr or lbm/hP·hr. Low values specific fuel consumption are desirable. Brake power gives the brake specific fuel consumption:

$$\text{bsfc} = \frac{\dot{m}_f}{P_b} \quad (4.23)$$

The bsfc will change at different engine speeds and throttle settings. It decreases as engine speed increases, reaches a minimum, and then increases again at high speeds. Fuel consumption increases at high speed because of greater friction losses. At low speeds, the longer time per cycle allows more heat loss and fuel consumption goes up. Brake specific fuel consumption generally decreases with engine size, and take it lowest value for very large engines. For SI engines, a typical value of minimum brake specific fuel consumption is about 270 gm/kW·hr. Once the indicated power has been determined, it is possible to calculate the indicated specific fuel consumption given by

$$\text{isfc} = \frac{\dot{m}_f}{P_i} \quad (4.24)$$

where  $\dot{m}_f$  is the mass of fuel supplied to the engine per unit time and  $P_i$  is the indicated power produced by the engine. The determination of indicated power is

discussed above, and the fuel mass consumed per unit time can be determined by using a scale to measure the amount of time required to use a given mass of fuel under the current engine operating conditions.

#### 4.10 MEAN EFFECTIVE PRESSURE

The mean effective-pressure is the average pressure in the engine that can exert on the piston through one complete operating cycle. Mean effective pressure (mep) is defined by

$$\text{mep} = \frac{W}{V_d} \quad (4.25)$$

Mean effective pressure is a good parameter for comparing the engines with regard to design or output because it is independent of both engine size and speed. Various mean effective pressures can be defined by using different work terms in Eq. 4.23. If the brake work is used, brake mean effective pressure is obtained. The bmep is composed of the average pressure of the gas in the engine cylinder during, the power stroke, less the pressure used for pumping in the intake air charge, pushing out the exhaust charge, and to overcome engine internal friction. Although it is a measure of an engine's ability to do work, torque cannot be used to compare different engines, since it depends on engine size. A more useful relative engine performance measure is obtained by dividing the work per cycle by the cylinder volume displaced. The parameter obtained thus is called as brake mean effective pressure and is defined shortly as the average pressure that the gas exerts on the piston through one complete operation cycle. The brake mean effective pressure can be found from the following formula;

$$\text{bmep} = \frac{2P_b}{V_d N} \quad (4.26)$$

Typical Maximum value of bmep for naturally aspirated engines is in the range of 850 to 1050 kPa. For CI engines, typical maximum values are 700 to 900 kPa for naturally aspirated engines and 1000 to 1200 kPa for turbocharged engines (Heywood, 1988). The area enclosed by the p-v diagram of an engine is the indicated

work done by the gas on the piston. The imep is a measure of the indicated work output per unit swept volume, a parameter independent of the size and number of cylinders in the engine and engine speed. imep is defined as (Stone, 1999):

$$\text{imep} = \frac{W_i}{V_d} \quad (4.27)$$

and also

$$\text{imep} = \frac{2P_i}{V_d N} \quad (4.28)$$

Indicated mean effective pressure (imep) is calculated in real time using the formula. This formula is identified which is resilient to large crank angle resolution.

$$\text{imep} = \sum_{i=0}^{719} P_i \frac{dV}{V} \quad (4.29)$$

By calculating the values of  $\frac{dV}{V}$  before acquisition begins, this provides a computationally efficient method of determining net imep. The combustion analysis software calculates indicated mean effective pressure using the following equation:

$$\text{imep} = \frac{\Delta\theta}{V_d} \sum_{i=n_1}^{n_2} P(i) \frac{dV(i)}{d\theta} \quad (4.30)$$

It can be seen that quantifying the performance of an internal combustion engine relies on the ability to acquire data accurately for the pressure verses volume curve.

#### **4.11 ACTUAL AIR-FUEL RATIO AND AIR FUEL EQUIVALENCE RATIO**

Energy input to an engine  $Q_{in}$  comes from the combustion of a hydrocarbon fuel. Air is used to supply the oxygen needed for this chemical reaction. For combustion reaction to occur, the proper relative amounts of air (oxygen) and fuel must be present. Air-fuel ratio is a parameter that is used to describe the mixture

quality. The actual air-fuel ratio is calculated from values of air and fuel mass flow rates obtained from the airflow manometer reading and the amount of fuel consumed.

$$\left(\frac{A}{F}\right)_{\text{actual}} = \frac{\dot{m}_{\text{air}}}{\dot{m}_f} \quad (4.31)$$

and

$$\phi = (A/F)_{\text{stoich}} / (A/F)_{\text{actual}} \quad (4.32)$$

#### 4.12 VOLUMETRIC EFFICIENCY

In the intake systems the air filter, carburetor, and throttle plate, intake manifold, intake port, intake valve restricts the amount of air which an engine of given displacement can induct theoretically. Volumetric efficiency is the ratio between the amount of air-fuel mixture that actually enters the cylinder and the amount that could enter under ideal standard atmospheric conditions. Because the engine runs at high speed, the cylinder seldom fills to 100% of its capacity. The volumetric efficiency is generally between 60% and 80% for a normally aspirated engine. Supercharged engines may have a volumetric efficiency of up to 200%.

$$\eta_v = \frac{\dot{m}_{\text{air}}}{\dot{m}_{\text{th-air}}} \quad (4.33)$$

The amount of theoretical air that could enter into a cylinder can be found from;

$$\dot{m}_{\text{th-air}} = i \left( \frac{2n}{j} \right) \rho_{\text{std}} V_d \quad (4.34)$$

Volumetric efficiency is also defined as:

$$\eta_v = \frac{2\dot{m}_{\text{air}}}{\rho_{\text{air}} N V_d} \quad (4.35)$$

The volumetric efficiency of the engine depends on the engine speed. Controlling the volumetric efficiency with the throttling butterfly valve in the carburetor regulates engine power. Air density is given by the following equation.

$$\rho_{\text{air}} = 0.4643 \frac{P_a}{273 + T_a} \quad (4.36)$$

The theoretical air mass (kg) can be converted into a theoretical airflow rate (kg/s).

#### 4.13 ENERGY ANALYSIS

Energy analysis states that energy is conserved, where the fuel energy transforms its form from heat to work. The energy components may be classified as indicated power, exhaust energy and heat rejection from the engine to cooling water, lubricating oil and environment.

The calculation procedure of the energy analyses was given in this section. As a beginning, from the first law of thermodynamics or energy balance equation for a thermodynamic system as shown in Fig.4.2 schematically can be formulated as:

$$\dot{Q} - \dot{W} = \Delta \dot{E} \quad (4.37)$$

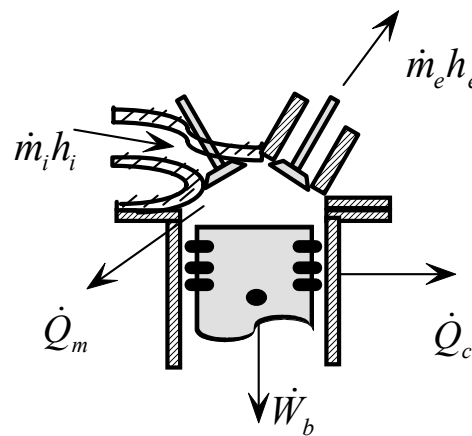


Figure 4.2: Typical Engine System

The total heat supplied by the fuel energy input for the left side of Eqn. (4.37) is given as in the following equation.

$$\dot{Q}_{in} = \dot{m}_f LHV \quad (4.38)$$



and

$$\dot{Q}_{out} = \dot{Q}_{cw} + \dot{Q}_{ex} + \dot{Q}_{un} \quad (4.39)$$

The oil heat transfer and the heat transfer from the walls of the engine by radiation and convection are the unaccounted losses which is given by

$$\dot{Q}_{un} = \dot{Q}_{convection} + \dot{Q}_{radiation} + \dot{Q}_{oil} \quad (4.40)$$

The unaccounted heat losses ( $Q_{un}$ ) is also given as

$$\dot{Q}_{un} = \dot{Q}_{in} - (\dot{Q}_{cw} - \dot{Q}_e - \dot{W}_b) \quad (4.41)$$

Exhaust enthalpy is calculated by

$$\dot{m}_e h_e = \dot{H}_s + \dot{E}_k + \dot{H}_{ic} + (\dot{Q}_{convection} + \dot{Q}_{radiation})_e \quad (4.42)$$

The losses except for sensible enthalpy are assumed negligible for exhaust flow. Hence the energy lost by the exhaust gases may be found by the following equations:

$$\dot{Q}_e = \dot{m}_e C_e (T_e - T_o) \quad (4.43)$$

It is impossible to directly measure the heat transfer by the exhaust gases as  $C_p$  is unknown for the exhaust gases and the mass flow rate is not directly measured. Exhaust gas calorimeter is used for measuring this term. The exhaust gas calorimeter is a heat exchanger where the exhaust gas is cooled by circulating cooling water. Energy lost by the exhaust gas is equal to energy gained by cooling water. Hence the multiplication of the mass flow rate of the exhaust gas by its  $C_p$  may be found. And finally the heat transferred by the exhaust gas as it leaves the calorimeter and cools down to the ambient temperature is found. The heat lost through the exhaust gases ( $\dot{Q}_e$ ) is also calculated by considering the heat necessary to increase the temperature of the total mass (water + air + propane fuel),  $\dot{m}_e$  (kg/sec), from outside conditions  $T_o$  ( $^{\circ}C$ ) to the temperature of the exhaust  $T_e$  ( $^{\circ}C$ ). This heat loss is also known as sensible heat, and to calculate it, it is necessary to estimate the mean specific heat of the exhaust gases, which, in this case, is assumed to be the value for air with a mean temperature of the exhaust (Ajav et al., 2000).

The heat transferred from the engine by the cooling water was determined by measuring the flow rate of water entering the engine as well as the temperature difference of inlet and outlet water as follows. Heat rejected to the coolant water ( $\dot{Q}_w$ ) is determined by

$$\dot{Q}_w = \dot{m}_w C_w (T_2 - T_1) \quad (4.44)$$

where  $\dot{m}_w$  is the flow rate of water measured, in (kg/sec),  $C_w$  is the specific heat of water, in (kJ/kg °C),  $T_1$  is the inlet water temperature, in (°C) and  $T_2$  is the outlet water temperature, in (°C). Friction power could be determined by measuring the power input from the dynamometer to the engine during motoring. Next, the engine could be loaded, data taken, and the corresponding brake power can be measured by the dynamometer. The resulting values should correspond with the equation:

$$IP = BP + FP \quad (4.45)$$

Where  $IP$  is the indicated power given by running the routine Analysis.m,  $BP$  is the brake power measured by the dynamometer.  $FP$  is the friction power measured while motoring the engine, which will include the power necessary to overcome mechanical friction as well as the pumping power (Heywood, 1988).

#### 4.14 SECOND LAW ANALYSIS

The second law of thermodynamics is a rich and powerful statement of related physical observations that has a wide range of implications with respect to engineering design and operation of thermal systems. For example, the second law can be used to determine the direction of processes, to establish the conditions of equilibrium, to specify the maximum possible performance of thermal systems, and to identify those aspects of processes that are detrimental to overall performance.

Sufficient data were measured and recorded during each test point for completing the first and the second law analysis of this typical engine. Energy terms were based on experimental measurements and availability terms were calculated then by using the experimental results. Availability (also called exergy) is defined as the maximum useful work that can be produced through intersection of the system

with its surroundings when the system reaches equilibrium (thermal, mechanical and chemical) with the environment. The determination of availability is based on the thermodynamic properties. An engine processes includes both closed (combustion and power strokes) and open system (intake and exhaust strokes) portions. The specific availability for the complete system is:

$$a = (u - u_0) + P_0(v - v_0) - T_0(s - s_0) \quad (4.46)$$

The specific flow availability for the open system is given by:

$$a_{flow} = (h - h_0) - T_0(s - s_0) \quad (4.47)$$

The total availability is obtained by

$$A = \dot{m} a \quad (4.48)$$

The change of availability of a thermodynamic system for a process as shown in Figure 4.3 schematically is defined as:

$$\Delta A = A_{in} - A_{out} - A_d \quad (4.49)$$

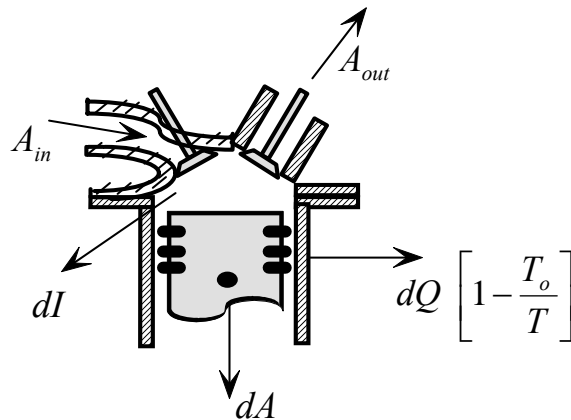


Figure 4.3: Engine Availability Streams

Heat transfer through a finite temperature difference, combustion, friction, and mixing processes for a typical internal combustion engine may destroy availability. The available energy equations for various processes are given in Table 4.1.

Szargut and Styrylska (1964) determined the availability of about 170 different fuels with known chemical composition. They were able to correlate the ratio of the fuel's availability rate at STP to its lower heating value. For gaseous fuels, they developed the following correlation,

$$A_m = \dot{m}_f LHV_f [1.0334 + 0.0183 \frac{H}{C} - 0.0694 \frac{I}{C}] \quad (4.50)$$

By definition, the fuel availability  $A_f$  is given by the Gibbs free energy.

$$A_f = -(\Delta G)_{T_0, P_0} \quad (4.51)$$

The ratio of the Gibbs free energy and the heating value is,

$$\text{ratio} = \frac{-A_f}{LHV} = \frac{\Delta G_{T_0, P_0}}{\Delta H_{T_0, P_0}} \quad (4.52)$$

This ratio, obtained above formulation, was used to determine the value of the fuel availability by multiplying this number with the heating value of the fuel:

$$A_f = \text{ratio } \dot{m}_f LHV \quad (4.53)$$

Table 4.1: General Availability Equations for Various Processes

Mechanism	Engine process	Equation
Work Transfer	Power Stroke	$dA_{\text{Work}} = dW$
Gas Transfer	Intake and Exhaust Stroke	$dA_{\text{gas}} = dm_{\text{gas}} [(h - h_0) - T_0(s - s_0)]$
Fuel Transfer	Combustion Stroke	$dA_f = dm_f (1.0661 LHV)$
Stored Energy	Heat Transfer to Oil Pan and Radiator	$dA_{\text{Stored}} = d[m_{\text{CV}}[(u - u_0) - T_0(s - s_0) + P_0(v - v_0)]]$
Heat Transfer	Convection, Radiation Loss, Exhaust Loss	$dA_{\text{heat transfer}} = dQ(1 - \frac{T_0}{T})$

The exhaust availability lost can be calculated as follows:

$$A_e = d\dot{Q}\left(1 - \frac{T_0}{T}\right) = \dot{Q}_e - T_0 \frac{\dot{Q}_e}{T_e} = \dot{Q}_e - T_0 \Delta\dot{S} \quad (4.54)$$

where

$$\Delta\dot{S} = \dot{m}_e C_{p_e} \ln \frac{T_e}{T_o} - \dot{m}_e R_e \ln \frac{P_e}{P_o} \quad (4.55)$$

The second law efficiency is defined as:

$$\eta_{II} = \frac{P_b}{\dot{W}_{rev}} \quad (4.56)$$

Where the reversible work which can be extracted from a reactant thermodynamic system that transfer heat with a reservoir at temperature  $T_r$ .

$$\dot{W}_{rev} = \sum_R \dot{N}_R (h_f + \Delta h - T_o s)_R - \sum_P \dot{N}_P (h_f + \Delta h - T_o s)_P - \sum_r \dot{Q}_r \left(1 - \frac{T_o}{T_r}\right) \quad (4.57)$$

The reversible work is determined using above formula. The last term of Eqn.4.57 represents the availability of cooling water and oil heat transfer to the reservoir at temperature  $T_r$ . The heat transferred to lubricating oil by the engine was neglected in the present study, since the amount of heat transferred to the lubricating oil can be assumed to be very small in comparison with the amount of heat transferred to the cooling water (Alkidas, 1989). The differential equations related to the analysis based on the second law of thermodynamics were further evaluated to predict exergy terms. The available energy equations for various processes were given in Table 4.1. An exergy balance was applied to all systems of the spark ignition engine such as the cylinder for the closed part of the cycle. Availability is not a conserved property, and it can be destroyed by irreversibilities due to processes such as heat transfer through a finite temperature difference, combustion, friction, or mixing processes. The change in availability of a thermodynamic system is defined as

$$\Delta A = A_{end} - A_{start} = A_{in} - A_{out} + A_Q - A_W - A_{dest} \quad (4.58)$$

Application of exergy-balance equation to spark-ignition engine subsystems as function of the crank angle is given as:

$$\frac{dA_{cyl}}{d\theta} = \frac{(\dot{m}_2 b_2 - \dot{m}_3 b_3)}{6N} - \frac{dA_w}{d\theta} + \frac{dA_L}{d\theta} + \frac{dA_f}{d\theta} - \frac{dI}{d\theta} \quad (4.59)$$

Each part of right hand side of Eqn. (4.59) is given as follows: Firstly, the availability transfer due to work is:

$$\frac{dA_w}{d\theta} = (p - p_o) \left( \frac{dV}{d\theta} \right) \quad (4.60)$$

The availability of the fuel that is introduced into the process is calculated by the following:

$$\frac{dA_f}{d\theta} = \left( \frac{dm_{fb}}{d\theta} \right) a_f \quad (4.61)$$

where  $a_f$  can be found from Eqn 4.51.

$$\frac{dA_L}{d\theta} = \frac{dQ_L}{d\theta} \left( 1 - \frac{T_o}{T} \right) \quad (4.62)$$

The change of availability of the cylinder contents is the term on the left hand side of Equation (4.59) as:

$$\frac{dA_{cyl}}{d\theta} = \frac{dU}{d\theta} + p_o \left( \frac{dV}{d\theta} \right) - T_o \left( \frac{dS}{d\theta} \right) - \frac{dG_o}{d\theta} \quad (4.63)$$

The term b in Eqn.(4.59), referring to the inflowing and out flowing exergy, is given by:

$$b = h - h_o - T_o(s - s_o) \quad (4.64)$$

This term is not needed for the closed part of cycle.

#### 4.15 EXPERIMENTAL PROCEDURE

The experimental procedures for the measurement of the engine parameter were summarized in this section. A variable speed-variable load test is performed on a spark ignition engine. The aim of this analysis is to obtain the variation of basic engine characteristics during the loading of the engine by the dynamometer while the engine speed is changing with load. A constant speed-variable load test is performed on a spark ignition engine. The aim of this experiment is to observe the variation of basic engine characteristics during the gradual loading of the engine by the dynamometer while the engine speed is kept as constant. All experimental measurements were conducted under steady state conditions, that is, when the change of temperatures over the surface of the engine block was measured as close to zero. For steady state condition, the engine was run for at least five minutes, and the measurements were recorded. The experiments for each case were repeated in a test point until the deviation between the results of two successive test is less than 5% errors. Averaging was performed to minimize the effects of variations than this error level. In addition, calibration check for the devices was made two times, before and after each successive test. Experimental procedures used in the thesis were summarized in Table 4.2.

Table 4.2: The Preset Conditions of the Tests

Experiment	Experimental Conditions			
	Speed (rpm)	Ignition Timing	Load	
Thermal balance Tests	Variable (1500 to 4500)	MBT	Variable	
	Speed	Ignition Timing	Load	$\phi$ (F/A)
Exhaust emissions tests	Constant 2000	MBT	Variable	0.8 to 1.2
	Speed	Ignition Timing	Load	$\phi$ (F/A)
Exergy analysis tests	Constant 2500	MBT	Variable	0.8 and 1.1
	Speed	Ignition Timing	Load	
Performance tests	Variable (1000 to 4500)	MBT	Variable	
	Speed (rpm)	Ignition Timing	Load	$\phi$ (F/A)
Exergy balance tests	Constant 2000	MBT	Constant	1.0

For exhaust emissions tests, the engine data were collected at 2000 rpm, which was selected as a moderate engine speed for internal combustion engines. The flow rate of fuel was adjusted for each different fuel air equivalence ratios. At each equivalence ratio and water to fuel mass ratio, the ignition timing was set at maximum brake torque (MBT). At each operating point, once for every 5 seconds during 4-minute period, about 48 values of speed, torque, water and fuel consumption rate, temperatures and exhaust emissions were recorded continuously. Tests for steam injection cases was realized at the same condition of the exhaust emissions tests.

For the energy and exergy analysis, the engine was running about 15 min for stable engine operation without misfire before the experiments. The engine was run with a 2500-rpm engine speed. At this speed, sufficient heat existed to evaporate the all injected water in the intake manifold since the ambient temperature and the intake manifold temperature during the test was sufficiently high. Thus, charge temperature was decreased by the water injection. This increased the charge density and also increased the power output similar to a supercharging effect. The tests were done under constant speed and MBT (maximum brake torque) settings for each water addition level. Engine power output varied because of the changes in the intake charge density with different water addition levels and was measured sensitively. In addition, all tests were made with local barometric pressures and with the ambient air humidity not over 45%. Two equivalence ratios of rich and lean mixture were selected for the test. The fuel flow rates were adjusted for each equivalence ratio values.

All tests for thermal balance analysis were performed at constant throttle opening position and variable engine speed. The engine was run at near three-fourth opening position of the throttle valve and its speed was adjusted from 4500 to 1000 rpm with 500-rpm steps for each case. The engine was run to attain uniform speed, and then it was loaded by the hydraulic dynamometer. At each engine speed and water to fuel ratio, the ignition timing was set at Maximum brake torque (here and after referred to as MBT). This also eliminated the effect of ignition angle.



For performance tests, each run the engine was started on pure LPG and then switched to the test water to fuel mass ratio. All tests were performed at constant load and variable engine speed and MBT ignition timing.

Experimental measurements used in the analysis of effect of water addition on the exergy balances were collected at 2000 rpm. Ignition timing was settled to MBT level.

#### 4.16 ERROR ANALYSIS

All measurements involve some level of uncertainty. In this work, the engine test system was made up of several different transducers and acquisition systems. Calibration check of the devices was made two times, before and after each successive test. Some of the experimental results were combination of the result of several independent measurements. They were connected into each other by a theoretical formula. An error analysis was conducted for both measured and calculated parameters. Error analysis for the derived quantities, such as engine power, brake specific fuel consumption, and thermal efficiency performed by considering the method of Kline and McClintok (Holman, 1989).

$$u_y = \left[ \left( u_1 \frac{\partial y}{\partial x_1} \right)^2 + \left( u_2 \frac{\partial y}{\partial x_2} \right)^2 + \dots + \left( u_n \frac{\partial y}{\partial x_n} \right)^2 \right] \quad (4.65)$$

Where  $u_y$  is the uncertainty,  $u_n$  is the error in the measured quantity  $u$ , and  $y$  is the function of the measured values,  $u_1, u_2, \dots u_n$ , to be calculated.

It should be noted that all data collected by the data acquisition systems used in this experimental study was subject to small errors. These errors were in the order of 0.02% for 12-bit system and 0.001% for 16-bit system and were considered negligibly small when compared to the other sources of error. For example, ADC may output a reading that is 16 bits in size. With  $\pm 10$  V range, a 16-bit ADC has a 0.31 mV resolution.

Equation 4.65 was applied to equations given in chapter 4. For the error calculations, all length measurements were considered to be accurate to within 0.2 mm, and the bore is considered to be accurate to within 0.1 mm. These estimations were derived from information found in the operator's manual for the engine. A shaft encoder that is accurate to within 0.36 degrees made this measurement. It was determined that the absolute errors in cylinder volume are approximately 2.5%, respectively. Knowing this, the error in indicated work was calculated. The pressure transducer made the cylinder pressure measurements. The manufacturer's specifications for this device state that it has a maximum error of  $\pm 4$  kPa. The error in cylinder volume has been determined to be approximately 2.5%. It was determined that the absolute error in indicated work is approximately 4.0%. The remainders of the performance quantifying parameters were derived from the work; therefore, it can be concluded that any errors in their values are of similar magnitude to the work error. Another measured parameter that has the potential to be a substantial source of error is the mass flow rate of the fuel and water. These values were determined by reading from digital scales the fuel consumed in a time that can be adjustable 2 to 20 seconds by the RS232 reader program. At each operating point, once for every 5 seconds during 4-minute period, about 48 values of water and fuel consumption rate were recorded continuously. Averaging was performed to minimize the effects of variations, it is felt that the error can be kept below a value of approximately 2%.

Maximum error in measured and calculated parameters was given in Table 4.3 for performance test.

Table 4.3: Maximum Estimated Experimental Uncertainties

Measurement	Maximum errors
Exhaust Temperature (K)	2.2
rpm	1.0
Torque (%)	0.67
Power (kW)	0.1
Brake power (%)	0.71
bsfc (g/kW·hr)	5
Thermal Efficiency (%)	1.3
In Cylinder Pressure (kPa)	0.4

Table 4.4 lists the accuracy and resolution of the instrumentation used in detail for exhaust emissions tests.

Table 4.4: Accuracy of Instrumentation

No.	Measured Value	Accuracy	Resolution
1	Fuel flow rate	1%	0.02 g/sec
2	Air flow rate	0.75%	0.01 g/sec
3	Water flow rate	1%	0.02 g/sec
4	Temperatures	0.75%, $\pm 0.1$ °C *	0.1 °C
5	Exhaust gas temperature	0.75%, $\pm 2.2$ °C *	1 °C
6	Torque	0.25%-0.1 N·m *	0.01 N·m
7	Speed	$\pm 1$ rpm	1 rpm
8	Ignition timing	0.5%	1 degree
9	NOx	1%, 5 ppm *	1 ppm
10	CO	1%	0.01%
11	HC	$\pm 12$ ppm	1 ppm

\*Whichever is greater.

The error analysis for thermal balance experiments is given. The error in the values of the engine torque was  $\pm 0.1$  N·m. Thus, the uncertainty in the values of torque was estimated to be in the range 0.14-0.07%. The error in the measurements

of the engine speed was  $\pm 1$  rpm. Thus, the uncertainty in the values of the engine speed was estimated to be in the range of 0.1 –0.02%. The error in the measurement of the fuel and water flow rates might be estimated by considering the error in the electronic balances, which have 0.1 g resolutions. The timer used in the test has a resolution 0.1 s. Hence, the uncertainties in the values of water and fuel flow rates were estimated in the range of 0.4-0.7%. The error in the measurements of temperatures during tests might be estimated by considering the error in the type of thermocouples used. Such an error for type T is 2.2 °C or 0.75%, whichever was greater and for type K is 2.2 °C or 0.75%. Thus, the uncertainty in the measurements of temperatures was estimated to be in the range 2-5%. An error analysis for the derived quantities, such as engine power, brake specific fuel consumption, thermal efficiency, heat rejection to the coolant water, heat lost through the exhaust gases, energy supplied to the engine and unaccounted heat losses performed. The error analysis by considering the method of Kline and McClintok (Holman, 1989) indicated that the uncertainty was in the range of 3-7%.

It should be clearly noted that the estimated errors in the measurements of the basic and derived quantities did not significantly influence the overall uncertainty in the final results.

## **CHAPTER 5**

### **EXPERIMENTAL AND THEORETICAL RESULTS**

#### **5.1 INTRODUCTION**

This chapter gives the detailed results of investigations. Effect of water addition on the LPG fuelled spark ignition engine was investigated experimentally in a detailed manner. Basic theoretical calculations were also done. These were included the effect of water addition on thermal balance, first and second law parameters, exhaust emission and performance. Inspection of the available literature indicated that there is a need for papers on the effect of water injection on LPG fuelled spark ignition engine. The results of this study had been published as three international journal papers (Özcan and Söylemez, 2005a; Özcan and Söylemez, 2005b; Özcan and Söylemez, 2005c) and additionally one report on this subject had been published (Özcan and Söylemez, 2004).

#### **5.2 THERMAL BALANCE OF AN LPG FUELLED, FOUR STROKE SI ENGINE WITH WATER ADDITION**

The thermal balance of the engine operating on LPG fuel and water injection into intake manifold was established at different engine speed conditions of the engine. The thermal balance was performed in respect of useful work, heat lost to cooling water, heat lost through the exhaust and unaccounted losses. The engine thermal balance for the pure LPG and various water to fuel mass ratios used in this work are presented in Figs. 5.1 and Tables 5.1 through 5.5. It can be seen from this figure that as the water injection level to the engine increased, the percentage of useful work increased, while the other losses decreased except for unaccounted

losses. Fig. 5.2 shows that the ratio of brake power to consumed fuel energy increases with water addition.

Table 5.1: Data of the Thermal Balance and Performance Parameters for LPG Fuel Only

$N$ (rpm)	$\dot{Q}$ (kW)	$P_b$ (kW)	$\dot{Q}_w$ (kW)	$\dot{Q}_e$ (kW)	$\dot{Q}_u$ (kW)	bsfc (g/kW·h)	$\eta_{th}$ (%)
1000	56.93	14.25	6.53	9.46	26.69	317.305	25.03
1500	66.27	18.36	8.34	15.81	23.76	286.667	27.70
2000	79.60	23.64	11.02	19.94	25.00	267.411	29.70
2500	94.15	28.33	13.32	24.3	28.20	263.932	30.09
3000	97.10	30.17	15.43	27.03	24.47	255.592	31.07
3500	101.13	31.23	16.92	29.46	23.52	257.176	30.88
4000	107.89	32.97	18.41	31.46	25.05	259.873	30.56
4500	115.46	34.35	20.48	33.86	26.77	266.934	29.75

Table 5.2: Data of the Thermal Balance and Performance Parameters with  $m_w/m_f=0.125$

$N$ (rpm)	$\dot{Q}$ (kW)	$P_b$ (kW)	$\dot{Q}_w$ (kW)	$\dot{Q}_e$ (kW)	$\dot{Q}_u$ (kW)	bsfc (g/kW·h)	$\eta_{th}$ (%)
1000	56.93	14.75	6.32	9.06	26.80	306.549	25.91
1500	66.27	18.84	8.07	15.16	24.20	279.363	28.43
2000	79.60	24.26	10.45	18.89	26.00	260.577	30.48
2500	94.15	29.12	12.89	23.1	29.04	256.772	30.93
3000	97.10	30.87	14.66	26.12	25.45	249.796	31.79
3500	101.13	31.96	15.95	28.56	24.66	251.302	31.60
4000	107.89	33.39	17.96	30.56	25.98	256.604	30.95
4500	115.46	35.46	19.41	32.83	27.76	258.579	30.71

Table 5.3: Data of the Thermal Balance and Performance Parameters with  $m_w/m_f=0.25$

$N$ (rpm)	$\dot{Q}$ (kW)	$P_b$ (kW)	$\dot{Q}_w$ (kW)	$\dot{Q}_e$ (kW)	$\dot{Q}_u$ (kW)	bsfc (g/kW·h)	$\eta_{th}$ (%)
1000	56.93	15.25	6.09	8.83	26.76	296.498	26.79
1500	66.27	19.34	7.88	14.91	24.14	272.141	29.18
2000	79.60	24.82	10.12	18.32	26.34	254.698	31.18
2500	94.15	29.81	12.51	22.21	29.62	250.829	31.66
3000	97.10	31.45	15.06	25.01	25.58	245.189	32.39
3500	101.13	32.61	16.42	27.41	24.69	246.293	32.25
4000	107.89	34.19	17.78	29.73	26.19	250.600	31.69
4500	115.46	36.18	19.19	32.17	27.92	253.433	31.34

The Tables 5.1 through 5.5 also show that as the ratio of injected water to charge increased, there was an increase in the quantity of useful work done by the engine as compared to pure LPG fuelled engine operation. The increases in useful work come from different sources. This increase may be because of the cooling effect of water, which yields to decrease the temperature of fresh air fuel charge in the inlet manifold as a supercharging effect and so more efficient combustion as compared to pure LPG fuelling case.

Results show that the heat flow rate to cooling water is a function of engine speed and water to fuel mass ratio. As the water to fuel ratio increased, there was a decrease in the average ratio of heat loss to cooling water as compared to pure LPG operation. Because, cooling water flow rate through the engine remains constant for each specified engine speed, while the temperatures of cooling water decrease due to reduction in the cylinder temperature. For pure LPG experiments, the average ratio of heat loss to cooling water was 15%, whereas it decreased to 13.5% for 0.5 water to fuel mass ratio. The results show an increase in heat flow rate to the exhaust with an increase in speed. As the water to fuel mass ratio increased, the heat lost through the exhaust gases was also decreased. Because, it is clear that as the water to fuel mass ratio increases, the exhaust temperature decreases. The heat absorbed by the additional water can explain the decrease in the exhaust temperature. Taymaz et al. (2003) investigated the heat losses at different engine loads and speeds with and without ceramic-coated diesel engine.

Table 5.4: Data of the Thermal Balance and Performance Parameters with  $m_w/m_f=0.33$

$N$ (rpm)	$\dot{Q}$ (kW)	$P_b$ (kW)	$\dot{Q}_w$ (kW)	$\dot{Q}_e$ (kW)	$\dot{Q}_u$ (kW)	bsfc (g/kWh)	$\eta_{th}$ (%)
1000	56.93	15.44	5.97	8.63	26.89	292.850	27.12
1500	66.27	19.52	7.72	14.71	24.32	269.631	29.45
2000	79.60	25.05	9.92	18.02	26.61	252.359	31.47
2500	94.15	29.74	12.22	21.75	30.44	251.419	31.59
3000	97.10	31.73	14.47	24.41	26.49	243.026	32.68
3500	101.13	32.92	15.6	27.43	25.18	243.973	32.55
4000	107.89	34.62	17.21	29.34	26.72	247.487	32.09
4500	115.46	36.68	18.79	31.51	28.48	249.978	31.77

Their results for the case of ceramic-coated one showed that an increase in exhaust energy due the high cylinder temperature at all load levels. Generally, lower exhaust temperature is an indication of a lower temperature through the entire engine cycle. During the pure LPG experiments, the average ratio of heat loss to exhaust gas was 26%, whereas it decreased to 23% for the 0.5 water to fuel mass ratio. It is clearly seen that as the engine rpm is increased, the time available for the combustion period decreases and the time for the heat transfer from the products of combustion to the surroundings is reduced, causing lower heat losses. However, an increase in water injection level reduced the average cylinder temperature.

It is clear from Fig 5.1 and Tables 5.1 through 5.5 that as the water to fuel mass ratio increases, the unaccounted losses increases. This may be attributed to an increase in the combustion period or a decrease in the flame speed that causes an increase in the heat loss since the products of combustion have more time to loose some of their heat to the surroundings. This effect dominates at lower engine speeds, perhaps due to lesser turbulence inside the cylinder. Additionally, the advancing the spark timing causes an increase in the percentage of heat losses, because advancing the spark causes the combustion to be completed within TDC, hence, more time would be available for the combustion products to loose heat to the surroundings. Harrington (1982) concluded that water addition leads to a decrease in burning rate with both ignition delay and burning intervals being extended. He also showed that the MBT (maximum brake torque) spark timings are advanced with water addition.

Table 5.5: Data of the Thermal Balance and Performance Parameters with  $m_w/m_f=0.5$

$N$ (rpm)	$Q$ (kW)	$P_b$ (kW)	$Q_w$ (kW)	$Q_e$ (kW)	$Q_u$ (kW)	bsfc (g/kW. h)	$\eta_{th}$ (%)
1000	56.93	15.86	5.82	8.36	26.89	285.095	27.86
1500	66.27	20.46	7.54	14.52	23.75	257.243	30.87
2000	79.60	25.8	9.59	17.31	26.90	245.023	32.41
2500	94.15	30.61	11.92	20.69	30.93	244.273	32.51
3000	97.10	32.55	14.04	23.31	27.20	236.903	33.52
3500	101.13	33.82	15.19	26.91	25.21	237.481	33.44
4000	107.89	35.45	16.82	28.91	26.71	241.693	32.86
4500	115.46	37.56	18.45	31.06	28.39	244.121	32.53



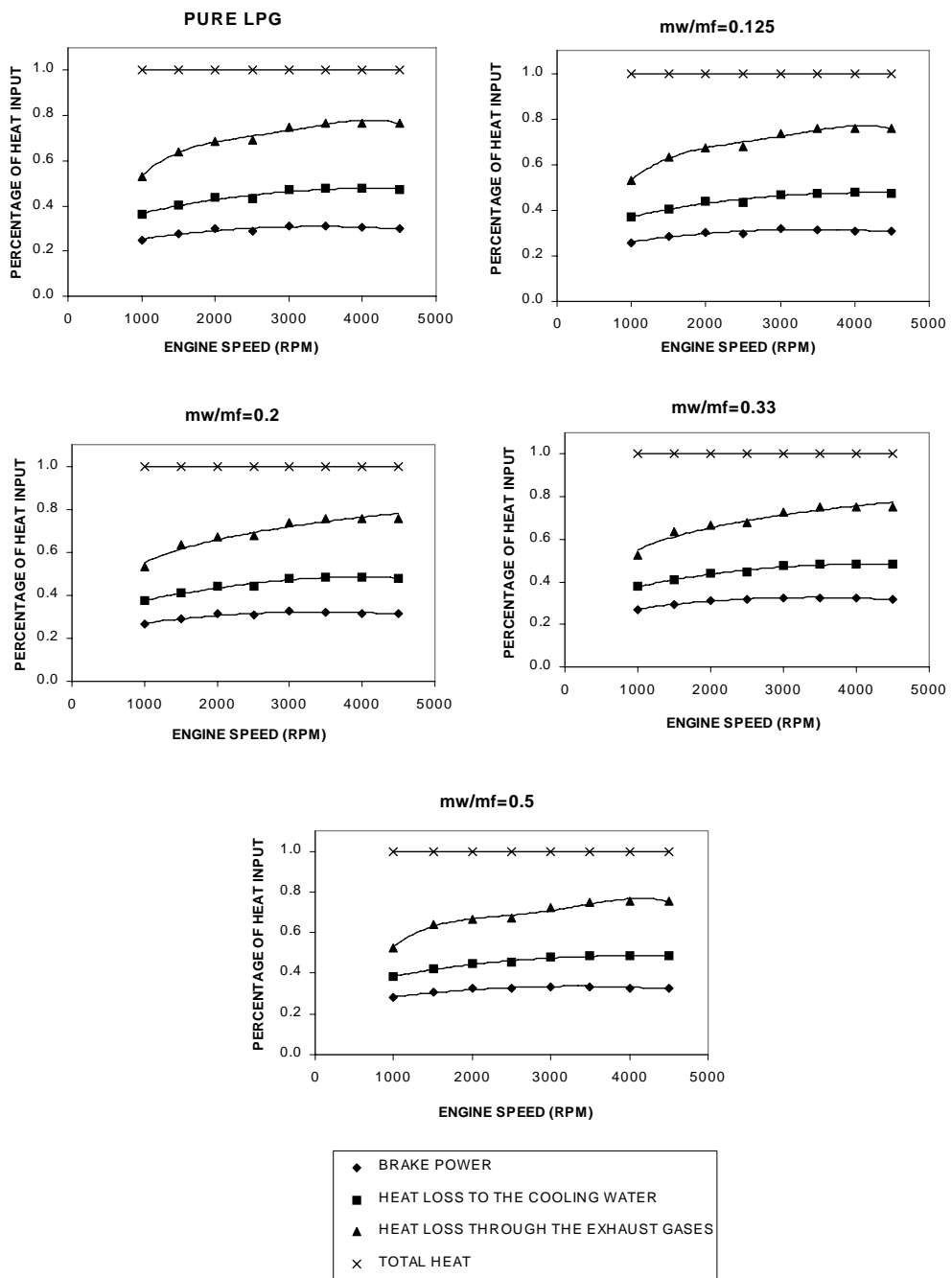


Fig. 5.1 Thermal Balance of Engine Operating with LPG Only and Various Water/Fuel Mass Ratio of Water Injection

Figure 5.2 shows that the effect of water addition on engine thermal efficiency for different water to fuel ratios. Results show that as the water to fuel mass ratio increases, the engine thermal efficiency increases due to the decrease in brake specific fuel consumption (bsfc). For pure LPG experiments, the average of the

thermal efficiency value is 29.3%, whereas it increased to 32% for a 0.5 water to fuel mass ratio, respectively. This trend agrees with the results of (Abu-Zaid, 2004), working on a single-cylinder diesel engine using water fuel emulsions. He concluded that as the water percentage in the emulsion increased, brake thermal efficiency increased. His results showed that the average increase in the brake thermal efficiency for 20% water emulsion is approximately 3.5% over the use of Diesel.

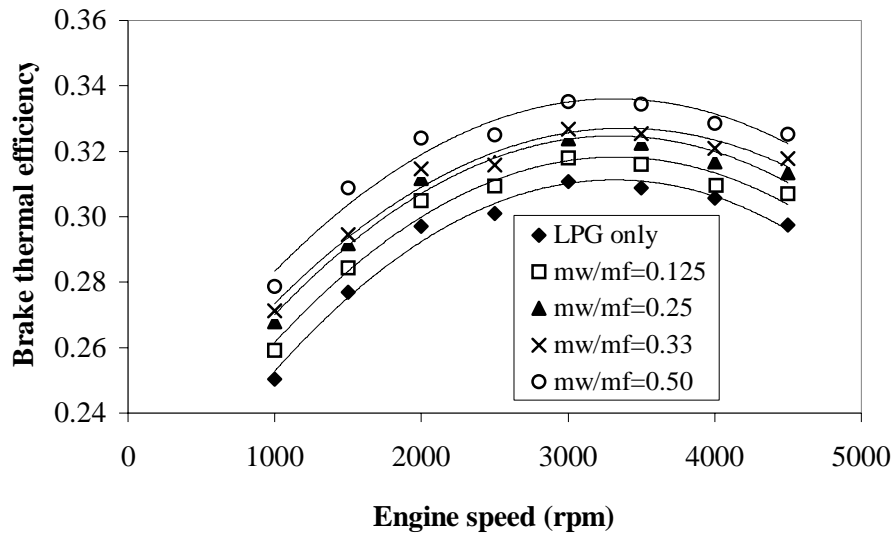


Fig. 5.2: Brake Thermal Efficiency Variations with Engine Speed for Various Water/Fuel Mass Ratio of Water Injection.

Fig. 5.3 shows that the brake specific fuel consumption decreases to a minimum and then it begins to increase at high speed as expected. Water to fuel mass ratio decreases the brake specific fuel consumption due to increase in brake power with water addition. Yamin and Badran (2002) concluded that the increase in percentage heat losses reduced the cylinder peak pressure and temperature, caused the engine power to drop because a lesser fraction of the thermal energy ended up as useful work.

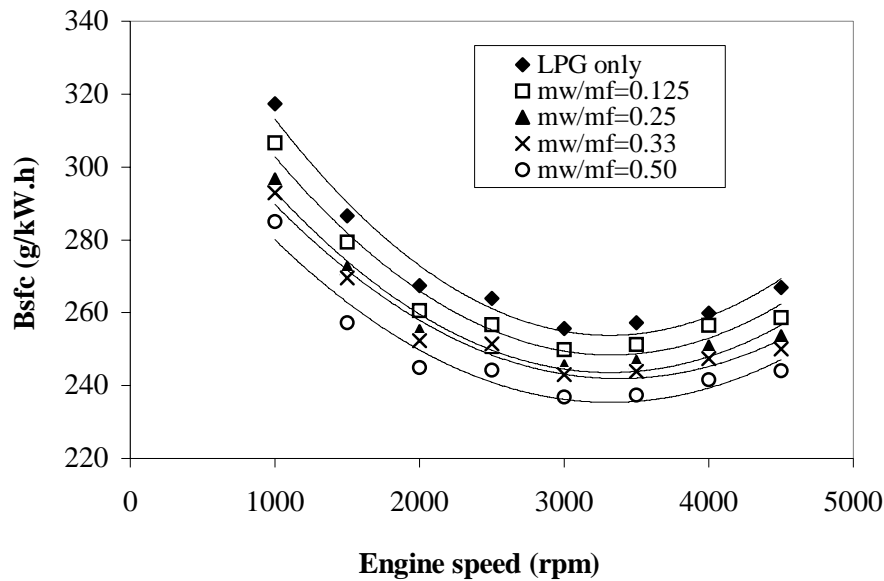


Fig. 5.3: Brake Specific Fuel Consumption Variations with Engine Speed for Various Water/Fuel Mass Ratio of Water Injection.

### 5.3 EXPERIMENTAL INVESTIGATION OF EFFECTS OF WATER ADDITION ON THE EXHAUST EMISSIONS

The effect of manifold water induction on LPG fuelled SI engine on knock and misfiring limits, exhaust temperature and emissions were searched at different fuel-air equivalence ratios. Results show that the water induction affects the information gathered such as knock, misfiring, exhaust emission and temperature during the tests. Production of  $\text{NO}_x$  depends on the fuel/air equivalence ratio, maximum cycle temperature and burning rate. Figure 5.4 shows the  $\text{NO}_x$  emission as a function of fuel/air equivalence ratio for different water to fuel mass ratio. Results indicate that the peak  $\text{NO}_x$  emissions occur at slightly lean conditions, where the combustion temperature is high and there is an excessive oxygen to react with the nitrogen as a result of the tendency of dissociation. Figure 5.4 also introduces that the water injection reduces the  $\text{NO}_x$  emission at lean region having a local maximum in between equivalence ratios of 0.9 and 1.0. Because the combustion process is closer to stoichiometric ratio and produces a higher flame temperature; therefore, the  $\text{NO}_x$  emission is increased, particularly by the increase of thermal Nitrogen Oxide. Experimental results also show that a maximum 35% of reduction in  $\text{NO}_x$  emission level was achieved with water injection.

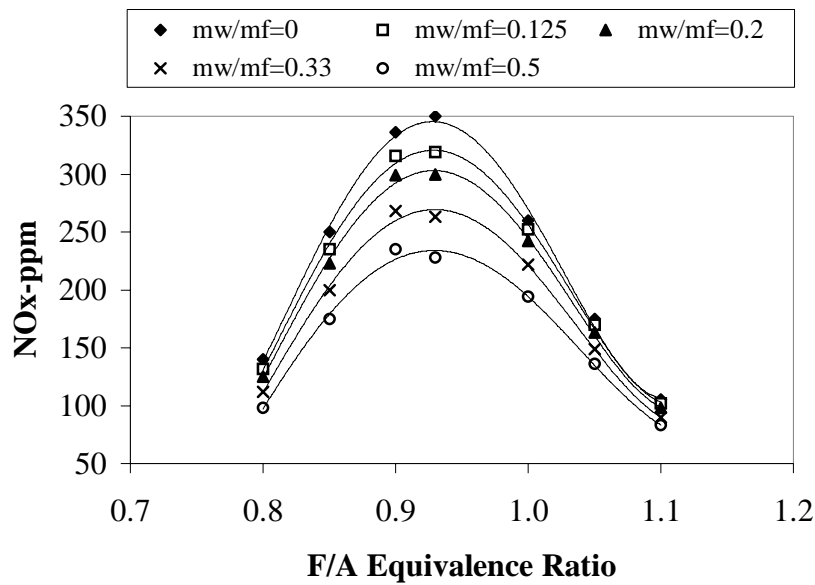


Figure 5.4: Effect of Water Addition on  $\text{NO}_x$  as a Function of F/A Equivalence Ratio

The reduction of  $\text{NO}_x$  emission level is evident in the lean mixture. The drop in temperature and reduction of the combustion rate with the water addition are the main reasons in the  $\text{NO}_x$  reduction. A basic thermodynamic analysis was performed for this purpose. The effect of 0.5 gm water addition per gm of fuel yields to lower the adiabatic flame temperature in the level of approximately 150 degrees K for stoichiometric fuel air mixture. It can be readily shown that, for Zeldovich mechanism at stoichiometric mixture, A 100 K drop in combustion temperature would cause to a 33% reduction in NO production rate. This result agreed with the measured trends in  $\text{NO}_x$ .

Several experimental results in the literature (Mozafari A.,1994; Woo Y. et al., 2004; Caton J. A., 2003) showed that EGR (exhaust gas recycling) lowers the  $\text{NO}_x$  concentration in the exhaust gas since the re-circulated exhaust gas is mixed with the fresh fuel–air mixture to dilute the concentration of fresh fuel air charge. The new mixture has reduced oxygen concentration due to higher mean specific heat and higher temperature than the air alone. This is like the effect of water induction. Water is added into the intake port and will produce a similar reduction in peak flame temperature as EGR, lowering thermal  $\text{NO}_x$  content. With EGR, a large reduction in  $\text{NO}_x$  emissions was obtained with significant increase in HC emissions. Substantial

reductions in  $\text{NO}_x$  concentrations are achieved with 10–25% EGR (Mozafari A., 1994). This result agrees with the results of (Woo et al., 2004) who worked on a modified commercial heavy-duty diesel engine using LPG as a fuel. Fig. 5.5 shows the HC emission as a function of fuel/air equivalence ratio and water to fuel mass ratio. HC emissions are not strongly affected near the stoichiometric mixture with increased water injection rate. The HC emission slightly increases at lean and rich regions as the water to fuel mass ratio increases. The higher heat of vaporization of water reduced temperature of the mixture. In addition, water addition decreases in burning rate of fuel-air mixture. The lower mixture temperature, combustion chamber deposits and longer burning period could have contributed to higher HC emissions from the engine.

EGR increases the HC emissions. The increase of HC emissions may reach over 60% at higher rates of EGR (Mozafari A., 1994). Woo et al. (2004) also concluded in their experimental work that  $\text{NO}_x$  decreased at the expense of HC increased and the increase rate in HC emissions was more moderate than  $\text{NO}_x$  reduction.

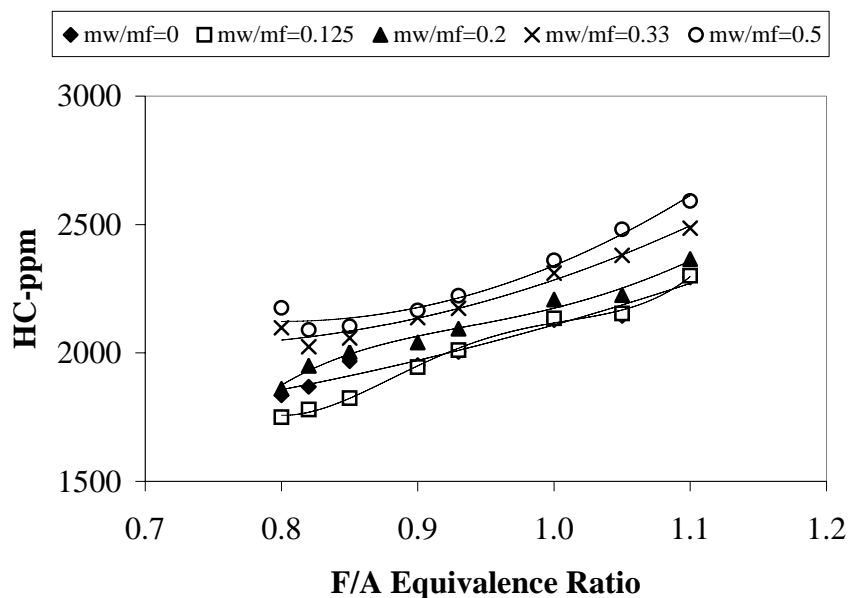


Figure 5.5: Effect of Water Addition on HC Emissions as a Function of F/A Equivalence Ratio

Results in Fig. 5.6 explain the variation of the CO concentrations as a function of fuel/air equivalence ratio and water to fuel mass ratio. For lean mixtures, CO concentrations vary little with equivalence ratio and increases rapidly as the fuel air mixture becomes richer than stoichiometric level.

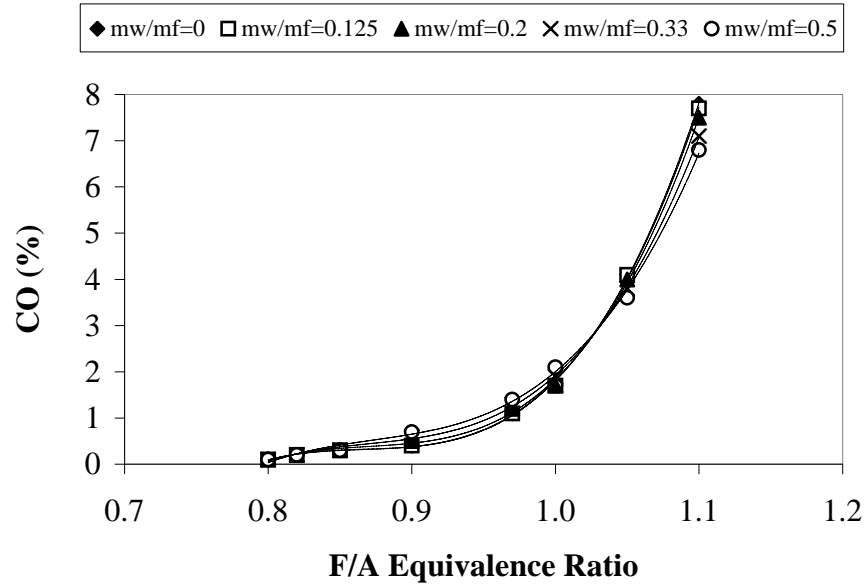


Figure 5.6: Effect of Water Addition on CO Concentration

CO concentrations in the exhaust increase, as the fuel/air equivalence ratio for fuel-rich mixtures increases in the amount of excess fuel naturally. A reduction in CO level of about 1% is observed in the rich mixture region since higher CO concentration exists and water in combustion helps to complete the combustion process by improving the oxidation of the CO. The combustion of CO occurs slowly and yields to a late burning in the combustion of the fuel. The presence of water vapour in the combustion process fundamentally changes the combustion chemistry. Specifically, it does help to the combustion of CO. EGR has little effect on CO emissions (Mozafari A., 1994).

Exhaust temperature significantly decreases for the lean mixture as presented in Fig. 5.7. This drop in exhaust temperature is relatively small for the rich mixture. This is because the addition of water has increased the total mass in the cylinder and water absorbs a great deal of heat due to its high specific heat similar to a

supercharging and inter-cooling effect. Woo et al. (2004) show that EGR reduced the exhaust gas temperature. This observation agreed with the results of (Caton J. A., 2003). He concluded that as the homogeneous EGR rate increased, the exhaust temperature decreased due to a slower burning rate.

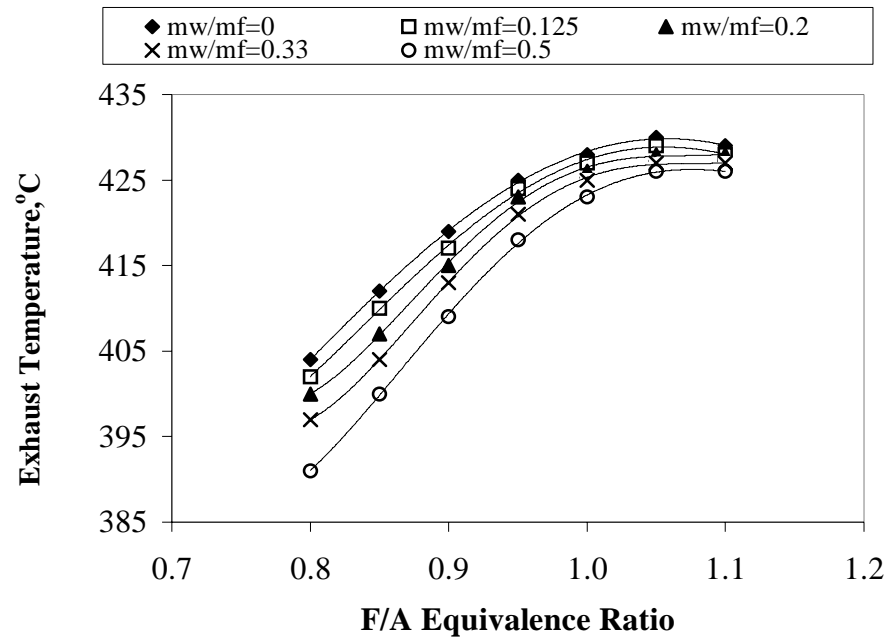


Figure 5.7: The Effect of Water Addition on Exhaust Temperature

Fig. 5.8 shows the MBT ignition timing for various fuel air equivalence ratios at different water addition levels. The MBT ignition timing for LPG fuelled engine increases as the water addition increases. Water addition to reactant mixture decreases in burning rate of fuel-air mixture during combustion in spark ignition engine. As a result of this, minimum MBT is advanced. The thermodynamic heat release analysis showed that the burning period was decreased in the case of stratified EGR. Combustion speed was increased as EGR rate was decreased. As the EGR amount was increased, fuel air mixture was diluted by the inert gas and total heat capacity was increased (Woo et. al., 2004). So, MBT spark advance requirement increases with the rate of EGR directly.

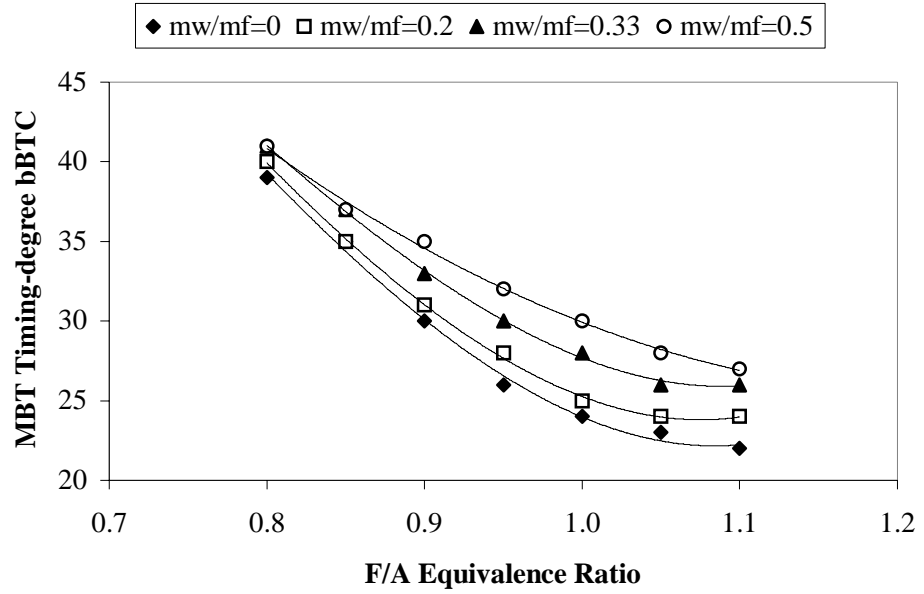


Figure 5.8: The Effect of Water Addition on MBT Timing

Experimental results in Fig.5.9 presents that as the water to fuel mass ratio decreases, the knock and misfire limits occur at less advanced ignition timing since water induction leads to slow down the burning rate and it increases the ignition delay period and combustion period.

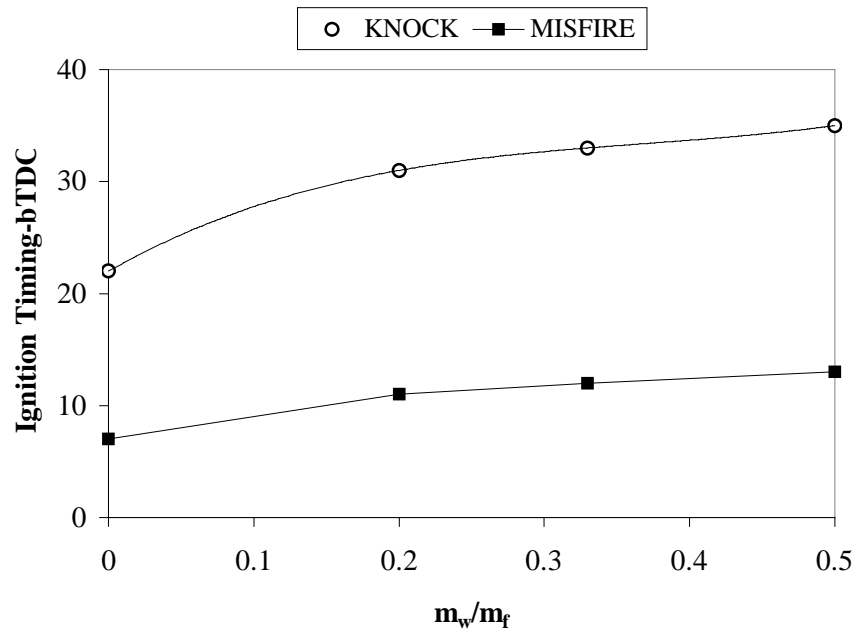


Figure 5.9: The Effect of Water Addition on Knocking and Misfire



In addition, the cooling effect due to evaporation of water has a significant effect on the reduction of charge temperature in the cylinder. As a result of these, water addition decreases the knock tendency, which yields to a desirable result for IC engines. The range of ignition timing between knock and misfire limits increases from 15 to 22 crank angle degrees when the water to mass fuel ratio increases from zero to 0.5.

Figure 5.10 shows the effect of water addition on the thermal efficiency of the engine for a fuel air equivalence ratio of 0.9. Results show that as the water addition level increases, the thermal efficiency increases. For this study, it was observed that water input caused a slight but sustained increase (0.2-2%) in thermal efficiency as compared to no water addition case. This occurs due to formation of steam at the compression stroke results in pressure drop that causes a decrease in the compression work. At the same time, an increase in thermal efficiency occurs as a result of the lowered tendency of dissociation reactions as a result of decrease in average cylinder temperature during the combustion. EGR also lowered the specific fuel consumption and decreased the heat transfer from the cylinder contents to the surrounding surface (Mozafari A., 1994). The engine thermal efficiency increased due to the decrease in brake specific fuel consumption with EGR.

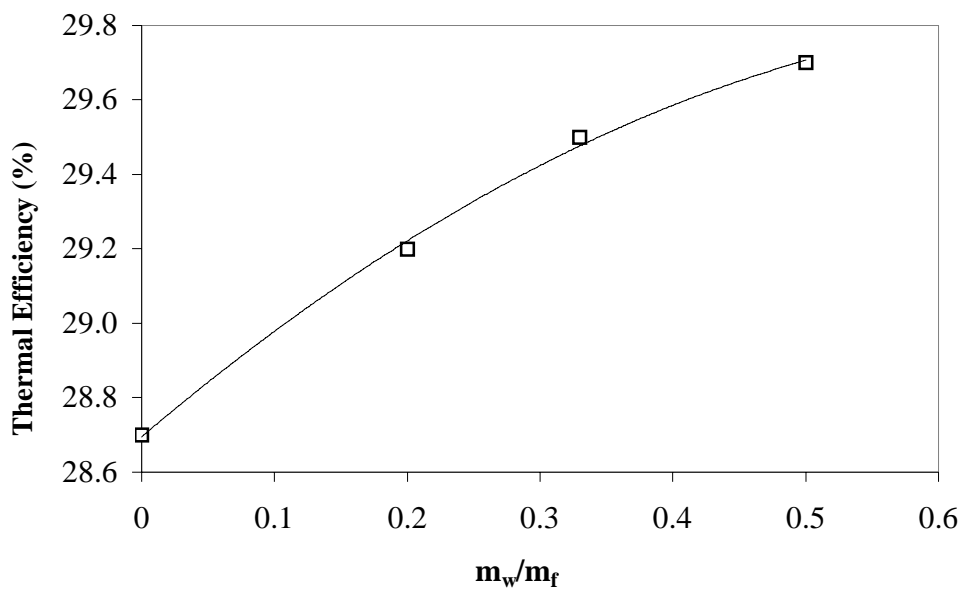


Figure 5.10: The Effect of Water Addition on Engine Thermal Efficiency

#### **5.4 EFFECT OF WATER ADDITION ON THE PERFORMANCE OF FOUR CYLINDER, LPG FUELLED SPARK IGNITION ENGINE**

The purpose of this study is to experimentally investigate the effect of water injection to intake manifold on the engine performance and exhaust gas temperatures of a commercial SI engine. A four stroke, four-cylinder SI engine was used for conducting this study. Water injections were used with five different water to fuel mass ratio; 0, 0.125, 0.2, 0.33 and 0.5 at constant load and variable engine speed ranging from 1000 to 4500 rpm.

Water was injected into suction port using a gasoline injector. This supplied water was sent into the intake manifold in the form of an ultra-fine mist. The amount of water injected was controlled by varying water supply pressure and/or by an adjustable valve controlled via a step motor with using computer parallel port. Throttle valve was also adjusted for each speed using another step motor with using same parallel port. For each run the engine was started on pure LPG and then switched to the test water to fuel mass ratio. All tests were performed at constant load and variable engine speed and MBT ignition timing. At each operating condition, the dynamometer load, speed, exhaust temperature, fuel and water flow were recorded after allowing sufficient time for the engine to stabilize. It has been demonstrated experimentally that the water addition produces some significant effects in the combustion of liquid fuels. The aim of the test is to investigate experimentally the effect of the water injection on the performance of a LPG fuelled SI engine.

As stated previously, the effect of water addition on engine horsepower, brake specific fuel consumption, brake thermal efficiency and the exhaust gas temperature were studied. The effect of water addition on the engine output torque and brake power for various speeds is shown in Fig. 5.11 and Fig. 5.12.

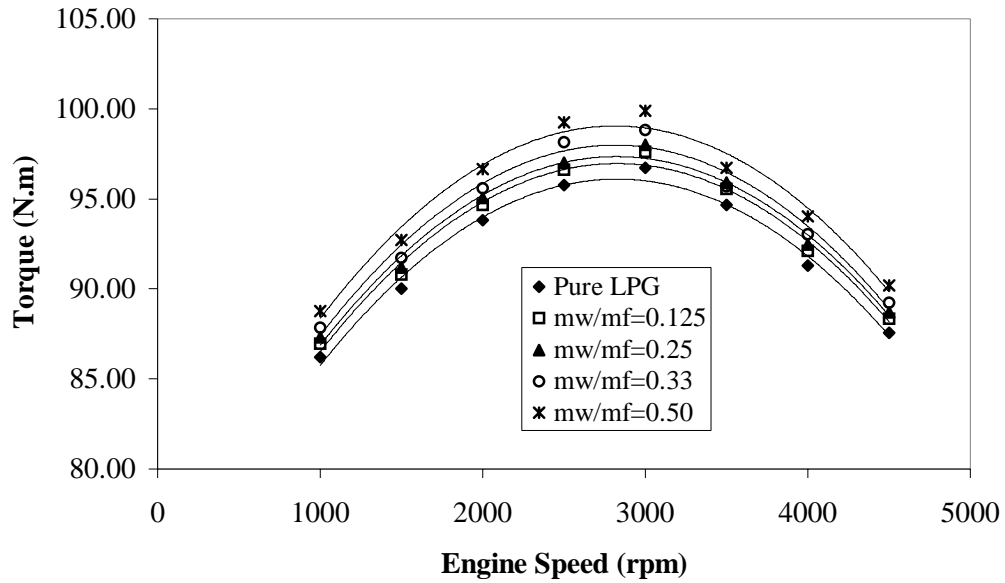


Figure 5.11: Effect of Water Injection on Engine Torque Output versus Engine Speed

Both torque and brake power values are functions of engine speed. At low speed, torque up to reach a maximum as the engine speed increases, and then, as engine speed increases further, torque decreases as shown in Fig. 5.11. The torque decreases because the engine is unable to ingest a full charge of air at the higher speeds. It is clear from Fig. 5.11 that as the mass ratio of water to fuel increases, the torque produced increases. The increases in torque come from different sources. When water changes state from a liquid to a high-pressure steam in the heat of combustion, this may be provided additional power. This increase in torque is also mainly as a result of supercharging effect of water injection.

The effect of the manifold water addition on the engine power is shown in Fig. 5.12. The brake power increases to a maximum and then decreases at higher speeds for a typical engine. This is because friction losses increase with speed and become the dominant factor at very high speeds.

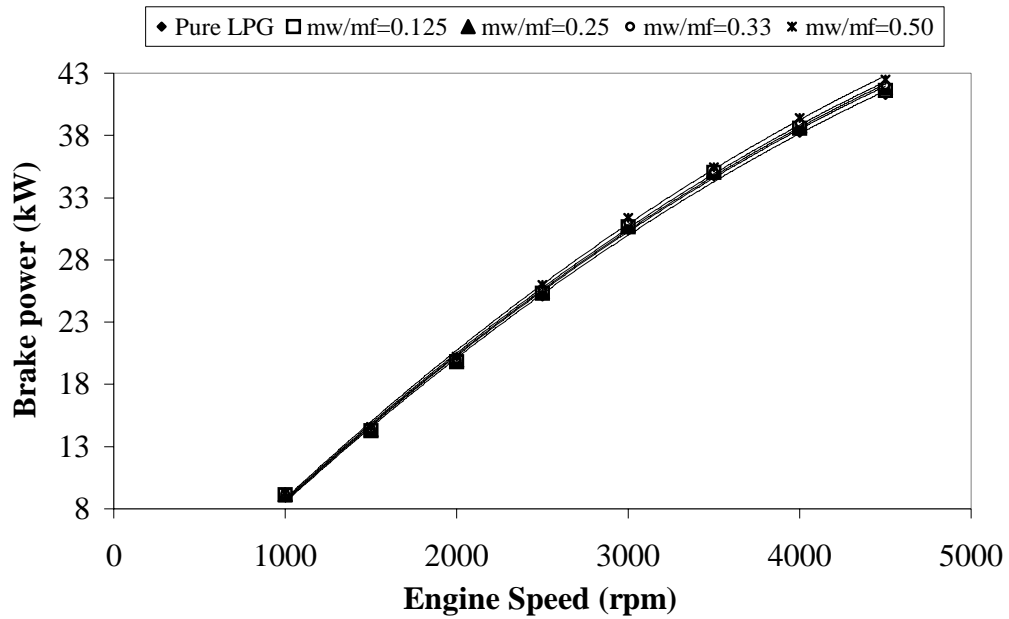


Figure 5.12: Effect of Water Injection on Engine Power Output versus Engine Speed

Fig. 5.12 shows that the power increases slightly as the water to fuel mass ratio increases. The increase in power output because several different combustion variables are affected by water injection. Harrington (1982) found that the water addition for a single cylinder engine leads to an increase in ignition delays. Thus, the charge requires less compression work than the LPG alone due to the longer ignition delay during the compression stroke. This helps to reach a higher peak pressure after TDC to produce more power output during the expansion stroke.

The BSFC decreases to a minimum as engine speed increases at low engine speed, and then increases at high speeds. At low speeds, the longer time per cycle allows more heat loss and lower combustion efficiency resulting in fuel consumption goes up for the power produced. Fuel consumption increases at high speed because of greater friction losses. As water addition is increased fuel consumption due to greater thermal efficiency. The variation of brake specific fuel consumption with engine speed for the different water to fuel mass ratio is shown in Figs. 5.13.

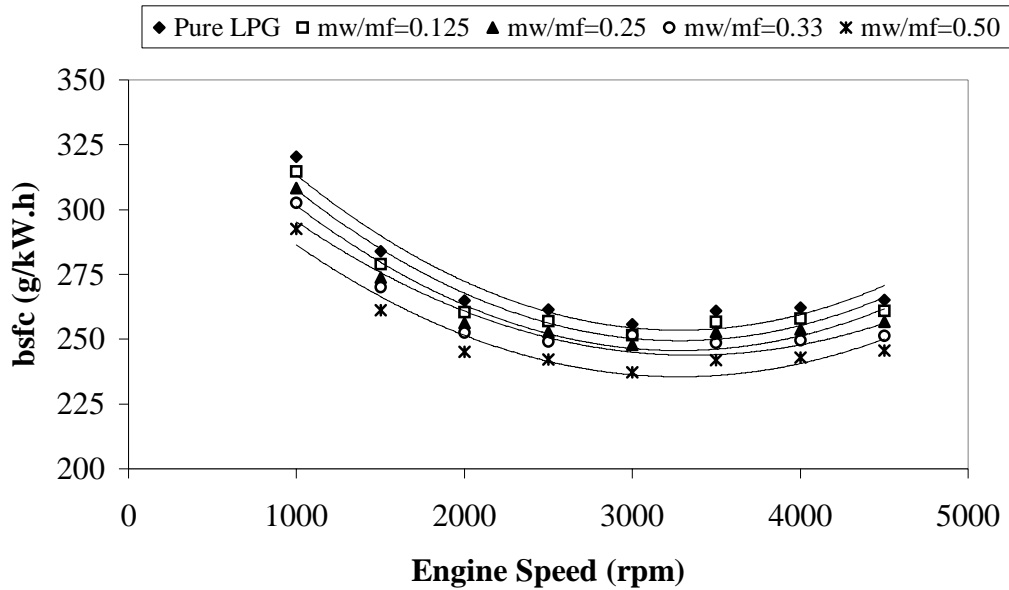


Figure 5.13: Effect of Water Injection on Brake Specific Fuel Consumption versus Engine Speed

Fig. 5.13 shows that as the water to fuel mass ratio increases, the BSFC increases. This is because, as the percentage of water in the gas increases, a larger amount of fuel is displaced by an equal amount of water. This means that less fuel is actually contained within each volume of the charge. It is clear from Fig. 5.13 that as the water to fuel mass ratio is increases, the BSFC decreases. The minimum value occurs when the water to fuel mass ratio is 0.5.

Fig. 5.14 shows the effect of water addition on the brake thermal efficiency. As expected, the maximum increase in brake thermal efficiency occurs when 0.5 of water to fuel mass ratio is used, and this is due to the fact that the BSFC was at its minimum value, as shown in Fig. 5.13. The average increase in brake thermal efficiency for 0.5 of water to fuel mass ratio is approximately 2.4% over the use of LPG alone for the engine speed range studied.

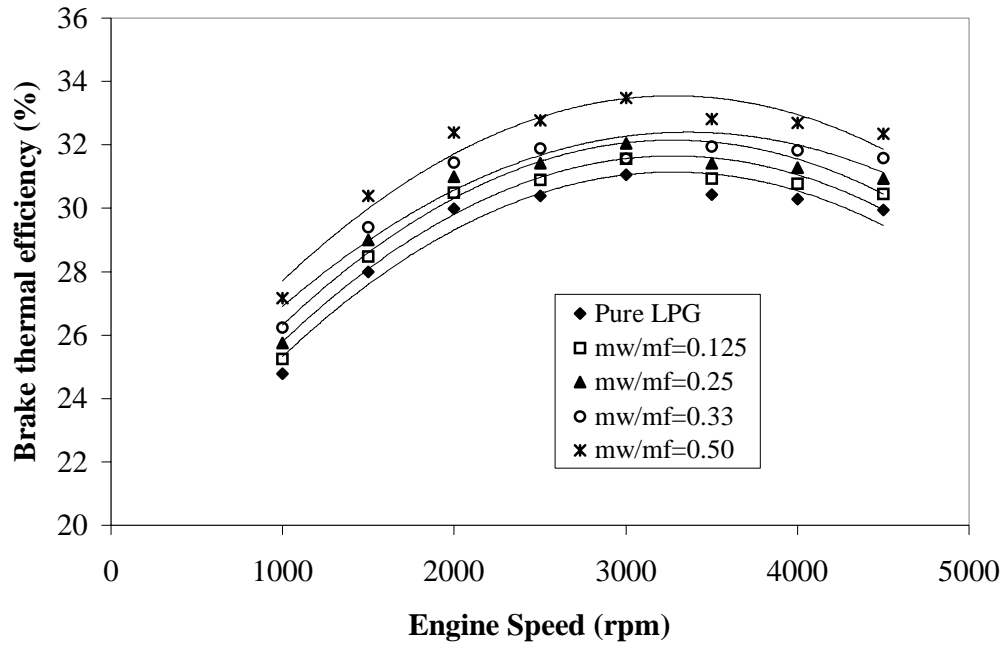


Figure 5.14: Effect of Water Injection on Brake Thermal Efficiency versus Engine Speed

The variation of the gases exhaust temperature with engine speed for the different water to fuel mass ratio is shown in Fig. 5.15.

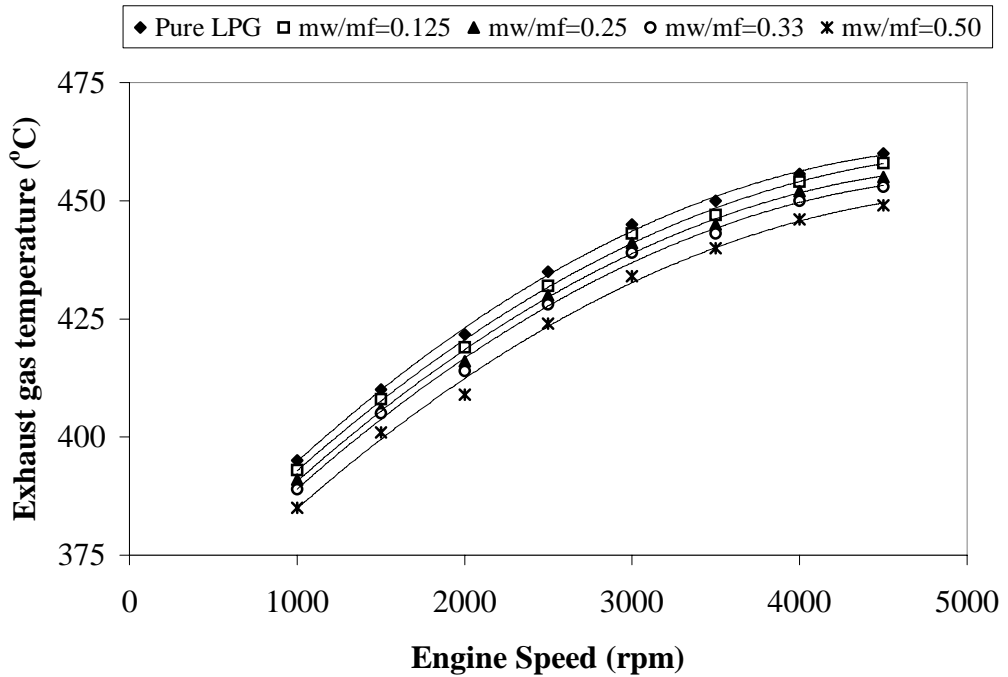


Figure 5.15: Effect of Water Injection on Gases Exhaust Temperatures versus Engine Speed

From Heywood (1988), it was discovered that typical exhaust gas temperatures for spark ignition engines are approximately 650 °C. The experimentally determined value of 450 °C seems to be reasonably close to the expected value but is lower a little bit. The exact reason for this deviation may be measurement point of the exhaust temperature. It is clear that as the water to fuel mass ratio increases, the exhaust temperature decreases. The exhaust gas temperatures with water injection decreased up to 7 °C. The heat absorbed by the additional water can explain the decrease in the exhaust temperature, because latent heat of the water will cool the charge. Lower exhaust gas temperature is an indication of a lower temperature through the engine cycle.

## 5.5 EFFECT OF WATER ADDITION ON THE COMBUSTION

Information for the recorded pressure is used to analyze the mass fraction burned when pure LPG and different water to fuel mass ratio. Figure 5.16 and Figure 5.17 show that ignition delay and combustion period as a function of engine speed and water injection rate.

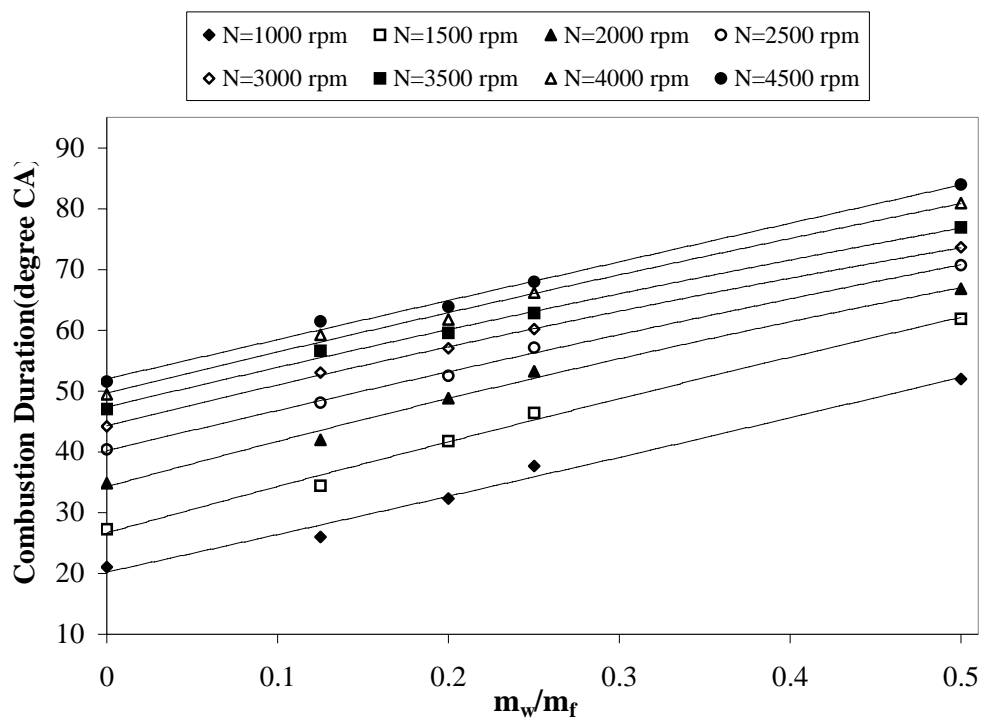


Figure 5.16: Combustion Period as a Function of Engine Speed and Water Injection Rate

Calculated results show that the ignition delay and combustion period were strongly affected by increased level of water addition. The ignition delay and combustion period increases as the water injection rate increases. The combustion period increases rapidly at low engine speeds.

Variation of cylinder pressure in the combustion chamber of the test engine with different water to fuel mass ratio values was given as a function of crank angle in Figure 5.18. Maximum pressure occur  $5^{\circ}$  to  $10^{\circ}$  a TDC (Obert, 1973). There is an optimum peak pressure position that, for a given mass of fuel and air inside the cylinder, gives maximum torque. Earlier peak pressure position could precipitate detonation. Studies done on aircraft engines between about 1935 and 1945 showed that the actual detonation reaction began behind the flame front in the partially combusted gases. Later peak pressure position causes power reduction. Note that the peak pressure position is moved later with water injection in Figure 5.18. This may be decreases the output torque.

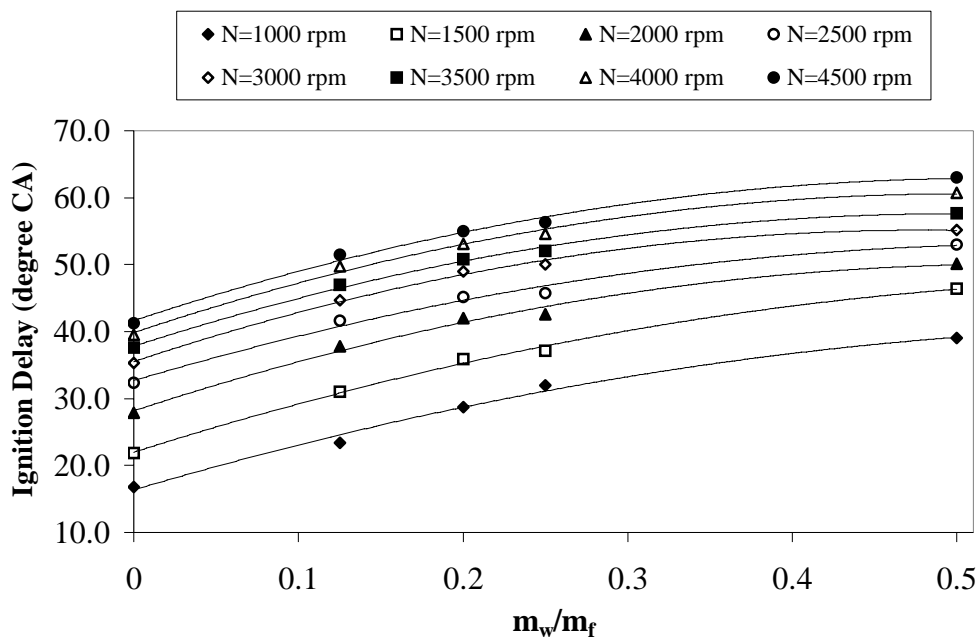


Fig. 5.17 Ignition Delay as a Function of Engine Speed and Water Injection Rate



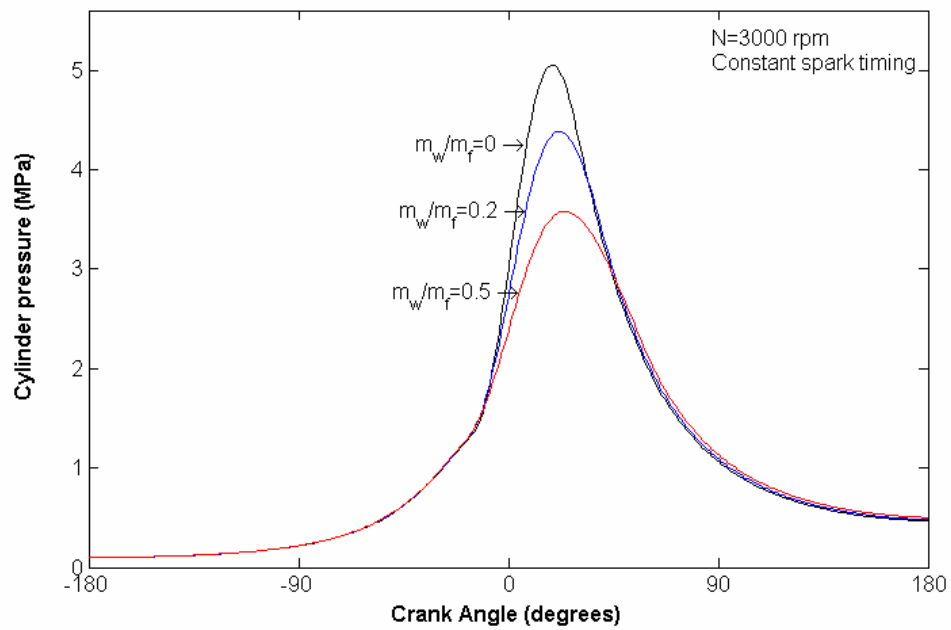


Figure 5.18: A P- $\theta$  Diagram for the Cylinder

Spark timing must be re-arranged to MBT spark timing for increasing the output torque. It was observed that the water injection could increase the engine efficiency. The pressure versus volume diagram values and the performance parameters for the engine were also calculated and are displayed in Table 5.6.

Table 5.6: Engine Performance Parameters for the Different Fuel to Water Mass Ratio at Constant Spark Timing

PARAMETER	Pure LPG	$m_w/m_f=0.2$	$m_w/m_f=0.5$
Average Engine Speed, rpm	3000	3000	3000
Average Gross Indicated Power, kW	35.42	35.16	34.81
Average Gross isfc, g/kWh	222.59	226.28	231.66
Average Gross imep, kPa	1092.7	1084.7	1073.9
Torque, N·m	97.11	96.32	95.14
bmepp, kPa	940.88	933.22	921.79
Bsfc, g/kWh	258.50	263.00	269.87

Water injection yielded to decrease the engine efficiency at constant spark timing. In addition, bmep, imep and torque decrease, isfc and bsfc increase as the water injection increases. Adjusting the spark advance can maximize engine efficiency with the water injection. As stated before, water injection affected the different combustion parameters. Sum of these effects do have a positive impact on engine performance. Water injection by itself may be giving a decrease in engine efficiency. Water injection is a well known method to increase engine power and efficiency at high loads and high compression ratios, the increase is obtained since water injection moves the knock limit and to gain the benefit of under these conditions and it is necessary to change the spark advance (Eriksson and Nielsen, 1998).

## **5.6 ENERGY AND EXERGY ANALYSIS OF WATER ADDITION**

### **5.6.1 Energy analysis**

Effect of water addition on the availability of a typical LPG (liquefied petroleum gas) fuelled conventional engine has been investigated based on experimental measurements. General engine performance results as a function of equivalence ratio are obtained. The results in terms of energy quantities: brake work, friction work, heat transfer to the coolant, energy out the exhaust, and unaccounted energy losses are used to determine the related second law quantities. The results of first and second law analyses for engine operation with water addition in different quantities are compared with the results of a similar analysis for no water addition case.

Maximum work can be produced from the original energy by using a Carnot heat engine theoretically. The amount of energy input is calculated by determining the energy of fuel air mixture in the engine. The theoretical thermodynamic derivation of Carnot heat engine performance is valid under ideal conditions. But, a heat engine cannot convert all the input heat energy into mechanical energy; some of the heat energy is rejected as illustrated in Fig. 5.19.

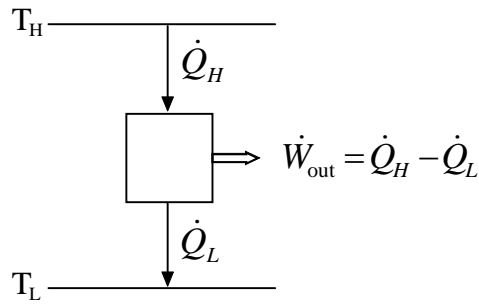


Figure 5.19: Schematic Presentation of Carnot Heat Engine

In an internal combustion engine, the engine absorbs energy from a heat source at a high temperature, converts part of the energy into mechanical work and rejects the remainder into a heat sink at a low temperature. Maximum power is obtained if one uses adiabatic flame temperature as source temperature. The greater the temperature differences between source and sink, the greater the efficiency. For a Carnot heat engine, the percentage of the energy that is available as a function of AFT (adiabatic flame temperature) for an environment temperature of 300 K as shown in Figure 5.20. The ambient temperature and temperature of products are extremely important since a system has potential to do work until the temperature of the system is equal to the ambient temperature. Fig. 5.20 shows that the percentage of available energy decreases as the amount of water addition rate increases.

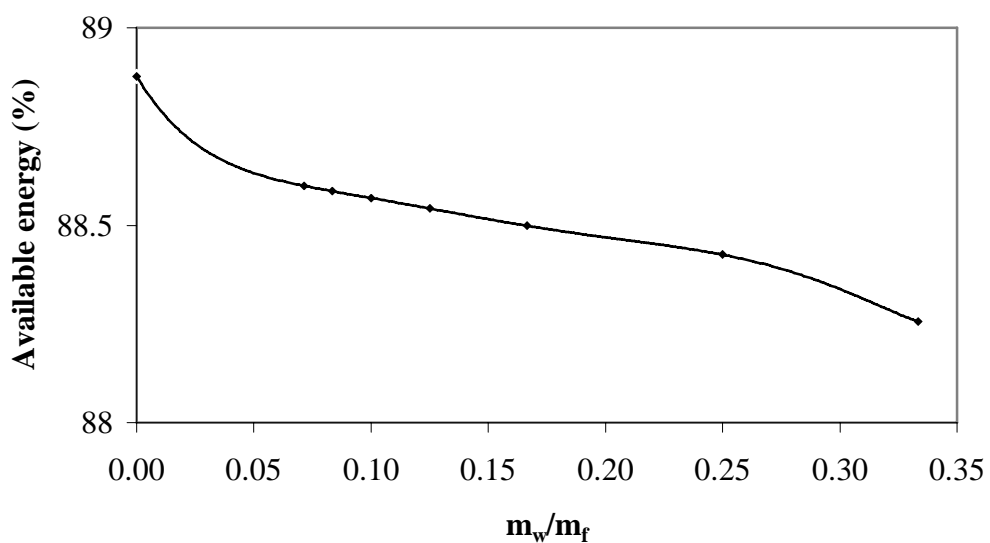


Figure 5.20: Change of Percent Available Energy with Water Injection Rate

Because, increase in the amount of water injection yields to decrease the AFT theoretically. For LPG, when containing pure propane, the effect of adding 0.5 gm water/gm fuel yields about 145 degrees K of reduction in the adiabatic flame temperature theoretically for a chemically correct fuel air mixture. There is a loss in maximum power when using LPG fuels as compared with that for gasoline, because there is a reduction in the fuel air breathing capacity. Water injection leads to cooling the fuel air mixtures because of its high specific and latent heat capacity. This increases the fuel air breathing capacity also for obtaining more power.

Fig. 5.21 shows the energy balance of cooling water, indicated and friction power for lean mixture. Results of experiments show that the indicated power and the coolant load are all increased with water injection.

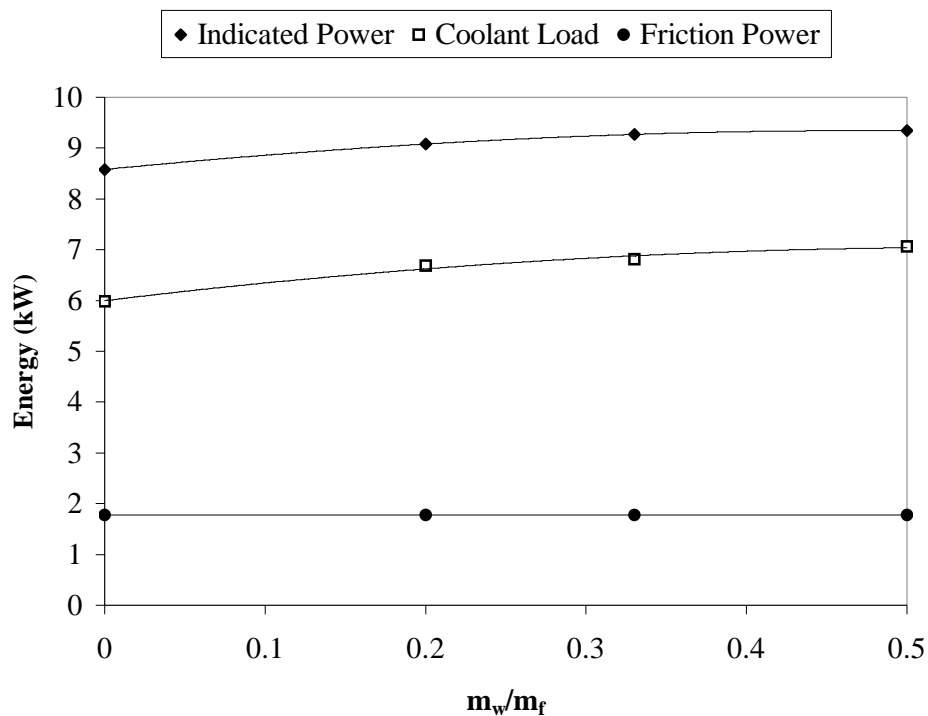


Figure 5.21: Energy Balance for Lean Mixture with Increasing Amount of Water Addition

Fig. 5.22 presents the energy balance for rich mixture. The indicated power slightly decreases with water addition. But, coolant load rapidly decreases. Indicated power, cooling water flow rate, inlet and exit coolant temperatures are measured and

then friction power and cooling water heat transfer rate values are calculated by using all of these measured quantities. Exhaust energy is also measured. So the remaining energy is assumed to be equal to the oil heat transfer and the engine heat transfer by radiation and convection plus auxiliary equipment energy consumption. These are called as the unaccounted energy terms.

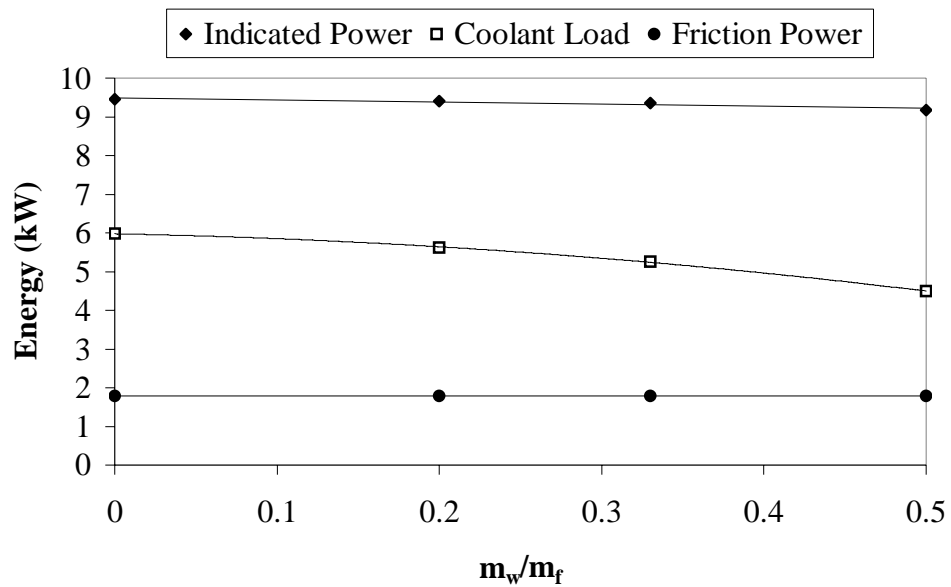


Figure 5.22: Energy Balance for Rich Mixture with Increasing Amount of Water Addition

Fig. 5.23 introduces these energy terms for lean and rich mixture. The exhaust gas temperature increases with large amount of water injection rate. Since water induction is reduced the inlet air temperature, this increases the density of inlet air charge and also increases sensible part of exhaust energy.

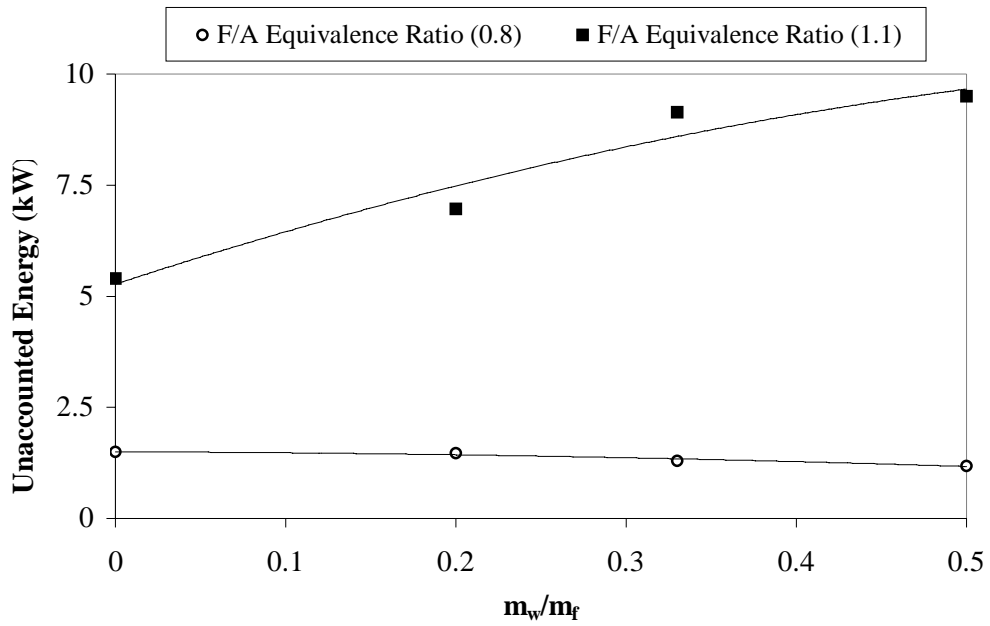


Figure 5.23: Unaccounted Energy for Lean and Rich Mixture with Amount of Water Addition

Figure 5.24 shows the distribution of energy use in the test engine given as a percentage of total fuel energy. It is noticed that at lean region only 37.9% of fuel energy for water to fuel ratio 0.5 has been used as an indicated power and 62.1% of fuel energy is not available for conversion to useful work due to the limitation of the second law of thermodynamics.

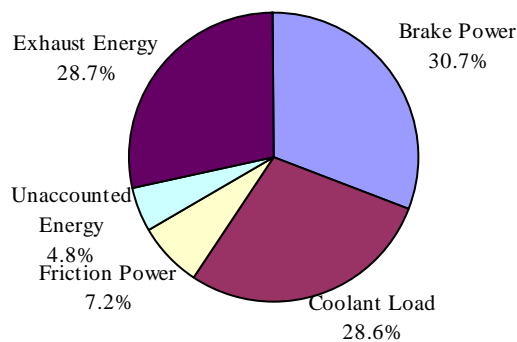


Figure 5.24: Energy Distribution for Water to Fuel Ratio 0.5 at Lean Region and  $Q_{in} = 24.62$  kW

The analysis of first law is completed with the thermal efficiencies. Fig. 5.25 indicates that the first law efficiency slightly increases with water injection for lean fuel air mixture. But it decreases for rich fuel air mixture. Since injected water reduces the compression work due to the drop in the gas pressure. In addition, water addition reduces the abnormal combustion for lean mixture and upper limit of power is advanced by water injection for spark ignition engines.

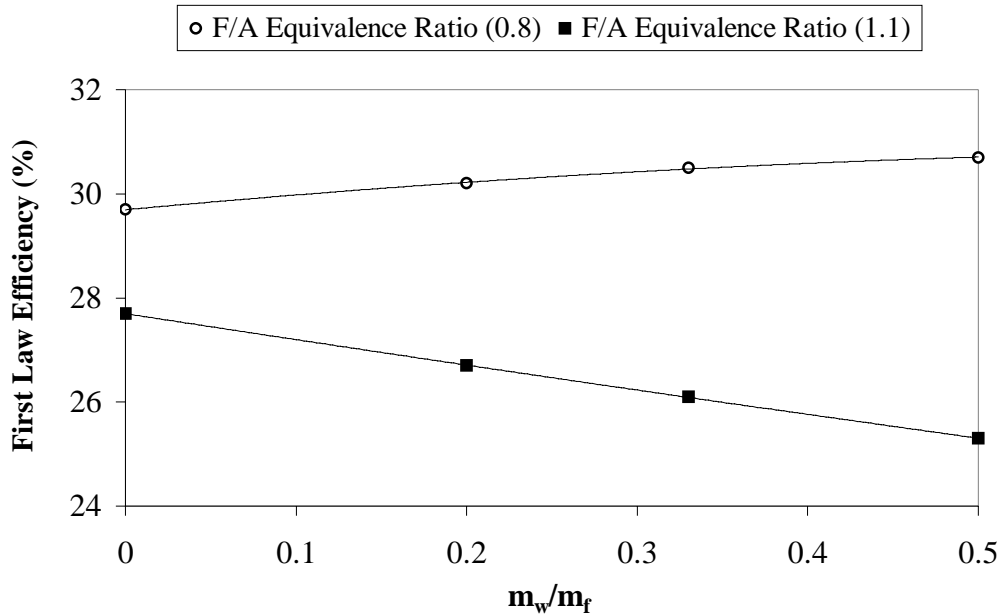


Figure 5.25: Effect of Water Addition on the First Law Efficiency

### 5.6.2 Exergy analysis

The second law of thermodynamics is the fact that a portion of a given amount of energy is “available” to produce useful work, while the remaining portion of the original energy is “unavailable” for producing useful work. Higher gas temperatures may minimize the destruction of available energy and also the percentage of available energy increases as the gas temperature increases at any ambient temperature. But, higher temperatures may lead to arise other losses of available energy such as higher heat transfer to oil and cooling water, higher availability expelled with the exhaust gases, higher nitric oxide formation rates in actual engine operations. Experimental results show that water is a perfect liquid for absorbing excess heat under certain engine operating conditions. Unlike energy,

availability is not conserved, and it can be destroyed by irreversibility. The availability energy of indicated power, friction power and cooling load as a function of water addition rate for lean and rich mixture conditions are shown in Figs. 5.26 and 5.27 respectively.

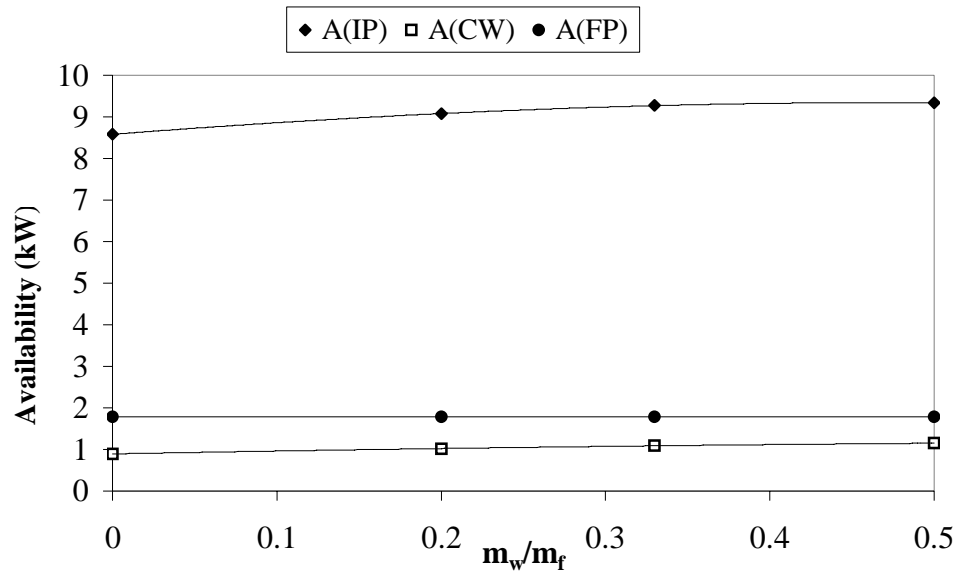


Figure 5.26: Availability versus Water Addition for Lean Mixture

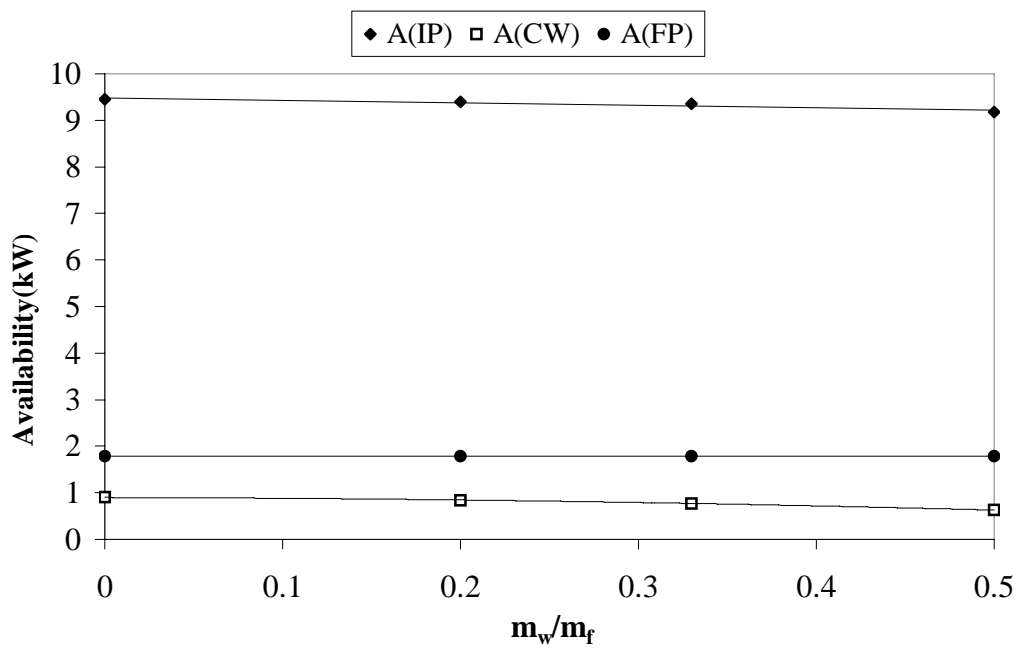


Figure 5.27: Availability versus Water Addition for Rich Mixture



Figs. 5.28 and 5.29 represent the exhaust and unaccounted availability values as a function of water addition for rich and lean mixture conditions respectively.

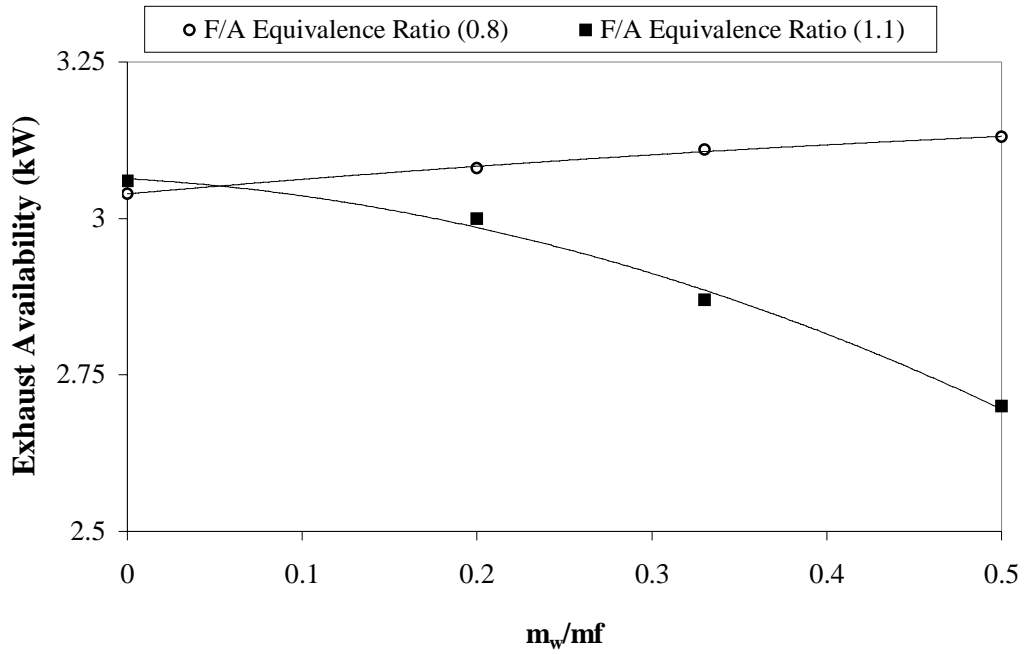


Figure 5.28: Exhaust Availability versus Water Addition for Rich and Lean Mixture

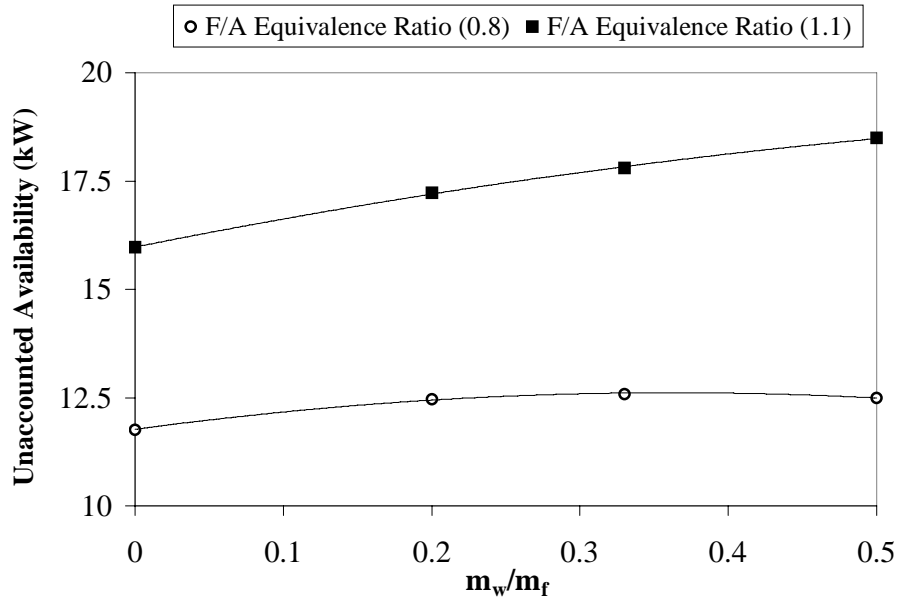


Figure 5.29: Unaccounted Availability versus Water Addition for Lean Mixture

Figure 5.30 summarizes the available energy for water to fuel ratio 0.5 at lean region. It is noticed that 47.9% of the total available energy cannot be utilized as useful work due to the irreversibility. The available energy represents 12% from the exhaust gas, while the available energy from cooling water represents only 4.4% of the total available energy.

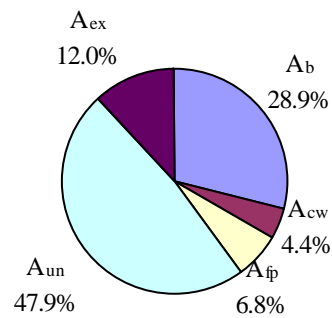


Figure 5.30: Availability Distribution for Water to Fuel Mass Ratio 0.5 at Lean Region and  $Q_{in} = 24.62$  kW

Figure 5.31 shows the variation of reversible power versus the ratio of mass rates of flow of water and fuel.

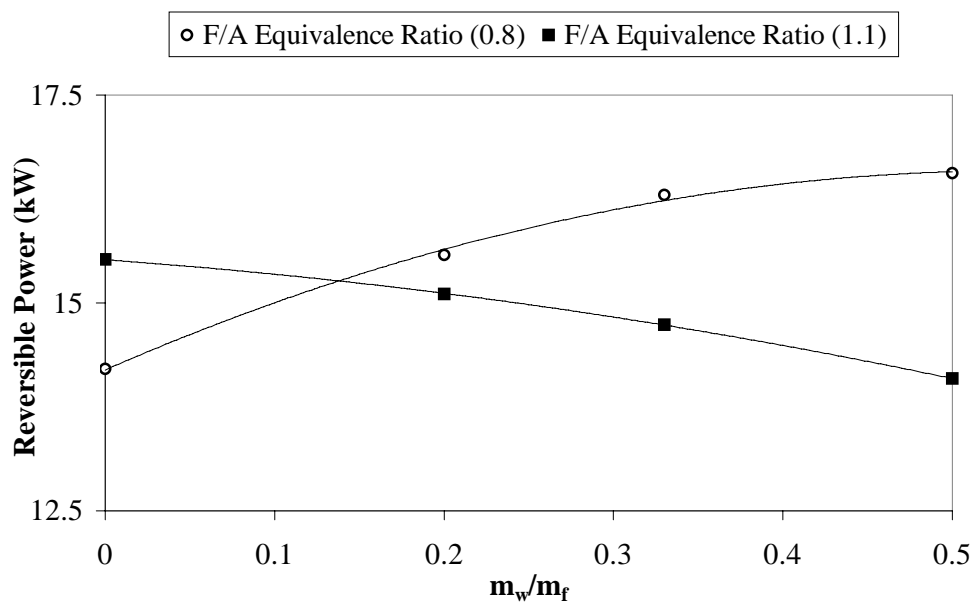


Figure 5.31: Reversible Power versus Water Addition

Reversible power increases with water addition for lean mixture as seen in this figure. The increase in cylinder temperature increases the availability of products. The temperature drop is higher for lean mixture than that for rich mixture.

Figure 5.32 shows the result of second law efficiency. The second-law efficiency is minimum at  $\phi=1.0$  where reaction reaches maximum values in temperature and in reversible work, theoretically (Alasfour, 1997). Results show the second law efficiency with water addition increases for rich mixture. But it decreases for lean mixture.

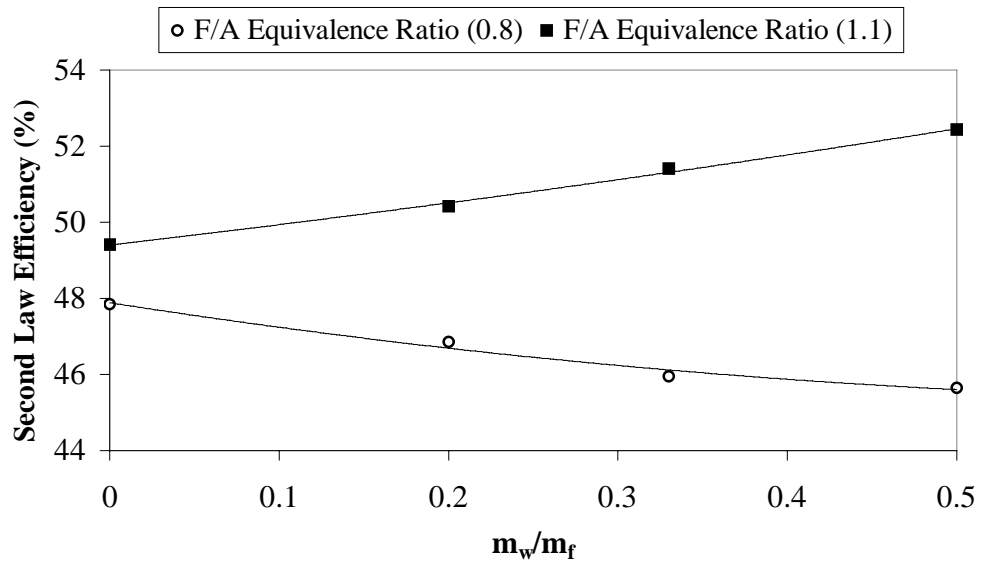


Figure 5.32: Effect of Water Addition on Second Law Efficiency

## 5.7 EFFECT OF WATER ADDITION ON THE EXERGY BALANCES

The present study describes the exergy changes with added water during the compression, combustion and expansion processes as a function of the crank angle, which runs for 360 degrees for a typical four stroke, spark ignition engine. The results of the second-law analysis of the engine operation with water addition are compared with the results of a similar analysis for cases with no water addition. This is an original work since the second law analysis is not applied.

An exergy analysis is presented for the combustion in a LPG fuelled spark ignition engine, and the effect of water addition was studied. Figure 5.33 shows the cylinder pressure as a function of crank angle with and without water injection cases. The peak pressure decreases with the amount of the injected water due to heat of vaporization and the specific heat capacity of the water. The water injection has shifted the peak pressure position slightly due to MBT spark timing. MBT spark timing causes the combustion to be completed within TDC.

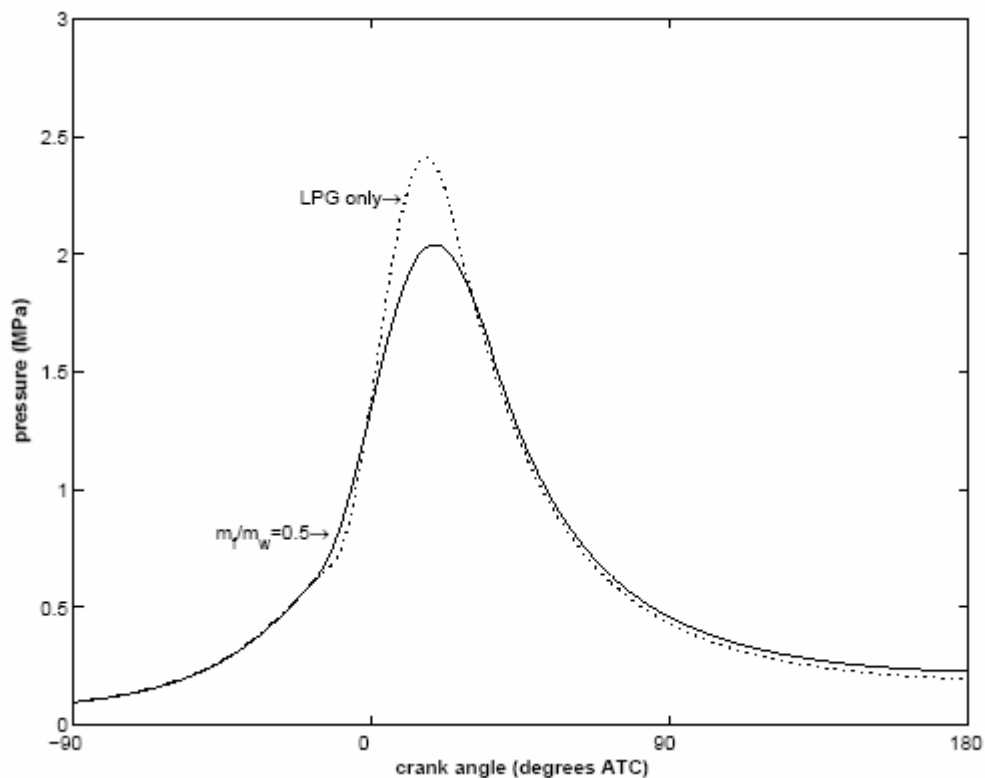


Figure 5.33: Effect of Water Injection over Pressure Traces

Figure 5.34 shows the mass fraction burned. It is found that MBT spark timing has advanced and combustion duration increased for water injection case. This result agrees with the result of Harrington (1982). His results showed that water injection leads to slow down the burning rate and it led to increase the ignition delay and combustion period.

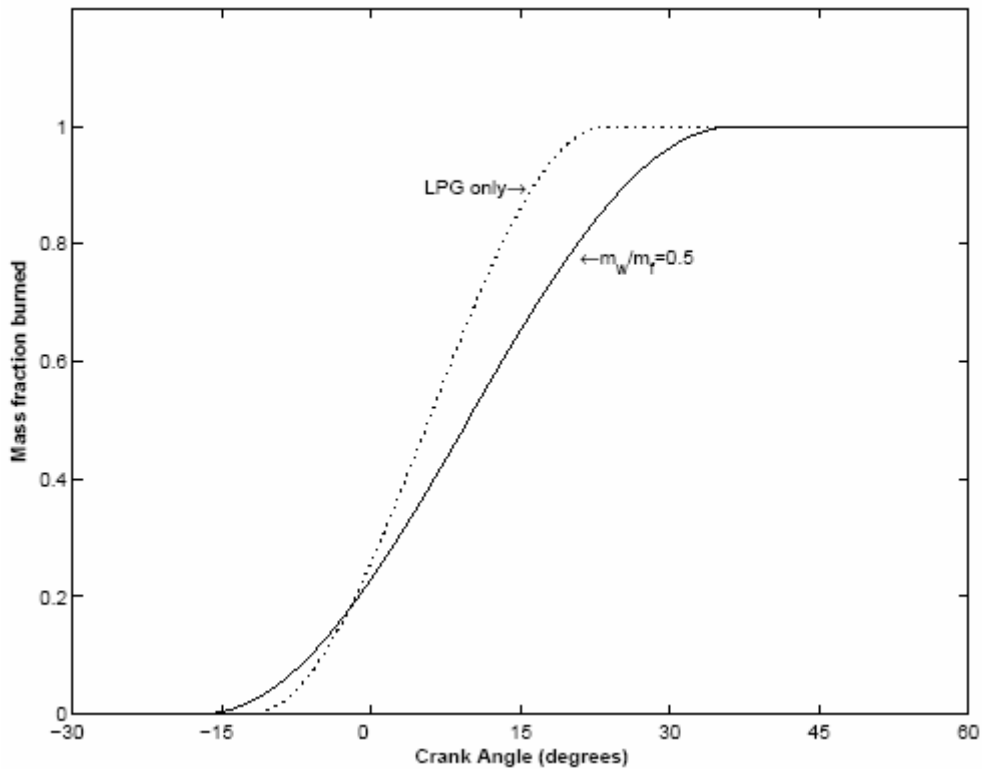


Figure 5.34: Effect of Water Injection on the Mass Fraction Burned

Figure 5.35 shows the effect of water addition on the availability transfer by work. The availability transfer due to work starts at zero, decreases due to the input work to the system during compression, and then rises to a positive value during expansion for both cases. The water addition reduces the cylinder peak pressure and temperature, causing the engine power to drop because a lesser fraction of the thermal energy ends up as useful work. Thus, this leads to a reduction in the availability work during combustion for the water injection case. In addition, the combustion period decreases the amount of work that can be extracted from the expanding gases due to the lowered cylinder pressure and prevents sharp pressure drop during expansion. Figure 5.36 shows the effect of water injection on the availability transfer by heat transfer. The availability transfer due to heat transfer also starts at zero and then increases slightly during compression. It decreases significantly after the start of combustion. It is seen from this figure that the availability transfer due to heat transfer decreases for water injection case. It is clear that the water injection decreases the heat loss during combustion and expansion due to lowered cylinder temperature.

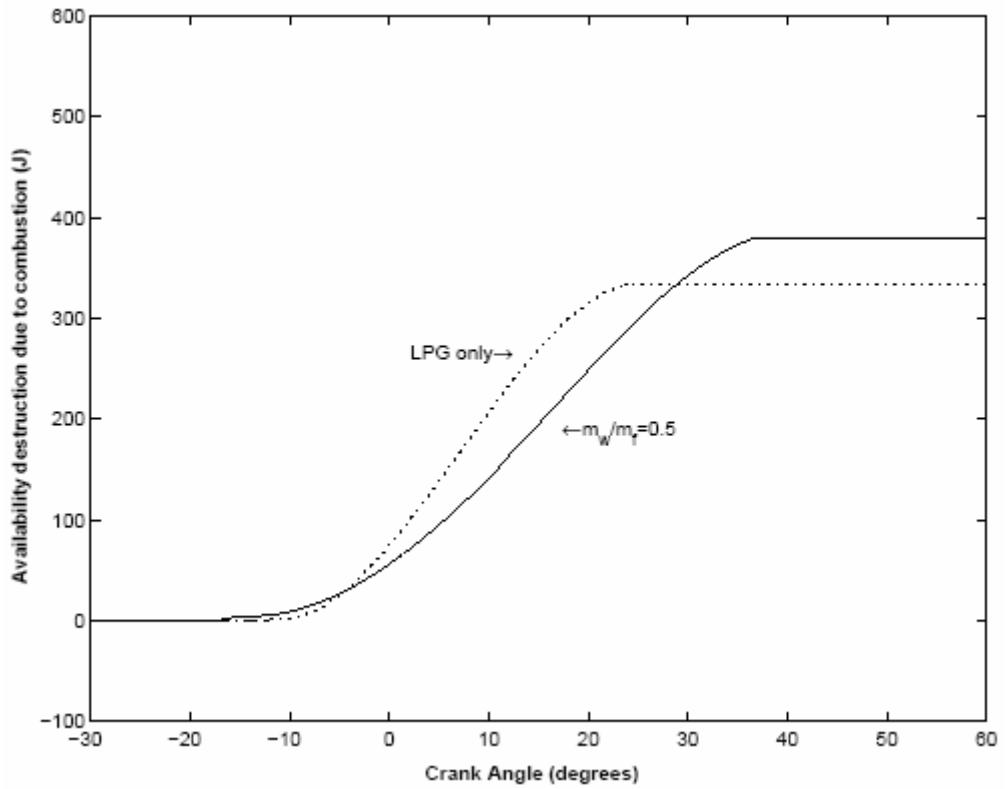


Figure 5.35: Effect of Water Injection on the Availability Transfer by Work

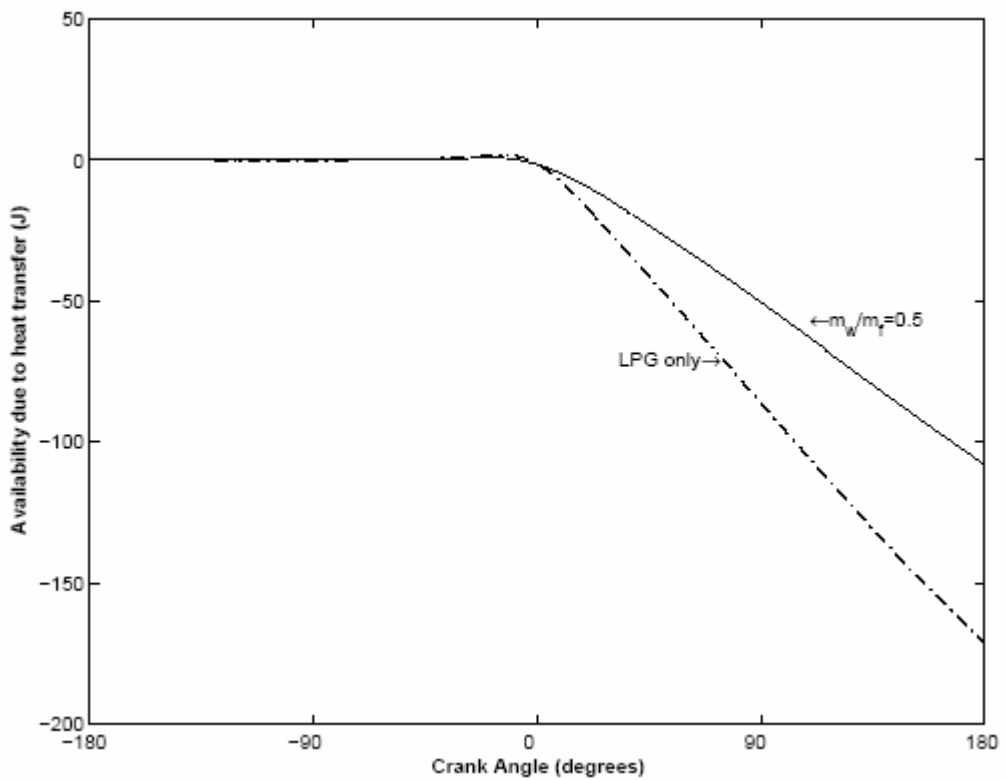


Figure 5.36: Effect of Water Injection on the Availability Transfer by Heat Transfer

Figure 5.37 shows the total system availability as a function of the crank angle. The availability transfer due to work increases slightly due to the addition of availability through the work done during compression and then rapidly decreases due to the destruction of availability during combustion, the work being extracted and the heat transfer.

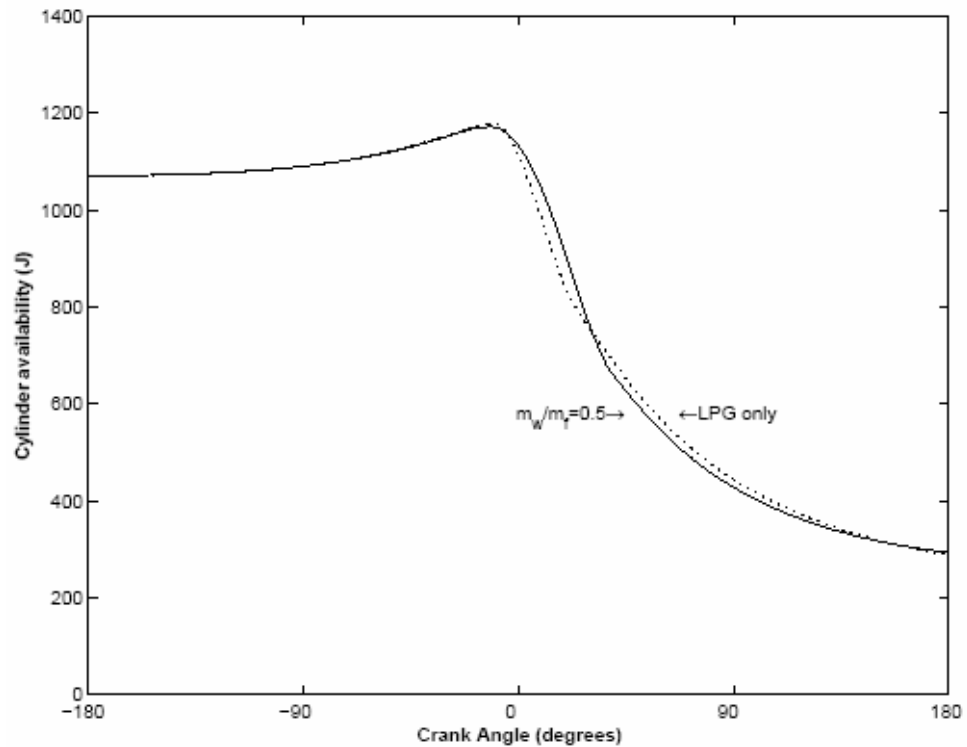


Figure 5.37: Total System Availability as a Function of Crank Angle

Figure 5.38 shows that the effect of water injection on the availability destruction as function of crank angle. The irreversibility starts out as zero and then increases to its final value during combustion. The combustion irreversibility rate is affected significantly by water injection. The destruction of availability due to combustion decreases with an increase in cylinder temperature. The combustion irreversibility at the end of combustion is 332.73 J for LPG only. It is 378.9 J for water addition case. Water injection leads to a reduction in the combustion temperature and an increase the ignition delay and combustion period.

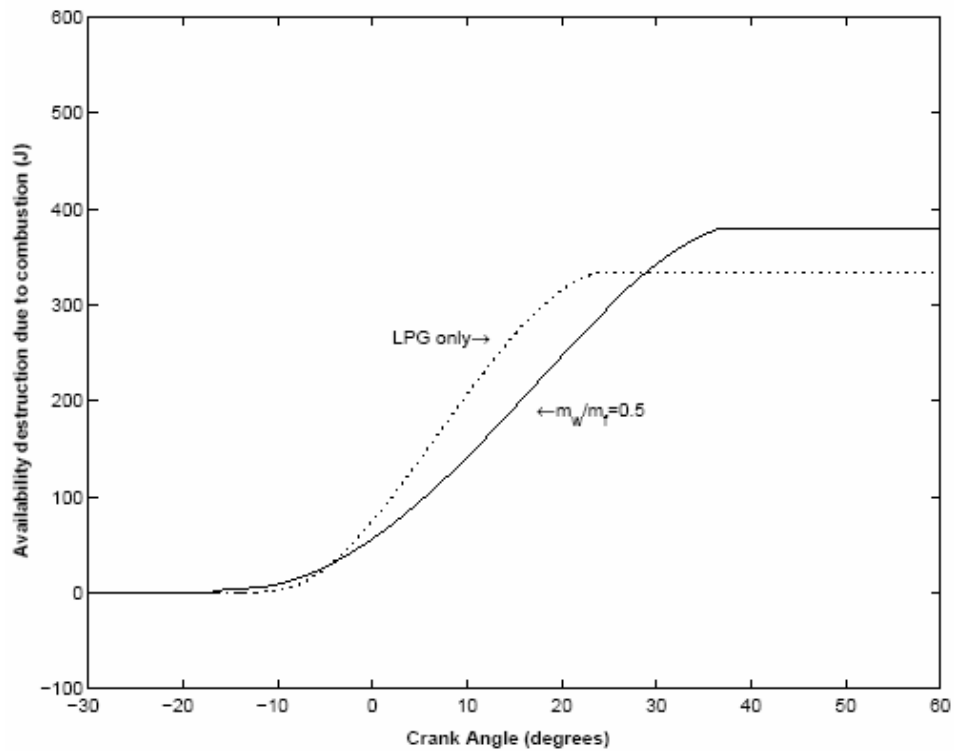


Figure 5.38: Effect of Water Injection on the Availability Destruction vs. Crank Angle

Figure 5.39 shows the terms from availability balance for no water injection case and for  $m_w/m_f = 0.5$  case. The cylinder availability increases due to the input of work to the system during compression, and then decreases due to irreversibility and heat transfer. For pure LPG case, the increase in the cylinder availability during combustion and the availability transfer due to heat transfer during combustion and expansion is greater than that for water injection case. Water injection yields to increase the combustion irreversibility.



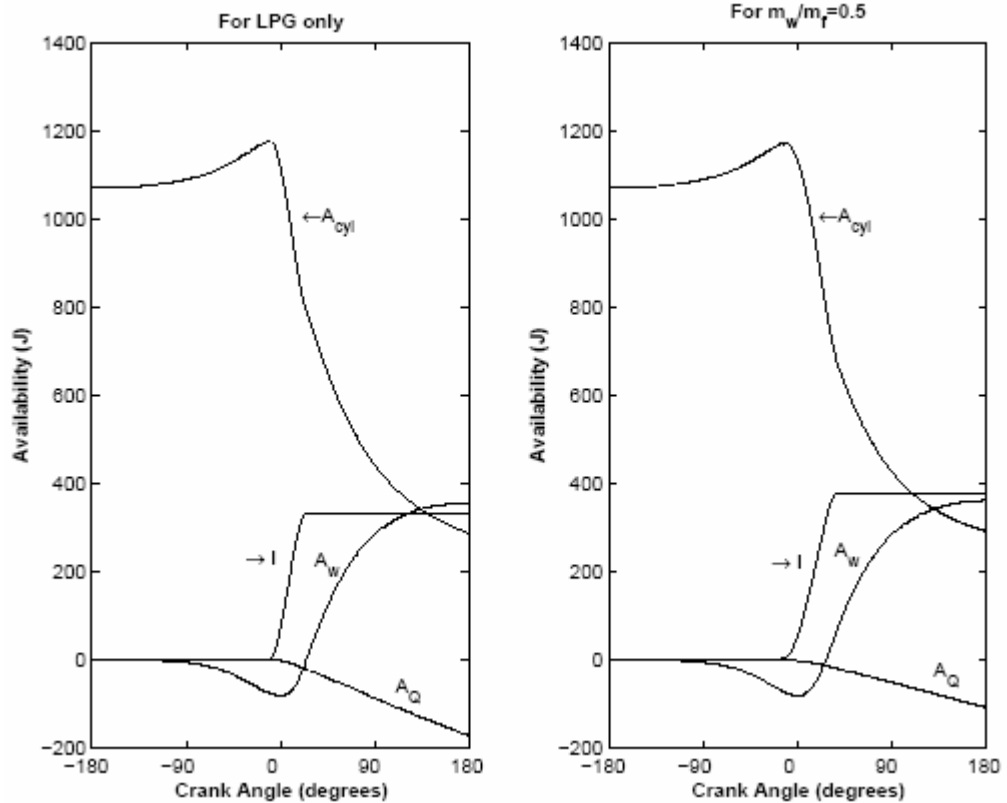


Figure 5.39: Terms of Availability Balance for No Water Injection Case and  $m_w/m_f=0.5$  Case

## 5.8 EFFECT OF STEAM WATER INJECTION

The aim of this analysis is to investigate the potential of steam injection to reduce the exhaust emissions, particularly  $\text{NO}_x$  emissions, and to examine the engine performance. A detailed analysis of previous and current results of water injection effects on the emissions and performance of spark ignition engine is introduced previously. In addition, in this part, these results are compared with the results from steam injection in Figure 5.40 to Figure 5.46. Addition of water in both the liquid state and the vapor state has a large effect on combustion, emissions, and performance. The magnitude of the effect increases as the water to fuel mass ratio increase. Effect of liquid water injection is stronger than the effect of steam injection.

Figure 5.40 shows the effect of water injection as a steam and liquid water on  $\text{NO}_x$  emission.

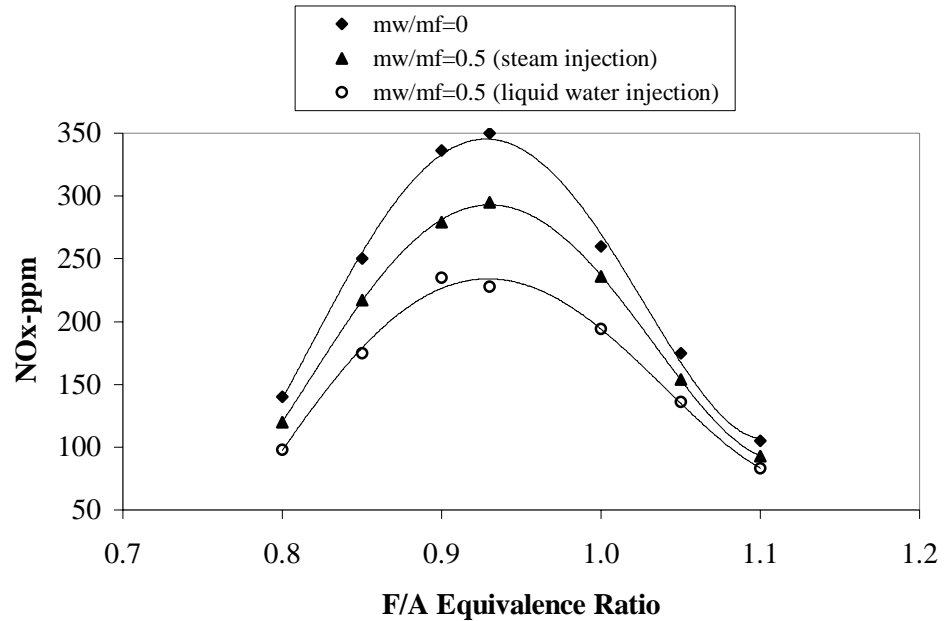


Figure 5.40: Effect of Water Injection as in the Form of Steam and Liquid Water on NO<sub>x</sub> Emission

When water is introduced in the charge air, this will lead to a reduction in the maximum combustion temperature level, but also cooling of the coldest zones in the combustion chamber. When using water in the form of steam, thermal capacity of the charge air increases. This results in lower peak temperature, and a reduction in the NO<sub>x</sub> formation. Liquid water based NO<sub>x</sub> reduction is probably preferable. Because peak reduction in NO<sub>x</sub> was about 16% with steam injection and about 35% with water injection under similar conditions. It was shown that the NO<sub>x</sub> reduction rate due to steam injection is about twice of the one due to the port water injection. It also lowered the specific fuel consumption and decreased the heat transfer from the cylinder contents to the surrounding surface.

Figure 5.41 shows the effect of water injection as in the form of steam and liquid water on HC emission and Figure 5.42 shows the effect of steam injection and liquid water injection on CO emission. Steam injection increases the HC emissions but has little effect on CO emissions. A reduction in the degree of dissociation in the high temperature burned gases, which allows more of the fuel's chemical energy to be converted to sensible energy near TDC.

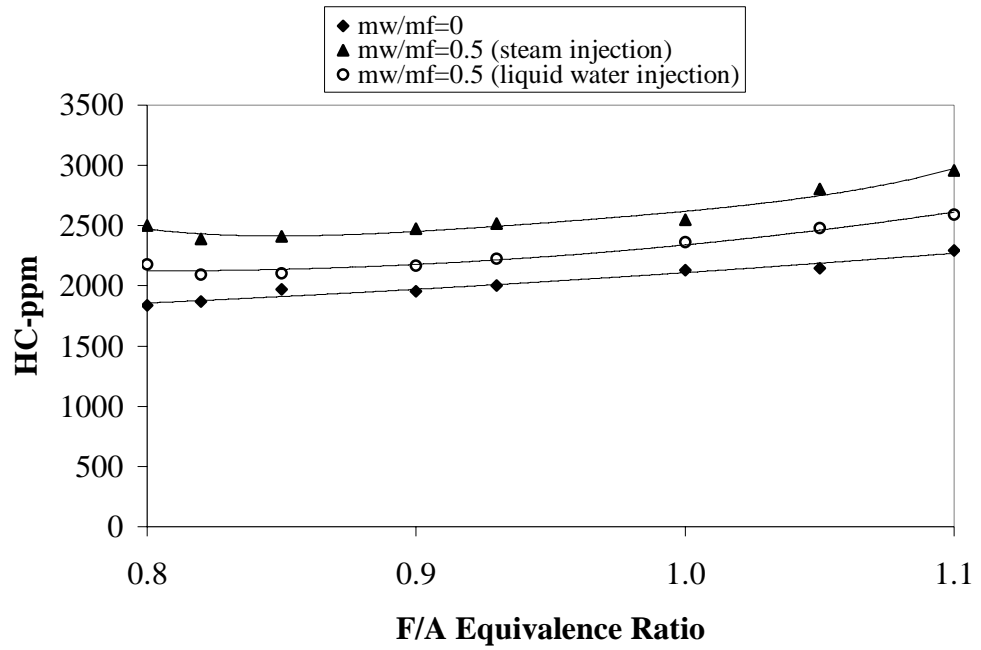


Figure 5.41: Effect of Water Injection as in the Form of Steam and Liquid Water on HC Emission

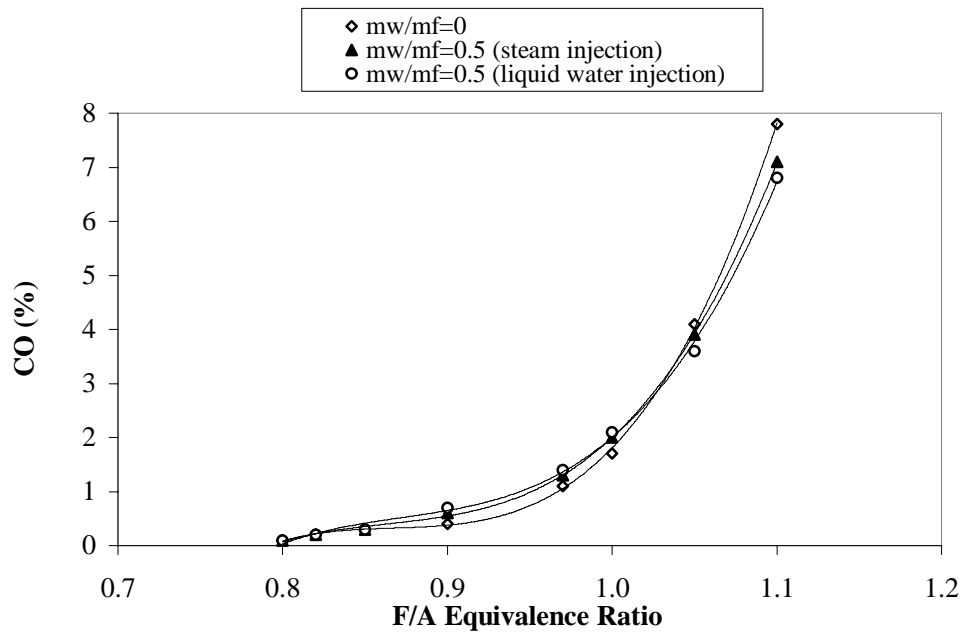


Figure 5.42: Effect of Steam Injection and Liquid Water Injection on CO Emission

Thermal efficiency is improved due to increased intake charge temperatures. Nicholls (1969) showed that nitric oxide concentration reductions of over 50% with a water-fuel mass ratio of unity. Conversely, water addition probably increases hydrocarbon emissions (Quader, 1971). Finally, with respect to carbon monoxide emissions, Kummer (1975) stated that the effect of water addition on CO emissions would be remained. Water addition is more effective for lean mixtures. The peak NO level was reduced in a small amount by steam injection. It is observed that the hydrocarbon emissions increased rapidly with water addition. In addition, injected water caused a small drop in carbon monoxide emission concentrations. This reduction was only noticeable at rich conditions where carbon monoxide levels were relatively high.

Figure 5.43 shows the effect of water injection as in the form of steam and liquid water on exhaust temperature. The temperature of the exhaust gas can be used as a tool to determine engine combustion efficiency. For instance, if engine combustion efficiency increases, then there should be more energy released in the cylinder, which will cause the exhaust temperature to rise due to more energy being lost in the form of heat.

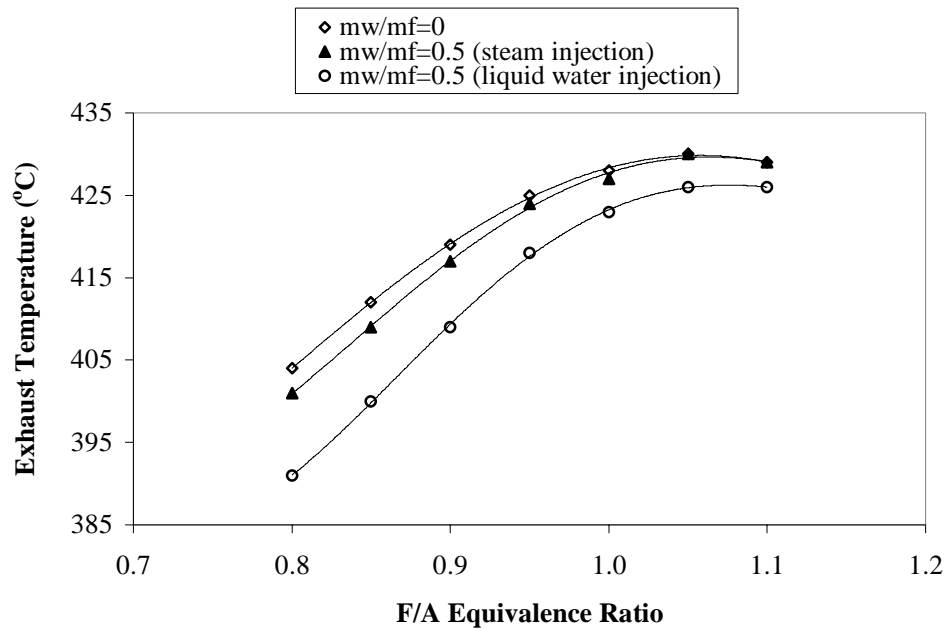


Figure 5.43: Effect of Water Injection as Steam and Liquid Water on Exhaust Temperature

The exhaust temperature did not significantly change for rich mixture conditions when water was added to the fuel. However, for lean mixture conditions exhaust temperatures decreased somewhat (Peters and Stebar, 1976).

Figure 5.44 and Figure 5.45 show the effect of steam injection and liquid water injection on combustion period and ignition delay respectively.

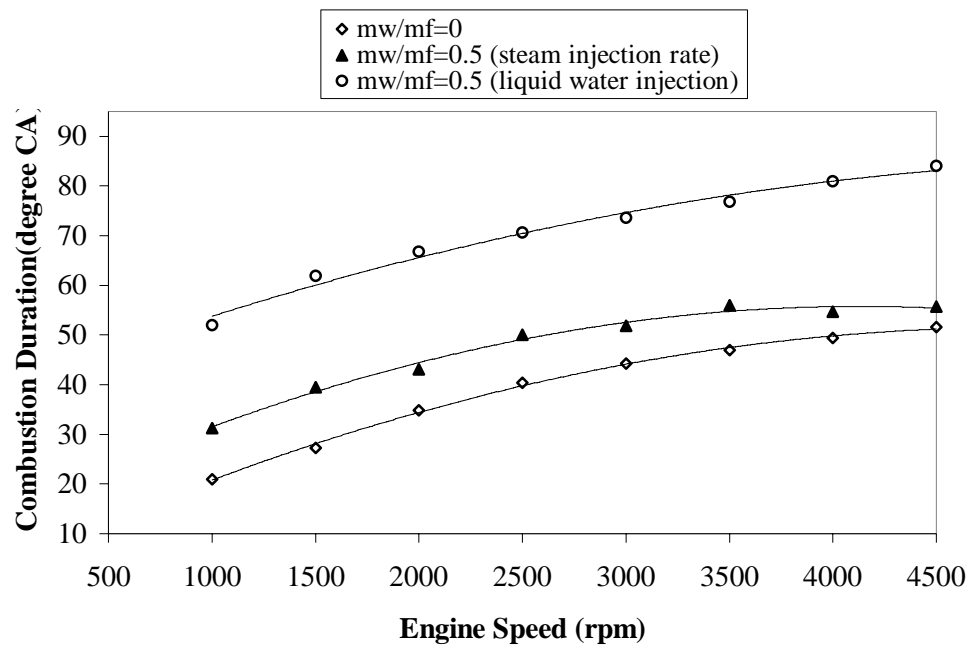


Figure 5.44: Effect of Steam Injection and Liquid Water Injection on Combustion Period

Steam injection increases the combustion duration and ignition delay. Steam injection also reduces the combustion rate. Obert (1948) and Zeilinger (1971) have showed that water addition to the reactant mixture slowed the combustion process in SI engines. Thus to maintain MBT spark settings, the timing must be advanced when using water-gasoline fuels.

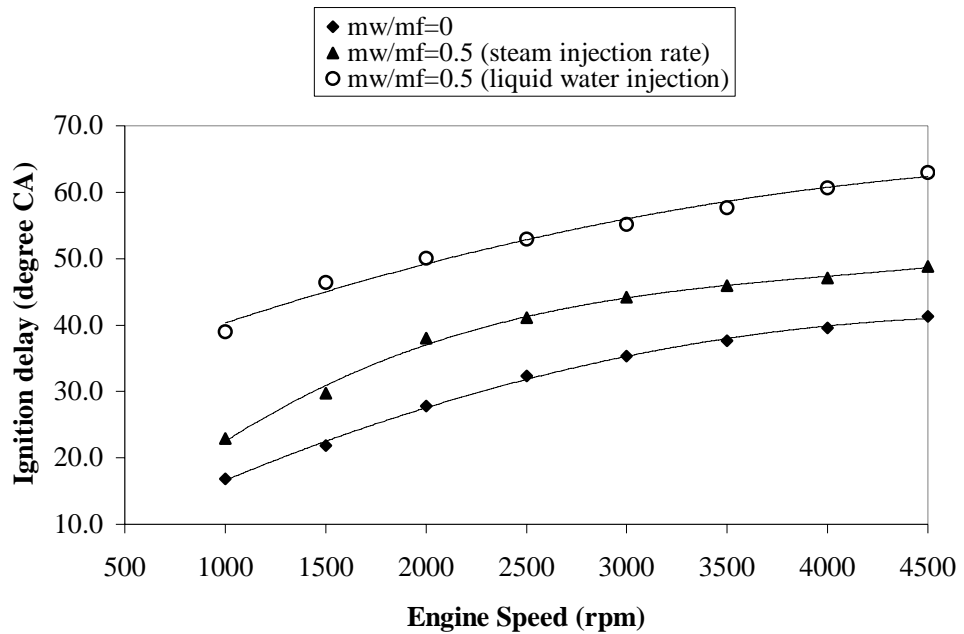


Figure 5.45: Effect of Steam Water Injection and Liquid Water Injection on Ignition Delay

Figure 5.46 and Figure 5.47 show the effect of water injection as a steam and liquid water on brake thermal efficiency and brake specific fuel consumption, respectively. Combustion temperature will decrease by the means of the very high specific heat and heat of vaporization of water. A decrease in combustion temperature will reduce the theoretical maximum possible efficiency of an Otto cycle engine that is operating correctly, but may improve efficiency in engines that are experiencing abnormal combustion for existing fuels. The steady state tests show that the brake thermal efficiency may be increased and the brake specific fuel consumption may be decreased with the steam injection. The improvement in fuel consumption with steam injection is due to three factors: firstly, reduced pumping work; secondly, reduced heat loss to the cylinder walls; and thirdly, a reduction in the degree of dissociation.

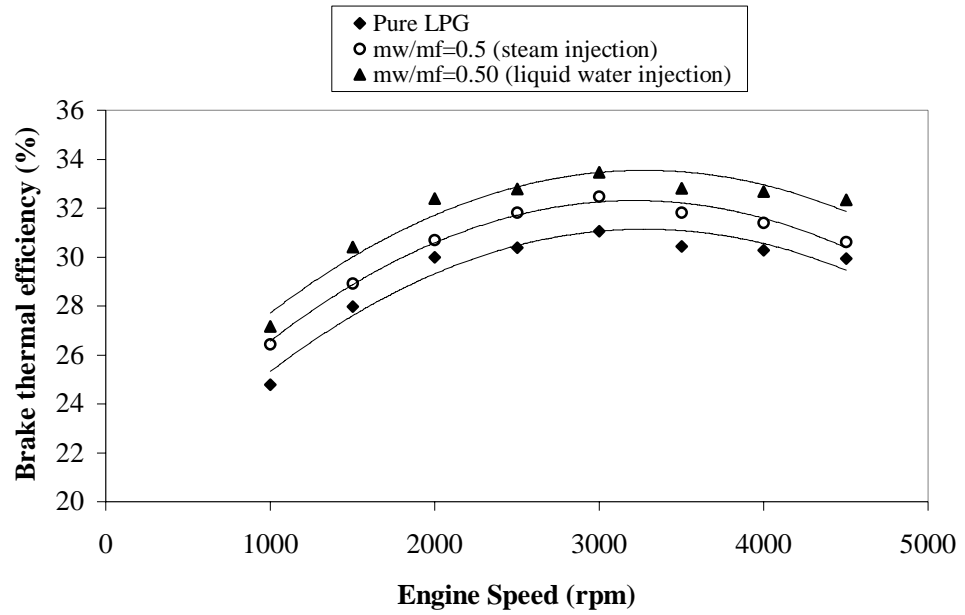


Figure 5.46: Effect of Water Injection as in the Form of Steam and Liquid Water on Brake Thermal Efficiency

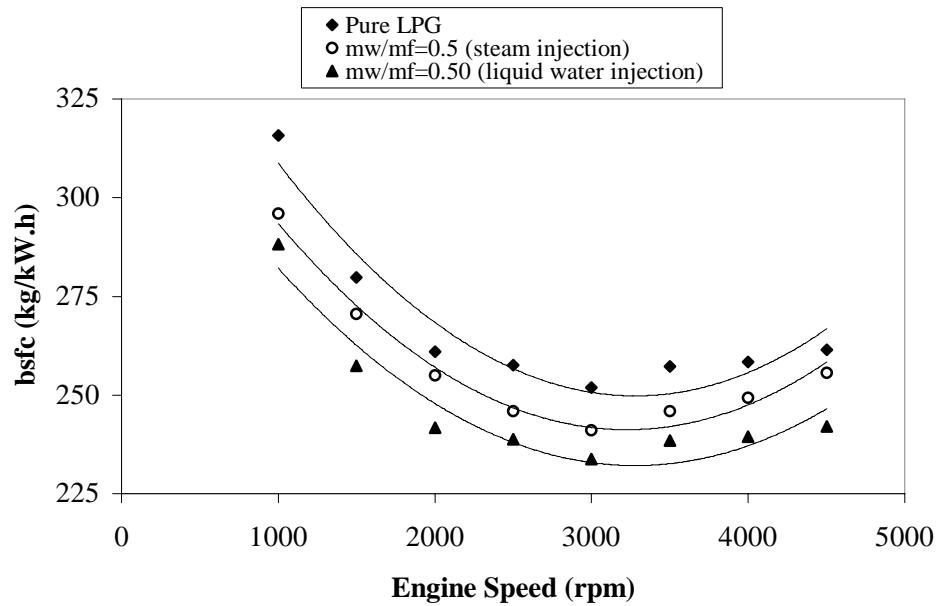


Figure 5.47: Effect of Water Injection as in the Form of Steam and Liquid Water on Brake Specific Fuel Consumption

The thermal efficiency is also improved due to increased intake charge temperatures and speed the oxidation of CO with steam injection. It is interesting to note that a dry mixture of CO and O<sub>2</sub> is almost impossible to ignite. Only when water vapor is

present a humid medium occurs it readily ignites and reacts with oxygen. Liquid water injection results in higher thermal efficiency than steam injection and makes possible lower NO<sub>x</sub> emissions. Unfortunately, despite expectations of improved efficiency, the reported gains are generally small and sometimes negative (Weiss and Rudd, 1989; Obert, 1948; Kettleborough and Quillian, 1955; so on). Fuel trend line thus for these experimental test conditions no significant improvement in indicated engine efficiencies was observed with water addition either directly to the manifold or via emulsified (Peters and Stebar, 1976). Evaporative cooling of the metal surfaces is a more efficient process and produces beneficial effects in the cycle. Also note that the fuel consumption improves from 0.65-0.54 lb/Bhp/hr for the best water injection condition. (Lestz, Melton and Rambie, 1975).

Figure 5.48 shows the effect of water injection as a steam and liquid water on volumetric efficiency. Water vapor in the intake charge also changes the thermodynamics of the intake process. As stated previously, injected water cools the hot cylinder wall and piston surfaces. It may be also change the heat gain in the fuel air charge during the intake stroke. At the end of the intake stroke the air pressure in the cylinder is actually very close to the manifold pressure. Most of the loss of volumetric efficiency is due to heating of the intake charge during the induction process. The high latent heat of evaporation and specific heat of water drastically reduce the temperature due to these processes, in addition to the outright cooling of the cylinder head, cylinder wall and piston head. A significant part of the cylinder heat losses occurs when the temperature is at its highest level. When water is added to the fuel, the cooling effect of the water is mainly exploited in the flame front and not all over the combustion chamber where additional cooling may have negative effects.



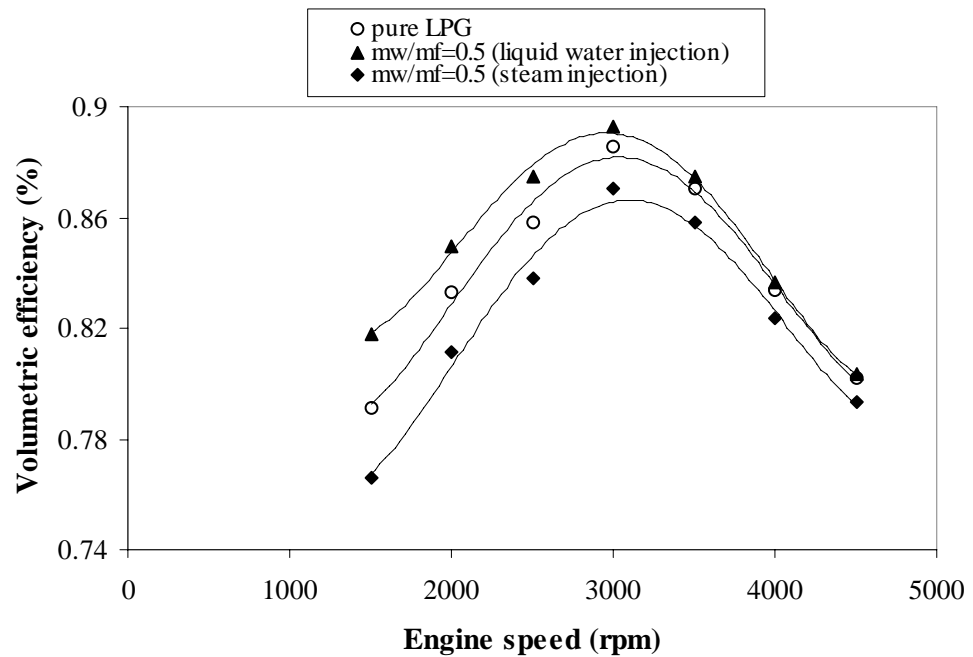


Figure 5.48: Effect of Water Injection as Steam and Liquid Water on Volumetric Efficiency

## 5.9 EFFECT OF WATER INJECTION ON THE ENGINE PARTS

Engine parts were controlled periodically after a number of test series. At the end of the water injection test, last, some engine parts were checked no severally stressed or damaged parts of the engine cylinder; piston, valves, or rings were observed due to water injection operation. This agreed with the previous investigators (Lestz, Melton and Rambie, 1975). The erosion on the exhaust manifold was only observed due to the water injection does decrease the dew point of the exhaust gases.

## 5.10 THEORETICAL CALCULATIONS

As an approximation, power produced in an engine can be assumed to be about proportional to inlet air density. Fuel is added in proportion to the mass of inlet air, and a percentage of this fuel energy is converted to power output. Inlet air density is inversely proportional to inlet air temperature. The effect of water injection

on AFT, volumetric efficiency and NO emission in the exhaust has been investigated theoretically in the first part.

The reduction in inlet air temperature due to water evaporation can be given by,

$$Q_{ev} = m_w h_{fg} = m_m C_p \Delta T = (m_a + m_f + m_w) C_p \Delta T \quad (6.1)$$

$$\Delta T = \frac{h_{fg}}{\left[ \left( \frac{m_f}{m_w} \right) \cdot \left( \frac{A}{F} \right) + \left\{ \left( \frac{m_f}{m_w} \right) + 1 \right\} \right] C_p} \quad (6.2)$$

Temperature of the air entering the engine after water evaporation

$$T_{with} = T_i - \Delta T \quad (6.3)$$

This approximate engine power with water injection is now increased by reduction in temperature.

$$\left( \dot{W} \right)_{with} = \left( \dot{W} \right)_{without} \left( \frac{T_{without}}{T_{with}} \right) \quad (6.4)$$

Above value is reduced somewhat when some of the mixture is displaced by water vapor. Engine output power is then:

$$\left( \dot{W} \right)_{output} = \left( \dot{W} \right)_{with} \left( \frac{N_m}{N_m + N_{vapor}} \right) \quad (6.5)$$

Figures 5.49 to 5.54 show the effect of water addition on output power, theoretically. It is calculated in Figure 5.49 where the effect of water addition on stoichiometric mixture of LPG shown. The density in the cylinder changes due to flow does not change, after the inlet valve closes.

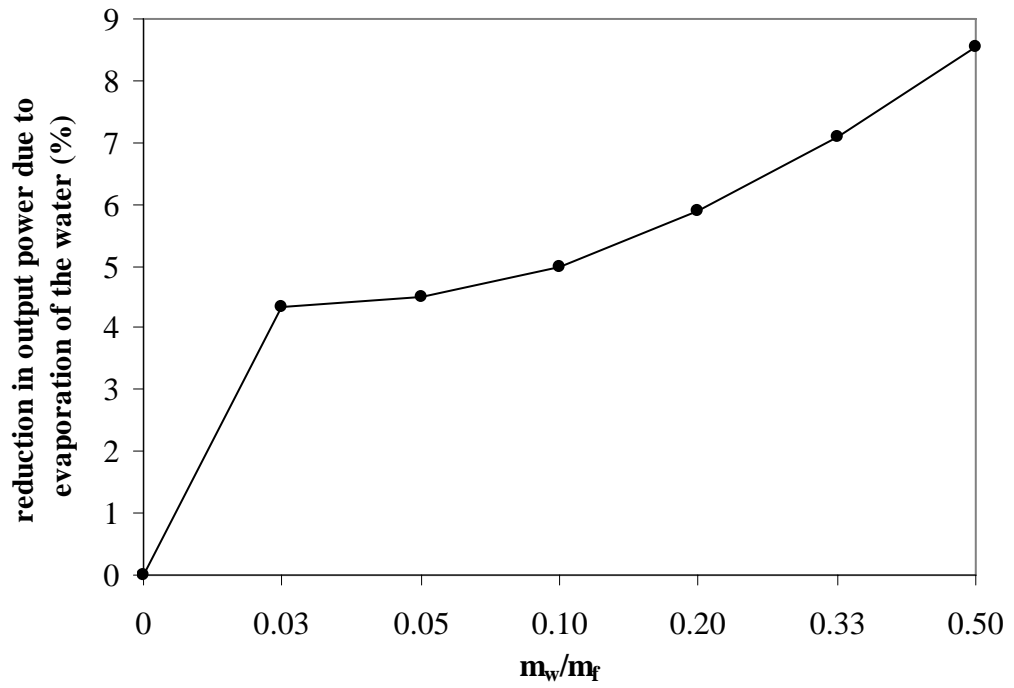


Figure 5.49: Percent Reduction in Output Power due to Evaporation of the Water

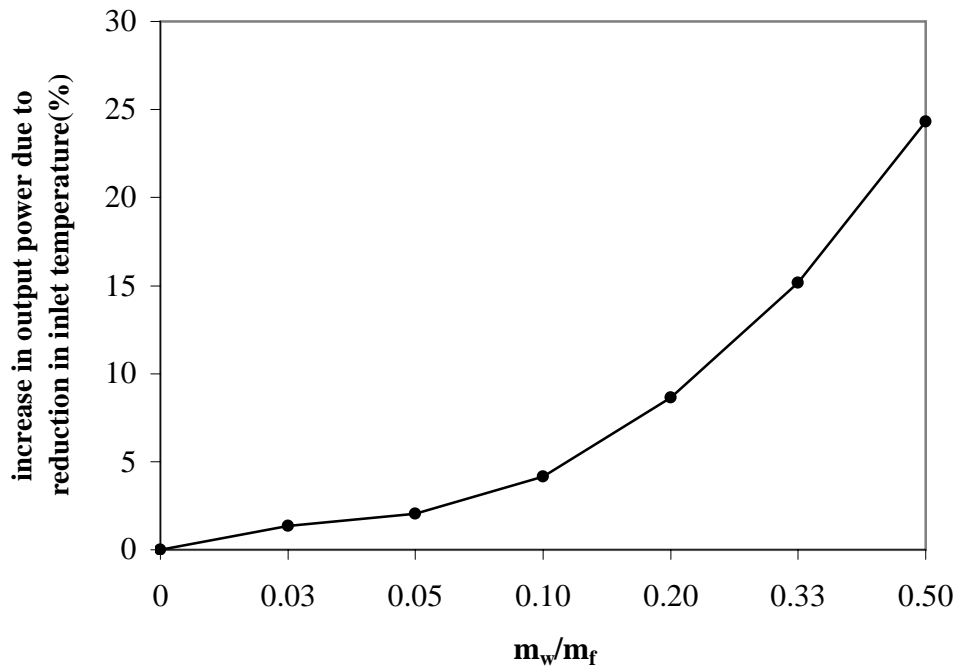


Figure 5.50: Percent Increase in Output Power due to Reduction in Inlet Temperature

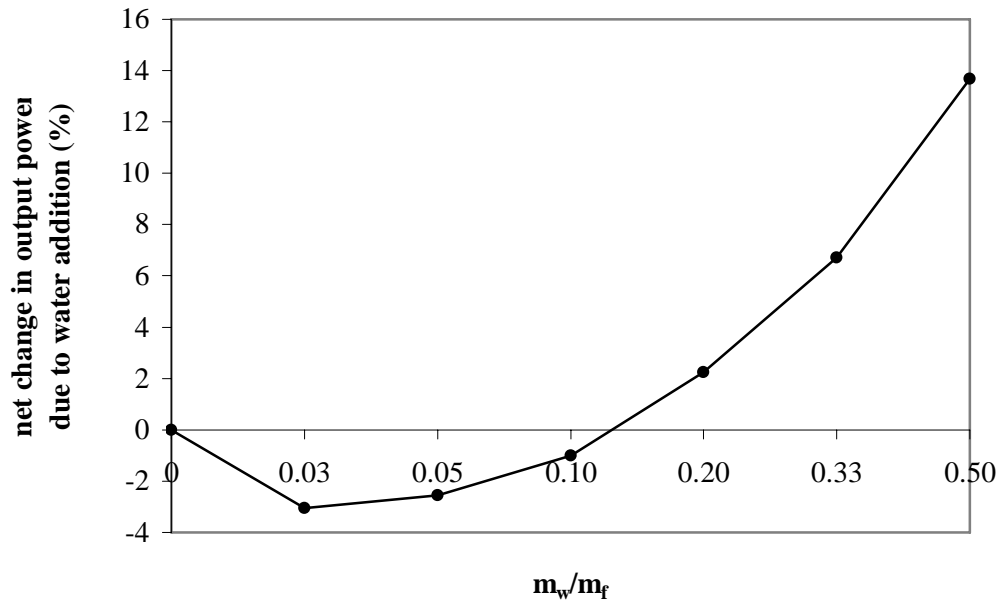


Figure 5.51: Net Change in Output Power due to Water Addition

If the water evaporates in the manifold, it cools the air, but also displaces it with water vapor, having a net reduction or increase in air density, consequently also reducing or increasing the mass of oxygen in the charge in the manifold.

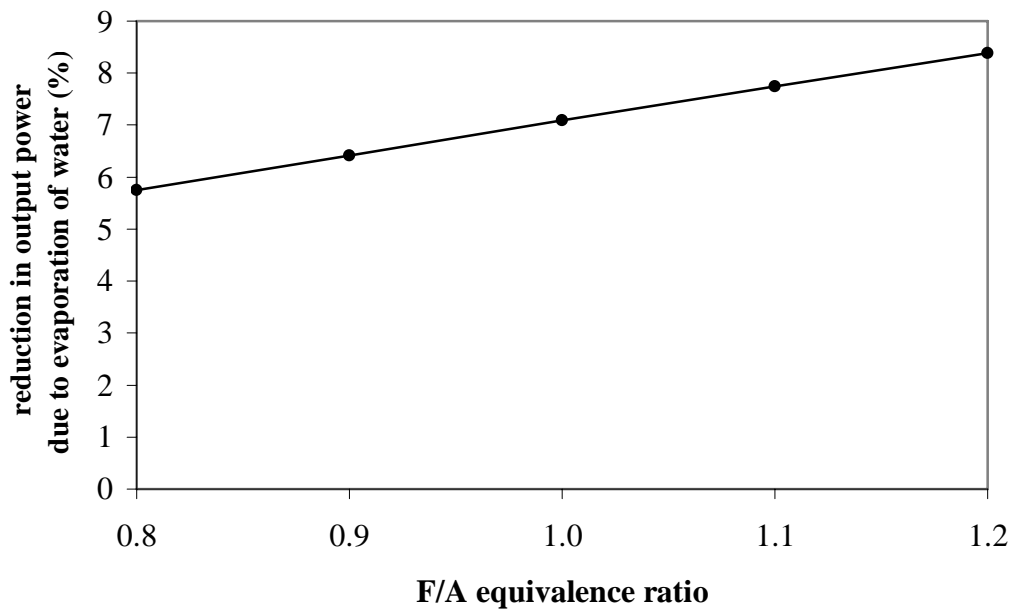


Figure 5.52: Percent Reduction in Output Power due to Evaporation of Water for 1/3 Water to Fuel Mass Ratio as Function of F/A Equivalence Ratio

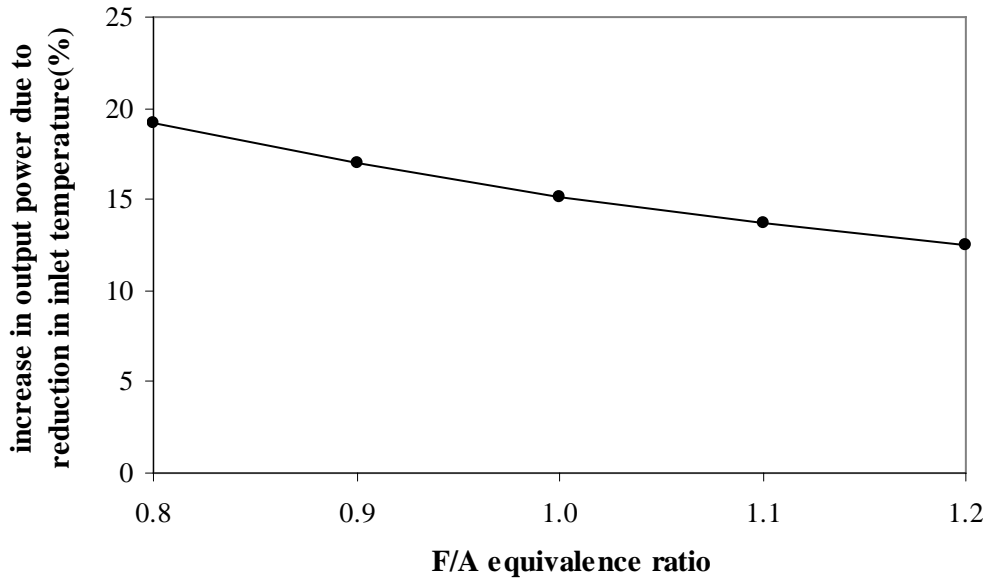


Figure 5.53: Percent Increase in Output Power due to Reduction in Inlet Temperature for 1/3 Water to Fuel Mass Ratio as a Function of F/A Equivalence Ratio

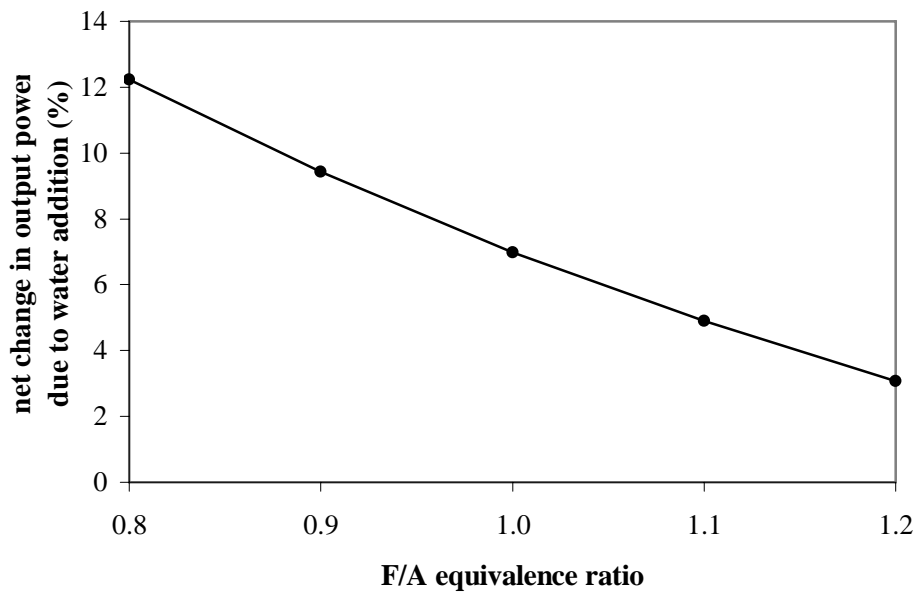


Figure 5.54: Percent Net Change in Output Power due to Water Addition for 1/3 Water to Fuel Mass Ratio as a Function of F/A Equivalence Ratio

Theoretically, water addition could either increase or decrease volumetric efficiencies, depending on the vaporization process and on whether the energy for

vaporization comes from the mixture or the exposed engine surface. It was observed in volumetric efficiency changes ranging from about 3% loss to a 13% gain were computed using a sample of the water addition data for water to fuel ratio range studied. Obert (1948) observed a 2% loss with a 50% water addition level. It was observed that water input caused a slight but sustained increase (2-3%) in volumetric efficiency, increases occur due to change and engine metal cooling, while decrease one due to the formation of steam on the intake stroke (Lestz, Melton and Rambie, 1975). Results show that power output was higher increase at lean mixture with water injection. This is due to the volumetric efficiency increase was dominant at this condition.

Heat of rejection by the combustion of a hydrocarbon fuel with air is the difference between the total enthalpy of the products and the total enthalpy of the reactants.

$$Q = \sum_{\text{prod}} N_i h_i - \sum_{\text{react}} N_i h_i \quad (6.6)$$

An estimation of the maximum temperature reached in an IC engine can be obtained by calculating the adiabatic flame temperature of the input air-fuel mixture. This is done by using above equation and setting  $Q=0$ . The reductions in AFT results in Table 5.7 are calculated by using enthalpy values that are obtained from (Raznjevic, 1976).

Table 5.7: Theoretical Calculations

$\frac{m_f}{m_w}$	$\Delta T_{\text{GAS}} \text{ (K)}$
0	0
3	142.5
4	105
6	88.6
8	78.6
10	72.6
12	68.5
14	65.5

During combustion, Nitrogen from the combustion air or fuel is converted to nitrogen containing pollutants such as NO, NO<sub>2</sub>, N<sub>2</sub>O, NH<sub>3</sub> and HCN. NO from combustion system results from three main processes: Thermal NO, prompt NO and fuel NO. Production of NO<sub>x</sub> in the cylinder depends on the fuel/air equivalence ratio, maximum cycle temperature, and combustion rate. The higher the temperatures or the higher combustion rate, the more NO<sub>x</sub> will be produced.

Zeldovic and Raizer (1966) studied the mechanism of NO formation from atmospheric nitrogen. They showed NO formation to rise exponentially with temperature.

$$\frac{d(NO)}{dt} \approx \exp(-E/RT), E/R=123000 R \quad (6.7)$$

Williams (1965) introduced the following equation for the flame temperature.

$$T_{fl} = T_f + \frac{1}{C_p} \left\{ \frac{(Q-L) \frac{Y_{ox}^\infty}{i} + C_p (T_\infty - T_f)}{\left(1 + \frac{Y_{ox}^\infty}{i}\right)} \right\} \quad (6.8)$$

Wilson, Muir and Pelliccitti (1974) re-arranged this expression by using below assumption,

1. Infinitely fast irreversible hydrocarbon oxidation,
2. Dissociation not considered,
3. Single C<sub>p</sub> common to both sides of the flame,

Based on these expressions, relative NO formation rate is given in Table 5.8 at the diffusion flame surface with different amounts of water injection. It was observed that production on NO<sub>x</sub> in the cylinder depends on the maximum cycle temperature. The higher the temperature, the more NO<sub>x</sub> will be produced.

For LPG fuel, T<sub>f</sub>=415 R, Q=21570 Btu/lbm, L=192.5 Btu/lbm and i=3.64 are taken. The required data for using calculation are taken from (Raznjevic, 1976).

Table 5.8: Calculated NO Formation Rate and  $T_{fl}$

$m_w/m_f$	$T_\infty$ (R)	$T_{fl}$ (R)	Calculated relative, $\frac{dNO}{dt}$
0	1260	4854,6	1
1/14	1218,6	4736,7	0,532
1/12	1213,2	4731,3	0,516
1/10	1204	4723,9	0,496
1/8	1190,2	4713,12	0,467
1/6	1167,2	4695,1	0,423
1/4	1131,2	4665,6	0,358
1/3	1089,2	4598	0,243

Figure 5.55 shows the theoretical Results of water addition quantity on the cycle temperatures.

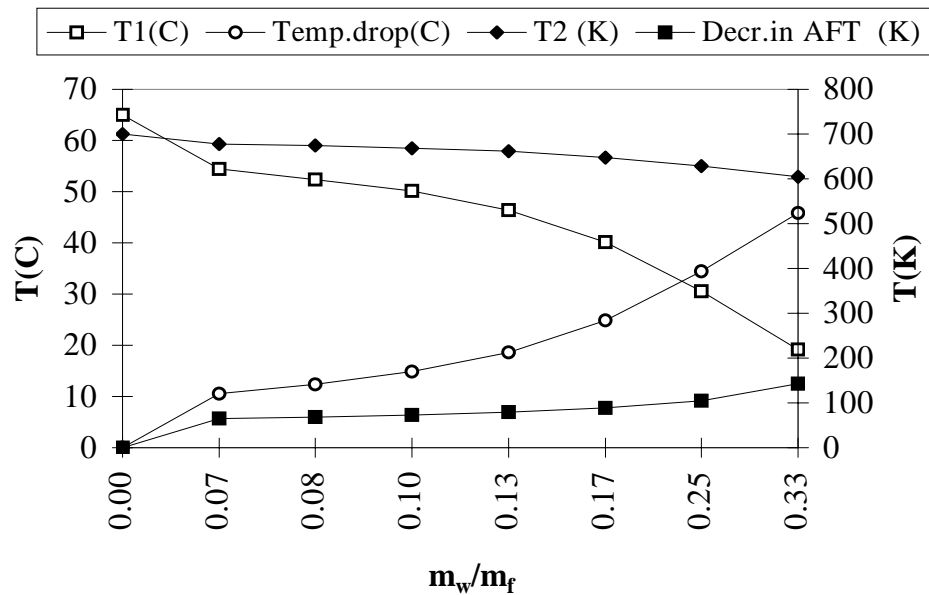


Figure 5.55: Theoretical Results of Water Addition Effect on  $T_1$ ,  $T_2$ , AFT and Temperature Drop of Inlet Air

Figure 5.56 show that water injection significantly affected  $NO_x$  production. First, when water is introduced in the charge, this will lead to a reduction of the maximum combustion temperature level, but also cooling of the coldest zones in the combustion chamber. The temperature levels at these locations are not high enough



to produce significant NO<sub>x</sub>, and the gases lose energy that could be transformed into mechanical work. On the other hand, the water vapor in the intake manifold will act as diluents for the combustion charge, reducing the flame temperature, and therefore, the reaction rates for forming NO.

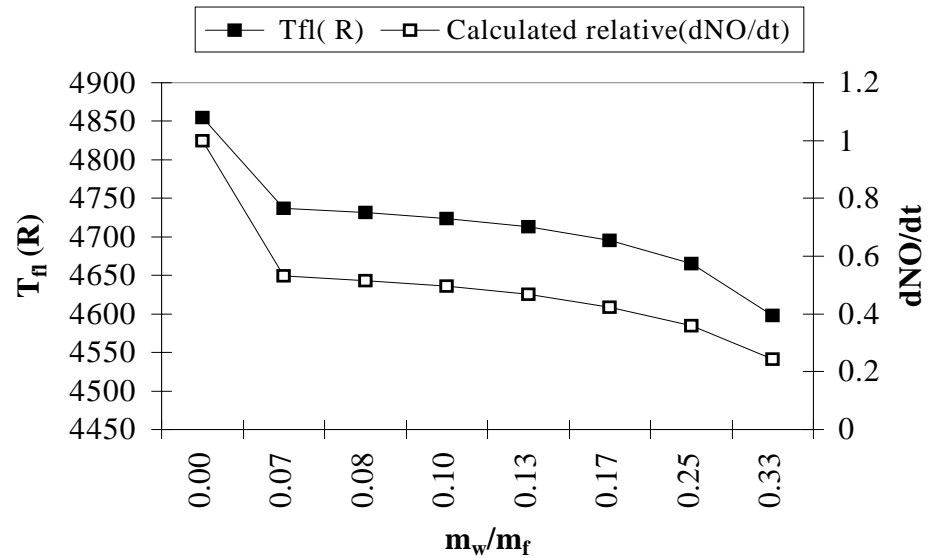


Figure 5.56: The Calculated the Relative NO Formation Rate at the Diffusion Flame Surface with Different Amount of Water Injection

Second, the dilution effect will slow down the fuel-burning rate, moving the average combustion later in the cycle where temperatures are lower due to the expansion cooling. Third, for a carbureted engine, an approximately fixed volume of air including humidity flows into the engine at a given throttle position. Water vapor displaces dry air, and therefore, increased humidity enriches the (dry) A/F of the engine, which effects all engine emissions.

The second part is included the second law analysis of the thermodynamics for Otto cycle with water injected working fluid. The stoichiometric combustion is assumed in the calculations. The exergy analysis was given below. Reversible work is defined as the maximum work that can be extracted from a thermodynamic system (Alasfour, 1997). Then the second law efficiency is defined as

$$\eta_{II} = \frac{W_b}{W_{max}} \quad (6.9)$$

Figure 5.57 shows the effect of water injection on the second law efficiency of an Otto cycle. Results show that the amount of water increases, the second law efficiency decreases.

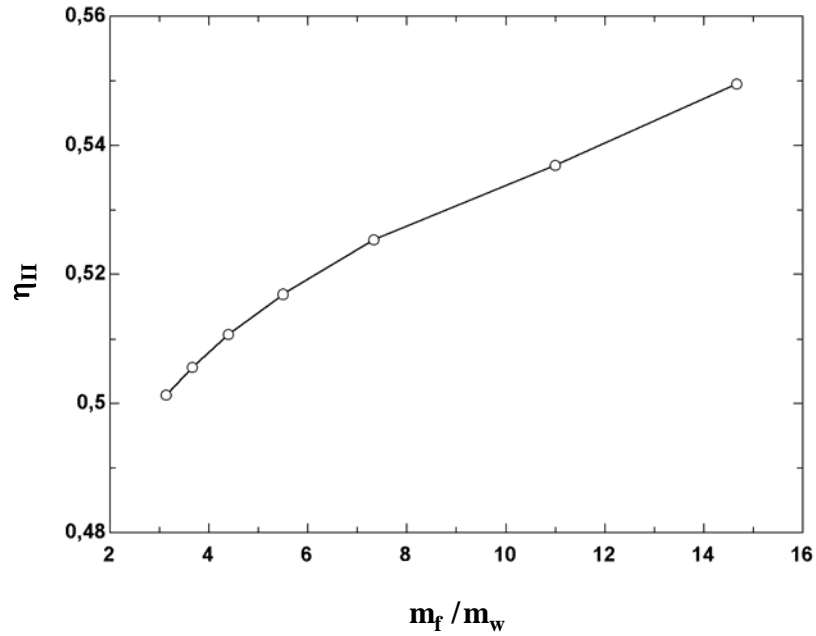


Figure 5.57: Effect of Water Injection on the Second Law Efficiency of the Otto Cycle

Figure 5.58 shows the effect of water injection on maximum work, actual work and lost work of combustion process for an Otto cycle.

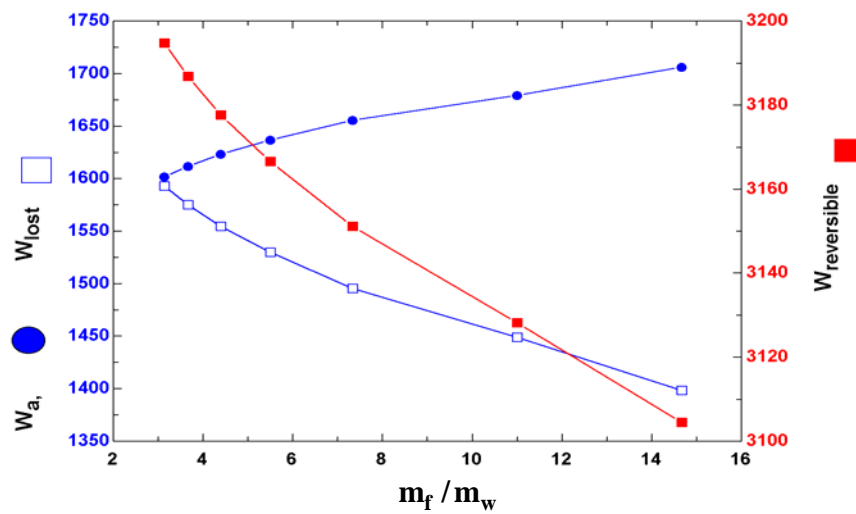


Figure 5.58: Effect of Water Injection on Maximum Work, Actual Work and Lost Work of Combustion Process in kJ for an Otto Cycle.

Present theoretical analysis shows that the reversible work decreases as the amount of injected water increases. This is due to reduction in the cycle temperature with water injection. The decrease in reversible work was reduced the second law efficiency.

## 5.11 CONCLUSIONS

The effect of water addition on the first and the second law efficiency of LPG fueled engine were investigated for both lean and rich fuel air mixture-operating conditions. This was the first study for water addition process that the calculated availability based on experimental measurements has been investigated. Following conclusions are drawn:

1. The optimal energy utilization as a useful work for the water to fuel ratio range studied is obtained for lean mixture and  $m_w/m_f = 0.5$ . But, water addition content must be decreased for energy utilization as a useful work for rich mixture. Brake thermal efficiency tends to increase with the increase in water addition rate for lean mixture. This is because injected water reduces the compression work due to the drop in the gas pressure and reduces the abnormal combustion.
2. The second law efficiency for the engine shows a reduction of 2.2% for lean mixture. But this second law efficiency shows an increase of within 3.01% for rich mixture. This is mainly because reversible work slightly increases with water addition in lean mixture region due to temperature profile. Conversely, reversible work tends to decrease with water addition for rich mixture.
3. Energy analysis shows that 37.9% of the fuel energy can be utilized as an indicated power at this specific point, while the availability analysis shows that 52.1% of fuel energy can be utilized as useful work for lean mixture and  $m_w/m_f = 0.5$ .

A computer program for test engine was prepared for the analysis of the first and the second law parameters by water injection. The followings are concluded.

1. The peak pressure decreases and peak pressure position shifts slightly by the affect of injection water.
2. The availability transfer due to heat transfer decreases as a result of the injection of water.
3. The combustion irreversibility rate is affected significantly with water injection. Combustion irreversibility increases as the amount of water injection increases.
4. The cylinder availability decreases during combustion and increases during expansion process as soon as the water is injected.

The experimental research investigated the effect of water injection on the engine performance and exhaust gas temperatures of a commercial SI engine. The following conclusions are drawn from this investigation:

1. As the water to fuel mass ratio increases up to 0.5, the engine torque, power and brake thermal efficiency increase.
2. The BSFC and the exhaust gas temperature decrease as the water to fuel ratio by mass increases.
3. The results indicate that the addition of water into the intake manifold reduces the compression work. The engine torque, power and brake thermal efficiency increase as the water to mass ratio increases. The average increase in the brake thermal efficiency for 0.5 water to fuel mass ratio is approximately 2.4% over the use of LPG only for the engine speed range studied. It was also found that the proper brake specific fuel consumption and gases exhaust temperature decrease as the water to mass ratio increases.
4. Calculated results show that the ignition delay and combustion duration was strongly affected by water injection rate. The ignition delay and combustion duration increase with the water injection. The ignition delay and combustion duration increase rapidly at low engine speeds.

Several different combustion parameters were affected with water injection. Based on the experimental test, the following conclusions are drawn on the effects of water addition.

1. During combustion process, all water is converted to steam. These steam particles get in between fuel and oxygen molecules, which slow combustion and the pressure, raise rate. The presence of water vapor in the combustion process fundamentally changes the chemistry of the combustion process. Specifically it accelerates the oxidation of the CO.
2. The ignition delay and combustion duration increases with the water injection. The ignition delay and combustion duration increases rapidly at low engine speeds.
3. Experimental results show that water injection leads to an increase in the range of ignition timing.
4. Combustion slows down by the water injection. This gives a peak pressure position that occurs too late.
5. The presence of water leads to shift the peak pressure position. Combination of water injection and the spark-advance can increase the engine torque.
6. Injected water to cylinder may reduce pumping work.
7. It was observed that water injection reduced heat loss to the cylinder walls.
8. Water injection may be cause a reduction in the degree of dissociation.
9. Water vapor in the cylinder has additive effect an expansion work.

The potential of steam injection on the exhaust emissions and performance parameter were investigated. Based on the engine test, the following conclusions may be drawn:

1. The magnitude of effects on combustion and exhaust emissions is much larger with water as in the form of liquid than that for steam due to the high latent heat of vaporization of water.

2. Liquid water injection based  $\text{NO}_x$  reduction is probably preferable since it was shown that the  $\text{NO}_x$  reduction rate due to steam injection is about half of the one due to the port water injection.
3. Steam injection causes a loss of volumetric efficiency due to heating of the intake charge during the induction process.
4. The steady state tests show that the brake thermal efficiency increased and the brake specific fuel consumption decreased with steam injection.
5. The steam injection results in the reduction of CO emission even in the increase of HC emission.
6. Steam injection increases the combustion period and ignition delay and reduces the combustion rate.
7. Steam injection reduces the exhaust gas temperature.

The effect of water injection on the engine parts were investigated at the end of engine test and the following conclusions are drawn:

1. No severally stressed or damaged parts of the engine cylinder; piston, valves, or rings were observed due to water injection operation.
2. The erosion on the exhaust manifold was only observed due to the water injection.

The present experimental study showed that water addition has a significant effect on the percentage heat losses from the engine. The following conclusions are drawn from this experimental investigation.

1. Since both the exhaust gas temperature as well as the peak cylinder temperatures, were lower in the case of water added operations, there was less heat loss through these channels, and as such, more useful work was available at the engine crankshaft.
2. As the water to fuel mass ratio increases, the unaccounted losses increases slightly.
3. The thermal efficiency increases as the water to fuel mass ratio increases due to the decreases in brake specific fuel consumption.

The effect of water addition on exhaust emissions of LPG fuelled SI engine was investigated experimentally. In the experimental measurements, water was added into the fuel air charge at the intake manifold with the induction method that are presumably the simplest and the most effective method. The following conclusions are drawn from the experimental measurements to investigate the effect of water addition on exhaust emissions with LPG fuels:

1. CO concentration is slightly affected by different water addition rates. This yields to a small drop in rich fuel-air mixture region. In addition, CO concentration slightly increases with water addition at lean fuel-air mixture region.
2. HC emissions increase with all water addition level for all equivalence ratios.
3. The experimentally observed reduction in  $\text{NO}_x$  levels by water injection for all cases in the rich mixture is significant than that for lean mixture.
4. The knock and misfiring occur at more advanced ignition timing by water injection. But, excessive amount of water addition relative to fuel air mixture mass caused to additional misfiring.
5. The exhaust gas temperature is reduced for all equivalence ratio values by increasing the amount of water addition. This reduction is more significant for lean mixture case as compared to rich mixture case.
6. Water addition to intake port seems as a simpler method of EGR since injected water certainly dilutes the charge, exactly as EGR does. But, due to the higher latent heat of evaporation of water, the magnitude of effects on combustion and emissions is relatively different.

A basic theoretical analysis was considered for the effect of water addition on engine power and second law efficiency and the following conclusions are drawn.

1. Results show that the percentage of available energy decreases as the amount of water addition rate increases due to decrease in AFT theoretically.
2. Results show that amount of water increases, the second law efficiency decreases. This is due to reduction in reversible work.

3. Theoretically, water addition could either increase or decrease volumetric efficiencies.
4. Theoretical results show that power output was higher increase at lean mixture with water injection. This is due to the volumetric efficiency increase that was dominant at this condition.



## CHAPTER 6

### SUGGESTIONS FOR FUTURE STUDIES

Some cases such as water injection into the cylinder, which could not be studied in the present work, and some main gaps observed in the literature are suggested as further works:

1. Water may be injected into the combustion chamber through separate nozzles in the cylinder head, or through the fuel injection valve. By using a dual nozzle system, the injection of water and fuel can be timed separately. For all these method can be applied to a spark ignition engine fuelled with LPG.
2. Injection of water into very highly compressed or supercharged engines has been successful as well as higher engine speeds. Therefore, the effect of water injection on highly compressed or supercharged engines fuelled with LPG should be investigated.
3. Water injection riches the water vapor in the exhaust gas. Exhaust gas fuel reforming should be investigated.
4. Positive effects of water injection are more than negative effects under some conditions. For example, amount of injected water was observed important under different loads and speeds. Different automatic control systems can be developed. Water injection can be applied successfully at different engine speed and load conditions by this way.
5. The change of effect of water addition should be investigated with combustion chamber geometry. The optimization of water injection with combustion chamber geometry should be investigated. At least, water injection literature shows the reduction of the  $\text{NO}_x$  emission is still possible.

6. Water may be added the LPG in the fuel tank. A type of water LPG emulsion can be achieved. The effect of this emulsion on engine performance and exhaust emissions should be investigated.
7. In many countries, a conventional mixer system is widely used in LPG fuel system. The liquid phase LPG injection is regarded as next generations LPG fuel supply system. This is known as LPLI fuel system. For example, MPI (multi point injection) LPG fuel system is one of application of this type injection system. The effect of water injection on the performance and the exhaust emissions of this type fuel system should be investigated. In addition, water can be injected to engine with using water LPG emulsion as stated above without additional injector. The effect of water fuel emulsion should be also investigated.
8. A method that how water can be injected into cylinder without any significant change should be investigated. At the start of this thesis, it is investigated. But it is not achieved due to technical impossibility. A method was considered that water might be injected into the engine passing through intake valves.
9. It should be investigated that the effects of swirling flow during induction process for the water-injected engine. This may increase the speed of evaporation of water and to enhance the homogeneity of air-fuel-water mixture.
10. Effect of water injection in the form of pulses to the intake air should be investigated together in internal combustion engines.

## REFERENCES

Abu-Zaid M. (2003). Performance of Single Cylinder, Direct Injection Diesel Engine Using Water Fuel Emulsions, *Energy Conversion And Management*, 45, 697-705.

Ajav E.A., Singh B., and Bhattacharya T.K. (2001). Thermal balance of single cylinder diesel engine operating on alternative fuels, *Energy Conversion and Management*, 41, 1533-1541.

Alasfour, F. D. (1997). Butanol- A Single –Cylinder Engine Study; Availability Analysis, *Applied Thermal Engineering*, vol. 17, pp. 537-549.

Alkidas, A. C. (1988). The Application of Availability and Energy Balances to a Diesel Engine, Trans. of ASME, *Journal of Eng. for Gas Turbines and Power*, vol. 110, pp. 462-469.

Alkidas, A. C. (1989). The Use of Availability and Energy Balances in Diesel Engines, *Society of Automotive Engineers*, SAE paper no: 890822.

Ament, F. and Patterson, D.J., and Mueller, A. (1977). Heat Balance Provides Insight into Modern Engine Fuel Utilization, *Society of Automotive Engineers*, SAE paper no:770221.

Alyea, John W. (1969). The Development and Evaluation of an Electronic Indicated Horsepower Meter, *Society of Automotive Engineers*, Technical Paper No.690181, International Automotive Engineering Congress, Detroit, MI, January 13 – 17.

Bignardi , L. et. al. (1981). Products of Combustion of Water in Fuel Emulsion, *14th International Congress on Combustion Engine*, Paper D-98, Helsinki.

Bass E., Bailey B., and Jaeger S. (1993). LPG Conversion and HC Emissions Speciation of a Light-duty Vehicle, *Society of Automotive Engineers*, SAE Paper 932745.

Bayraktar H, Durgun O. (1998). The Effects of Using Gaseous Fuels on Engine Combustion and Performance. *The Sixth Combustion Symposium*. Istanbul, Turkey, p. 273–85 [in Turkish].

Bayraktar H. and Durgun O. (2005). Investigating the Effects of LPG on Spark Ignition Engine Combustion and Performance, *Energy Conversion and Management*, 46, 2317–2333

Bedford F., Rutland C., Dittrich P., Raab A. and Wirbeleit F. (2000) Effects of Direct Water Injection on DI Engine Combustion, *Society of Automotive Engineers*, SAE paper no: 2000-01-2938.

Beer T, Grant B, Williams D, Watson H. (2002). Fuel-cycle Greenhouse Gas Emissions from Alternative Fuels in Australian Heavy Vehicles. *Atmos Environ*;36:753–63.

Bozza, F., Nocera, R., Senetore, A., and Tuccillo, R. (1991). Second Law Analysis of Turbocharged Engine Operation, *Society of Automotive Engineers*, SAE paper no: 910418.

Brown, William L. (1973). The Caterpillar imep Meter and Engine Friction, *Society of Automotive Engineers*, Technical Paper No. 730150, International Automotive Engineering Congress, Detroit, MI, January 8 – 12.

Brusca S. and Lanzafame R. (2003). Water injection in IC-SI engines to control detonation and to reduce pollutant emissions, *Society of Automotive Engineers*, Document Number: 2003-01-1912.

Caton, J.A. (1999). Results From the Second-law of Thermodynamics For a Spark-Ignition Engine Using a Cycle Simulation, proceedings of the 1999 Fall Technical Conference, *the American Society of Mechanical Engineers*, Internal Combustion Engine Division, Ann Arbor, MI.

Caton, J.A. (2000a). A Review of Investigations Using the Second Law of Thermodynamics to Study Internal-Combustion Engines, , *the Society of Automotive Engineers*, SAE paper no:2000-01-1081, pp. 9–22

Caton, J.A. (2000b). Operation Characteristics of a Spark-Ignition Engine Using the Second Law of Thermodynamic: Effect of Speed and Load, *the Society of Automotive Engineers*, 2000 SAE International Congress Exposition, Cobo Center, Detroit, MI, 6-9 March 2000.

Caton, J.A. (2002). A Cycle Simulation Including the Second Law of Thermodynamics for a Spark-Ignition Engine: Implications of the Use of Multiple-Zones for Combustion, the Society of Automotive Engineers, *Society of Automotive Engineers*, Technical Paper No. 2002–01–0007.

Caton, J. A. (2001). A Thermodynamic Cycle Simulation for Spark-Ignition Engines Including the Second Law of Thermodynamics Using Multiple Zones for Combustion, *Report No. ERL–2001–01*, Version 1.0, Engine Research Laboratory, Department of Mechanical Engineering, Texas A&M University.

Chambers, W.J., (1998). Engine Instrumentation and Data Analysis for Ignition System Testing, MS Thesis, West Virginia University.

Colwell A.T., Cummings R.E. and Anderson D.E. (1945). Alcohol-Water Injection, *SAE Journal (Transactions)*, Vol.53, No.6.

Cummins, Lyle C. (1989). *Internal Fire*, Warrendale, PA, Society of Automotive Engineers, Inc.

Dodge, I.G., Leone, D.M., Neageli, D. W., Dickey, D.W. and Swenson, K.R. (1996). A PC-Based Model For Predicting NOx Reductions in Diesel Engines, *Society of Automotive Engineers*, SAE Technical Paper 962060.

Doebelin, Ernest O. (1990). *Measurement Systems Application and Design*, New York, NY, McGraw-Hill Publishing Company, 1990.

Eaton D.C. (1946). Cruising Economy by Use of Water Injection, Wright Aero, Ltd. *SAE Journal (Transactions)*, Vol.54, No.2, February.

Edward F. (1948). Detonation and Internal Coolants (Water Injection), *SAE TRAN.*, Document Number: 480173, VOL. 56, No.1, pp.52-58.

Gallo, W. L. R., and Millanez, L. F. (1992). Exergetic Analysis of Ethanol and Gasoline Fueled Engines, *Society of Automotive Engineers*, SAE paper no: 920809.

Gross S. (1991). *Low Emissions for Ship's Machinery*, the motor Ship, special supplement 16-9.

Harrington, J. A. (1982). Water Addition to Gasoline - Effect on Combustion, Emissions, Performance, and Knock, *Society of Automotive Engineers*, SAE paper no: 820314.

Heywood, John B. (1988). *Internal Combustion Engine Fundamentals*, New York, NY, McGraw-Hill Book Company.

Holman, J.P. (1989). *Experimental method for engineers*, 5th ed. McGraw-Hill, Inc; p.41.

Ishida, M. and Chen, Z. (1994). An Analysis of the Added Water Effects on NO Formation in D.I. Diesel Engines, SAE Technical Paper 941691, (1994).

Ishida, M., Ueki, H., and Sakaguchi, D. (1997) Prediction of NO<sub>x</sub> Reduction Rate due to Port Water Injection in a DI Diesel Engine, *Society of Automotive Engineers*, SAE paper no: 972961.

Jost, K. (1995). Future Saab Engine Technology, *SAE International*, vol.103, no.12.

Kegl, B. and Pehan, S. (2001). Reduction of Diesel Engine Emissions by Water Injection, *Society of Automotive Engineers*, SAE paper no. 2001-01-3259.

Kettleborough, C.F. and Milkins, E.E. (1955). Water Injection into Internal Combustion Engines, *The engineers Digest*, Vol. 16, No. 7, pp 319-321.

Kohketsu, S., Mori, K., Sakai, K., and Nakagawa, H. (1996). Reduction of Exhaust Emission with New Water Injection System in a Diesel Engine, *Society of Automotive Engineers*, SAE paper no. 960033.

Kuhring, M.S. (1938). Water and Water-alcohol Injection in a Supercharged Jaguar Aircraft Engine, *Canadian Journal of Research*, Vol 16, pp 67-76.

Kumar, S. V., Minkowycz, W. J., and Patel, K. S., Thermodynamic Cycle Simulation of the Diesel Cycle; Exergy as a Second Law Analysis Parameter, *International Communications in Heat and Mass Transfer*, vol. 16, pp. 335-346, (1989).

Kummer, J.P. (1975). *Letter to technology Review*, pp. 4, 64-65.

Lancaster, D. R., Krieger, R. B. (1975). Lienesch, J. H., "Measurement and Analysis of Engine Pressure Data, *Society of Automotive Engineers*, SAE Paper 750026.

Lanzafame, R. (1999). Water Injection Effects In A Single-Cylinder CFR Engine, *Society of Automotive Engineers*, SAE paper no: 1999-01-0568.

Lestz, S.S. and Meyer, W.E. (1972). Emissions from a direct-cylinder water-injected spark-ignition engine, *SAE TRAN.*, VOL. 810. Document Number: 720113.

Lestz, S.J, Melton, R.B., and Rambie, E.J. (1975) Feasibility of Cooling Diesel Engines by Introducing Water Into the Combustion Chamber., *SAE Trans.*, Document Number: 7501289 . Pp. 606-619.

Lipkea, W. H., and Dejoode, A. D. (1989). A Comparison of the Performance of Two Direct Injection Diesel Engines from a Second Law Perspective, *Society of Automotive Engineers*, SAE paper no: 890824.

Measurement of Indicated Power (1970). New York, NY, *The American Society of Mechanical Engineers*.

Modak A. and Caretto L.S. (1972) Engine Cooling by Direct Injection of Cooling Water, *Society of Automotive Engineers*, SAE TRAN.,VOL.810, Document.Number:720113.

Murillo S., Miguez J.L., Porteiro J., Lopez Gonzalez L.M., Granada E. and Moran J.C., (2005). LPG: Pollutant Emission and Performance Enhancement for Spark-ignition Four Strokes Outboard Engines, *Applied Thermal Engineering*, (Article in Press).

Nicholls, J.E., El-Messiri, I.A. and Newhall, H.K. (1969). Inlet Manifold Water Injection for control of Nitrogen Oxides-Theory and Experiments, *Society of Automotive Engineers*, SAE TRAN., VOL.780, Document Number: 690018.



Obert E.F. (1948). Detonation and Internal Coolants, *SAE Quarterly Trans.*, pp. 52-59.

Ozcan, H. and Soylemez, S. (2004). Experimental Investigation of the Effect of Water Injection on the Performance of LPG Fuelled Engine, Report No. MF-01-06, University of Gaziantep.

Ozcan, H. and Soylemez, S. (2005a). Effect of water addition on the exergy balances of an LPG fuelled spark ignition engine, *Int. J. Exergy*, Vol. 2, No. 2, pp.194-206.

Ozcan, H. and Soylemez, S. (2005b). Experimental Investigation of Effects of Water Addition on the Exhaust Emissions of a Naturally Aspirated, LPG Fuelled Engine, *Energy and Fuels*, Vol.19, issue4, pp. 1468-1473.

Ozcan, H. and Soylemez, S. (2005c). Thermal Balance of a LPG Fuelled, Four Stroke SI Engine with Water Addition, *Energy Conversion And Management*, (Article in Press)

Park, J.W., Huh, K.Y., and Lee J.H. (2001) Reduction of NO<sub>x</sub>, Smoke and Brake Specific Fuel Consumption with Optimal Injection Timing and Emulsion Ratio of Water-Emulsified Diesel, *Proc Instn Mech Engrs*, Part D, Vol 215, pp. 83-93.

Peters B.D. and Stebar R.F. (1976). Water-Gasoline Fuels-Their Effect on Spark-Ignition Engine Emissions and Performance, *Society of Automotive Engineers*, SAE Technical Paper 760547.

Primus, R. J. (1984). A Second Law Approach to Exhaust System Optimization, *Society of Automotive Engineers*, SAE paper no: 840033.

Pulkrabek, W.W. (1997), *Internal Combustion Engine*, Prentice-Hall, Inc.

Randolph, Andrew L. (1990). Methods of Processing Cylinder-Pressure Transducer Signals to Maximize Data Accuracy, *Society of Automotive Engineers*, Technical Paper No. 900170, International Congress and Exposition, Detroit, MI, February 26 – March 2.

Rakopoulos, C. D. (1993). Evaluation of a Spark Ignition Engine Cycle Using First and Second Law Analysis Techniques, *Energy Conversion and Management*, vol. 34, pp. 1299-1314.

Rakopoulos, C. D., and Andritsakis, E. C. (1993). DI and IDI Combustion Irreversibility Analysis, in Thermodynamic and the Design, *Analysis and Improvement of Energy Systems*, ed. By H.J. Richter, Proceedings of ASME-WAM, AES, vol. 30, pp. 17-32, New Orleans, LA.

Rakopoulos, C. D., and Andritsakis, E. C., and Kyritsis, D. K. (1993). Availability Accumulation and Destruction in a Diesel Engine with Special Reference to the Limited Cooled Case, *Heat Recovery Systems&CHP*, vol. 13, pp. 261-376.

Rakopoulos, C. D and Giakoumis, E. G. (1997). Simulation and Exergy Analysis of Transient Diesel Engine Operation, *Energy*, vol. 22, pp. 875-885.

Raznjevic K. (1976). *Handbook of Thermodynamic Tables and Charts*.

Rowe M. R. and Ladd G.T. (1946). Water Injection for Aircraft Engines, *SAE Journal (Transactions)*, vol.54, No.1.

Satpov, E. B. and Luksho, B.A. (1982). A Study on the Effect of Water in Fuel on the Performance of SI Engine, *published in Engine Manufacturing in Russian*.

Selim M.Y.E. (2004). Sensitivity of Dual Fuel Engine Combustion and Knocking Limits to Gaseous Fuel Composition. *Energ Convers Manage*,45:411–25.

Shapiro, H. N., and van Gerpen, J. H. (1989). Two Zone Combustion Models for Second Law Analysis of Internal Combustion Engines, *Society of Automotive Engineers*, SAE paper no. 890823.

Stone, R. (1999). *Introduction to Internal Combustion Engines*, Macmillan Press Limited, Basingstoke, Hampshire.

Szargut, J., and Styryiska, T. (1964). Angenäherte Bestimmung der Exergie von Brennstoffen, *Aeitschrift für Energietechnik und Energiewirtschaft, Bennisstoff-Wörme-Kraft*, Bd. i6, pp. 589-596.

Taylor, C.F. (1960). *The Internal Combustion Engine in Theory and Practice*, New York: John Wiley and Sons, Inc., p. 440.

Taymaz, K. Cakir, Gur M. and Mimaroglu A. (2003) Experimental Investigation of Heat Losses in a Ceramic Coated Diesel Engine, *Surface and Coatings Technology*, 169 – 170, 168–170.

*The Clean Fuels Report* (1992), J.E Sinor Consultants Inc, Volume 4, No. 5

Thring R., H. (1983). Alternative Fuels for Spark Ignition Engines, *Society of Automotive Engineers*, SAE paper no:831685.

Traupel, W., Reciprocating Engine and Turbine in Internal Combustion, *Proceedings of the International Congress of Combustion Engines (CIMAC)*, Zurich, Switzerland, (1957).

Tsao K.C. and Wang C.L. (1984). Performance of Gasoline-Water Fuel in a Modified SI Engine, *Society of Automotive Engineers*, SAE Document Number: 841399 (SP-587).

Tsukahara, M., and Yoshimoto, Y. (1992). Reduction of NOX, Smoke, BSFC and Maximum Combustion Pressure by Low Compression Ratios in Diesel Engine Fuelled by Emulsified Fuel, *Society of Automotive Engineers*, SAE paper no. 920464.

Thsukahara, M., Murayama, T. and Yoshimoto, Y. (1982). Influence of Fuel Properties on the Combustion in Diesel Engine Driven by the Emulsified Fuel. *J. Jap. Soc. Mech. Engrs.*. 25(202), 612-619.

Quader A.A. (1971). Why Intake Charge Dilution Decreases Nitric Oxide Emission from Spark Ignition Engines, *Society of Automotive Engineers*, SAE Document Number:710009, Vol. 80, pp.20-30.

Ulrich, O. and Wallace, I. S. (1987). Liquid Propone Injection for Diesel Engines, *Society of Automotive Engineers*, SAE paper no: 872095.

Van Gerpen, J. H., and Shapiro, H. N. (1990). Second-Law Analysis of Diesel Engine Combustion, *Journal of Engineering for Gas Turbines and Power*, vol. 112, pp. 129–137.

Yüksel F. and Ceviz M. A. (2003). Thermal Balance of a Four-Stroke SI Engine Operating on Hydrogen as a Supplementary Fuel, *Energy*, 28, 1069-1080.

Wallace S.J. (1989). Assessment of “First Generation” Propane Conversion Equipment, *Society of Automotive Engineers* , SAE paper no. 892133.

Weiss K. and Rudd J.W. (1959) Engine Performance Improvement, *Auto Engineer*, Vol.49, No.11, pp. 424-432.

Weatherford, W.D., and Quilian R.D. (1970). Total Cooling of Piston Engines by Direct Water Injection, *Paper 700886 presented at SAE Combined National Fuels & Lubricants and Transportation Meetings*.

Wilson R.P., Muir E.B. and Pellicciotti F.A (1974). Emissions Study of a Single-Cylinder Diesel Engine, White Motors Corp. *Society of Automotive Engineers, SAE TRAN.*, Vol.830, Document Number:740123.

Yamin J.A.. and Badran O.O. (2002). Analytical Study to Minimize the Heat Losses from a Propane Powered 4-Stroke Spark Ignition Engine, *Renewable Energy*, 27, 463–478.

Zeilinger K. (1971). Influence of Water Injection on Nitric oxide Formation in Petrol Engines, Paper C122171, *Ins. of Mech. Eng. Con. on Air Pollution Control in Transport Engines*, pp.7-13.

## **APPENDICES**

## APPENDIX 1

### TECHNICAL SPECIFICATIONS OF THE TEST ENGINE

Data collection has been performed on a four cylinder, four strokes, normally aspirated and LPG fueled engine. Data for the engine that was used in the experiments are tabulated in table below.

<b>Parameter</b>	<b>Value</b>
<b>Engine type</b>	Four stroke, In-line
<b>Number of cylinder</b>	4
<b>Bore</b>	76 mm
<b>Stroke</b>	71.5 mm
<b>B/S ratio</b>	1.06
<b>Displacement</b>	1297 cm <sup>3</sup>
<b>Compression Ratio</b>	7.8
<b>Intake valve opening</b>	3 ° bTDC
<b>Intake valve closing</b>	45 ° aBDC
<b>Exhaust valve opening</b>	43 ° bBDC
<b>Exhaust valve closing</b>	5 ° aTDC
<b>Ignition order</b>	1-3-4-2
<b>Max. Power at rpm (DIN)</b>	66 HP@5200 rpm
<b>Max. torque at rpm (DIN)</b>	102 N-m@3000 rpm
<b>Coolant</b>	Water

## APPENDIX 2

### TECHNICAL SPECIFICATIONS OF THE PRESSURE TRANSDUCERS

Piezoelectric pressure transducer was used for the purpose of acquiring in-cylinder pressure data. This piezoelectric pressure transducer have the following technical specifications;

<b>Type</b>	Water cooled piezoelectric
<b>Application</b>	Cylinder Pressure
<b>Dynamic Measuring Range</b>	0-100 bar
<b>Sensitivity</b>	7.5 pC/bar
<b>Resolution</b>	0.004 bar
<b>Capacitance</b>	3.1 pF
<b>Natural Frequency</b>	160 kHz
<b>Damping</b>	0.9 log decrement
<b>Acceleration sensitivity</b>	0.0008 bar/g
<b>Linearity</b>	$< \pm 1\%$ FSO
<b>Max. Operating Temperature</b>	200 °C

The absolute pressure of the inlet manifold was used to absolute pressure correction of the piezoelectric pressure transducers. For this purpose, the pressure transducer was fitted to the inlet manifold. The specifications of the absolute pressure transducer are given in table below.



<b>Type</b>	Differential Pressure Transducer
<b>Application</b>	Intake Manifold Pressure
<b>Range</b>	0 to 15 psi
<b>Accuracy</b>	±0.13% full scale
<b>Output</b>	0.1 to 5.1 V
<b>Temp range (compensated)</b>	-4 to 176°F (-20 to 80°C)
<b>Process connection</b>	1/4" NPT(M)
<b>Electrical connections</b>	2-ft cable
<b>Media compatibility</b>	gases or liquids compatible
<b>Operating temperature</b>	-40° to 260°F (-40° to 125°C)
<b>Dimensions</b>	5"L x 2" dia
<b>Power</b>	12 to 28 VDC (unregulated)
<b>Housing</b>	NEMA 6 (IP68)

Another pressure transducer was mounted on the hydraulic load cell of the dynamometer. This pressure transducer has the following technical specifications;

<b>Range</b>	0 to 250 psig
<b>Application</b>	Torque Measurement
<b>Accuracy</b>	±0.25% full-scale
<b>Output</b>	0.5 to 5.5 V
<b>Temp range (compensated)</b>	-4° to 176°F (-20° to 80°C)
<b>Process connection</b>	1/4" NPT(M)
<b>Electrical connections</b>	2-ft cable
<b>Operating temperature</b>	-40° to 260°F (-40° to 125°C)
<b>Dimensions</b>	2 3/4"L x 1 1/2" dia
<b>Power</b>	9 to 30 VDC
<b>Wetted parts</b>	17-4 PH stainless steel

A pressure transducer was mounted on the air-flow meter. The specifications of this transducer are tabulated in table below.

<b>Type</b>	Differential Pressure Transducer
<b>Application</b>	Air-flow rate measurement
<b>Range</b>	0-5'' WC
<b>Accuracy</b>	0.5% FS
<b>Output</b>	4-20 mA; (1-6 V) with a resistance
<b>Excitation</b>	13-36 VDC
<b>Standard Response Time</b>	250 msec
<b>Stability - Max. Change (F.S./year)</b>	±0.5%
<b>Hysteresis</b>	±0.02%
<b>Non-repeatability</b>	±0.05%
<b>Non-linearity</b>	±0.4%

## APPENDIX 3

### TECHNICAL SPECIFICATIONS OF THE CHARGE AMPLIFIER

The Charge Amplifier takes the charge signals from the piezoelectric pressure transducer, converts them to voltages which can be logged on the computer. Therefore, a charge amplifier was used. The specifications of the charge amplifier are tabulated in table below.

<b>Output resistance</b>	10 $\Omega$	
<b>Operating temperature range</b>	0-60°C	
<b>Output voltage</b>	< $\pm 11$ V	
<b>Output current</b>	< $\pm 2$ mA	
<b>Range</b>	Sensitivity	Max. Input Q
<b>1</b>	100 mV/pC	100 pC
<b>2</b>	10 mV/pC	1000 pC
<b>3</b>	1 mV/pC	10000 pC
<b>Maximum charge drift</b>	< 0.2 pC/s	
<b>Continuous span adjustment</b>	Min.X1 to Max. X11 $\pm 1\%$	

## APPENDIX 4

### TECHNICAL SPECIFICATIONS OF THE SHAFT ENCODER

Crank angle encoder is a precision instrument in a modular system for use wherever rotational position must be measured to a high level of accuracy. Therefore, a crank angle encoder was used in all cases where the angle or volume information from the combustion chamber. The specifications of the shaft encoder are given in table below.

<b>Type</b>	Incremental
<b>Resolution</b>	1000 pulse/rev.
<b>Max Shaft Speed</b>	6000 rpm
<b>Freq Response</b>	1 MHz
<b>Rise Time</b>	Less than 1 microsecond
<b>Input Voltage</b>	4.75 to 28 VDC
<b>Operating Temp</b>	-10° C to 70° C
<b>Max Acceleration</b>	$1 \times 10^5$ rad/sec <sup>2</sup>
<b>Allowable Shaft Loads</b>	
<b>Radial</b>	2.5 Max. kg
<b>Axial</b>	1.5 Max. kg
<b>Starting Torque</b>	80 Max. g-cm
<b>Index</b>	Occurs once per revolution.
<b>Input Current</b>	100 mA max with no output load
<b>Input Ripple</b>	100 mV peak-to-peak at 0 to 100 kHz

## APPENDIX 5

### TECHNICAL SPECIFICATIONS OF THE USED READOUT AND RECORDING DEVICES

A data logger was used for reading and recording data from the transducers to computer. The specifications of the data logger are given in table below.

<b>Type</b>	Data logger
<b>Input channels</b>	43
<b>Resolution</b>	8 bits
<b>Analogue Inputs</b>	
<b>Temperatures</b>	15 differential DC millivolt input
<b>Single ended DC Voltage channels</b>	8 single ended input channel
<b>AC current Channels</b>	3 AC current channel
<b>Internal voltage measurement channel</b>	1
<b>Inputs Voltage</b>	Up to +50 V
<b>Digital Inputs</b>	
<b>Number of digital inputs</b>	8
<b>Types of digital inputs</b>	Frequency inputs (pulses), Logic inputs
<b>Digital Outputs</b>	
<b>Number of digital outputs channel</b>	8
<b>Switches type</b>	Sinking type
<b>Interface</b>	RS 232

In addition data logger has -5 V, + 5 V,-12 V and +12 V auxiliary power outputs to drive the transducers and solid state switches. All input, output and auxiliary power output connections are via 84 removable high quality screw terminals. Data Logger has menu driven software. This software allows transducers to be easily and quickly configured to return data in the engineering units selected by the operator and for these configurations to be simply stored using a standard Windows format.

High speed data acquisition system was used for the analysis in-cylinder events. This system is a very capable acquisition device which is supported by very comprehensive analysis and reporting facilities in DATS for windows. The specifications of this system are tabulated in table below.

<b>Type</b>	High speed data acquisition system
<b>Application</b>	In-cylinder measurements
<b>Analogue Inputs</b>	8 channels per unit
<b>Expansion</b>	Up to 64 channels using multiple units
<b>Sampling Rate</b>	Up to 100 kHz per channel
<b>Internal storage capacity</b>	From 256 bytes to 2 Mbytes/channel
<b>Programmability</b>	All features under software control
<b>Resolution</b>	16 bit
<b>Overall accuracy</b>	$\pm 0.10\%$ full scale at gain<1000
<b>Non-linearity</b>	Less than 1 LSB
<b>Sensitivity</b>	(gain=01) $\pm 300 \mu V$ (gain=1000) $\pm 0.3 \mu V$
<b>Input voltage range</b>	$\pm 10 V$
<b>Input impedance</b>	10 Mohm
<b>Analogue over voltage protection</b>	70 V p-p
<b>Communications</b>	High speed serial
<b>Connectors</b>	BNC, Lemo (full functions)
<b>Shock and Vibration</b>	Suitable for mobile use

Digital storage oscilloscope was used for the display of on-line in-cylinder measurements. The specifications of the DSO are tabulated in table below.

<b>Type</b>	Digital Storage Oscilloscope
<b>Application</b>	Display in-cylinder measurements
<b>Analog input channel</b>	4
<b>Resolution</b>	Voltage 0.4% of FSD, time 0.2% of FSD
<b>Trigger delay range</b>	20 ns to 5000 s
<b>Trigger delay accuracy</b>	$\pm 0.01\%$ , $\pm 1$ ns
<b>Rise time</b>	3.5 ns to 800 ps
<b>Interface</b>	GPIB, RS 423
<b>Analog BW</b>	20 MHz
<b>Max. sample rate</b>	100 Ms/s
<b>Sample Rate Accuracy</b>	$\pm 0.01\%$ (% of sample time)
<b>Operating Temp</b>	0° C to 50° C

Multi port RS 232 card with 8 port female adaptor was used for communications of the devices with computer.

<b>Type</b>	32 bit PSI bus Multiport serial card
<b>Application</b>	Serial port communications
<b>Operating temperature</b>	0 to 60 °C.
<b>Storage temperature</b>	-20 to 70 degree °C.
<b>Humidity</b>	5% to 95% in non-condensing.
<b>UART Type</b>	16550
<b>Base Addresses</b>	Any address selected by Plug and Play BIOS
<b>IRQs</b>	Any address selected by Plug and Play BIOS
<b>Status Register</b>	Bit mapped to indicate which port has data
<b>RS232 Signals</b>	TxD, RxD, RTS, CTS, DTR, DSR, RI, CD, GND
<b>Cables</b>	Expansion box with 8 DB25 female adapters
<b>Maximum Baud Rate</b>	460K baud
<b>OS Compatibility</b>	Windows XP, Windows 2000, Windows 98, MS-DOS, Windows 3.x, Windows 95, Windows NT, UNIX, Linux

## APPENDIX 6

### TECHNICAL SPECIFICATIONS OF THE DYNAMOMETER

Engine torque was measured with a dynamometer. Water brake dynamometer was used to measure engine torque at different speeds; by changing the water level in the dynamometer, the load applied to the engine could be varied. The specifications of the dynamometer are given in table below.

<b>Type of absorption</b>	Momentum exchange Water brake
<b>Loading Capacity</b>	100 HP
<b>Maximum allowable speed</b>	7400 rpm
<b>Opposing torque speed</b>	400 rpm
<b>Direction of rotation</b>	Right hand and left hand
<b>Torque transducer system</b>	Hydraulic
<b>Measuring device</b>	Pressure transducer
<b>Accuracy</b>	±0.25% full-scale
<b>Output</b>	0.5 to 5.5 V



## APPENDIX 7

### TECHNICAL SPECIFICATIONS OF THE AIRFLOW METER

Inlet airflow rate was determined by measuring the pressure drop across a calibrated venture nozzle attached to a large surge tank. The specifications of the air flow meter are tabulated in table below.

<b>Application</b>	Intake air flow rate	
<b>Range</b>	0 to 510 lbs/hr	
<b>Output</b>	1 to 6 V	
<b>Accuracy</b>	±0.13% full scale	
<b>Dumping drum capacity</b>	50 gallons	
<b>Air flow nozzle</b>		
<b>HP Range</b>	<b>Air-flow Range</b>	<b>Nozzle Size</b>
<b>0 to 6 HP</b>	0 to 40 lbs/hr	0.5'' diameter
<b>5 to 14 HP</b>	30 to 94 lbs/hr	0.75'' diameter
<b>12 to 35 HP</b>	80 to 230 lbs/hr	1.183'' diameter
<b>30 to 78 HP</b>	220 to 510 lbs/hr	1.75'' diameter

## APPENDIX 8

### TECHNICAL SPECIFICATIONS OF THE EXHAUST EMISSION TESTING APPARATUS

An exhaust gas analyzer was used for the analysis of exhaust gas. The specifications of the gas analyzer are shown in table below.

<b>Type</b>	Portable			
<b>Operating Temp.</b>	10 °C-40 °C			
<b>Condensation Trap</b>	Inline with integrated filter			
<b>Filter</b>	In-line - four micron – washable			
<b>Calibration</b>	Automatic 3-minute zero calibration, 30-second re-calibration.			
<b>Interface</b>	RS 232			
<b>Repeatability</b>	0.5% of full scale			
<b>Linearity</b>	1% of full scale			
<b>Parameter</b>	<b>Principle</b>	<b>Resolution</b>	<b>Accuracy</b>	<b>Range</b>
O <sub>2</sub>	Electrochemical sensor	0.01 Vol.%	± 3% of point	0-25 Vol.%
CO	Electrochemical sensor	0.01%	± 3% of point	0-15 Vol.%
NO <sub>x</sub>	Electrochemical sensor	1 ppm	± 3% of point	0-2000 ppm
HC	NDIR	1 ppm	± 3% of point	0-5000 ppm

## APPENDIX 9

### TECHNICAL SPECIFICATIONS OF THE USED ELECTRONIC BALANCE FOR FLOW MEASUREMENTS

For fuel and water flow rates, electronic balances were used with home made software. Fuel and water flow rate was calculated from the time elapsed to consume amount of fuel and water. The technical specifications of these balances are presented in table below.

<b>Application</b>	Water flow rate	Fuel flow rate
<b>Type</b>	High precision lab. Balance	High precision lab. balance
<b>Capacity</b>	3000 gr	20000 gr
<b>Resolution</b>	0.1 gr	0.1 gr
<b>Repeatability</b>	$\leq 0.1$ gr	$\leq 0.1$ gr
<b>Linearity</b>	$\leq 0.1$ gr	$\leq 0.2$ gr
<b>Response time</b>	$\leq 1$ s	$\leq 1$ s
<b>Display</b>	Liquid crystal display	Liquid crystal display
<b>Output</b>	RS 232 interface for data output	RS 232 interface for data output
<b>Power source</b>	AC 220 v, 50/60 Hz	AC 220 v, 50/60 Hz

## APPENDIX 10

### TECHNICAL SPECIFICATIONS OF THE OTHER SENSORS USED IN THE THESIS

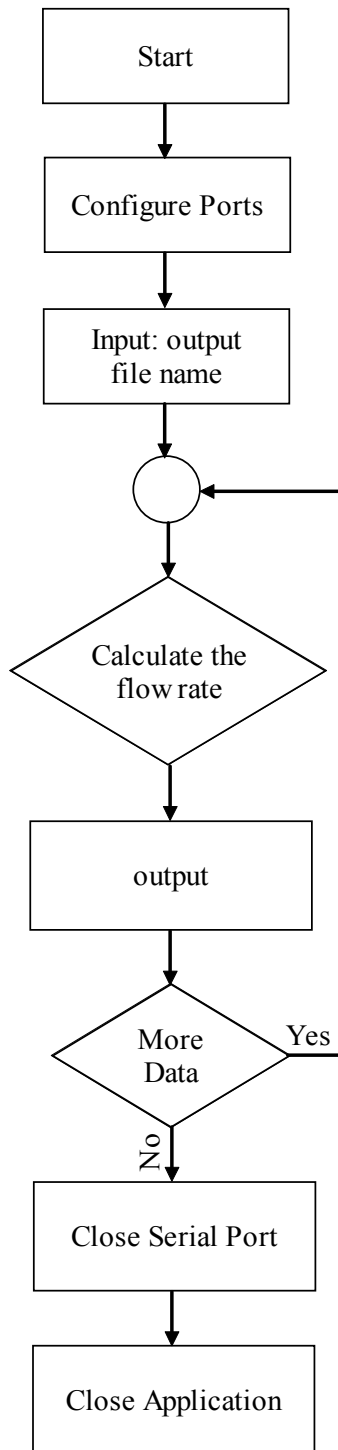
The technical specifications of the sensor used in thesis study are illustrated in table below.

<b>Sensor</b>	<b>Thermocouples</b>	
<b>Type</b>	<b>T</b>	<b>K</b>
<b>Names of Materials</b>	Copper (+), Constantan (-)	Chromel (+), Alumel (-)
<b>Measuring range</b>	-200 to 350 °C	95-1260 °C
<b>Accuracy</b>	0.75% of point	0.75% of point
<b>Resolution</b>	0.1 °C	1 °C
<b>Sensor</b>	<b>Speed</b>	
<b>Type</b>	Inductive pick-up Clamp	
<b>Range</b>	0 to 9999 rpm	
<b>Resolution</b>	1 rpm	
<b>Accuracy</b>	± 0.5%	
<b>Interface</b>	RS 232	
<b>Sensor</b>	<b>Ignition timing</b>	
<b>Type</b>	Capacitive coupling	
<b>Resolution</b>	0.36 °	
<b>Output</b>	+5 V	

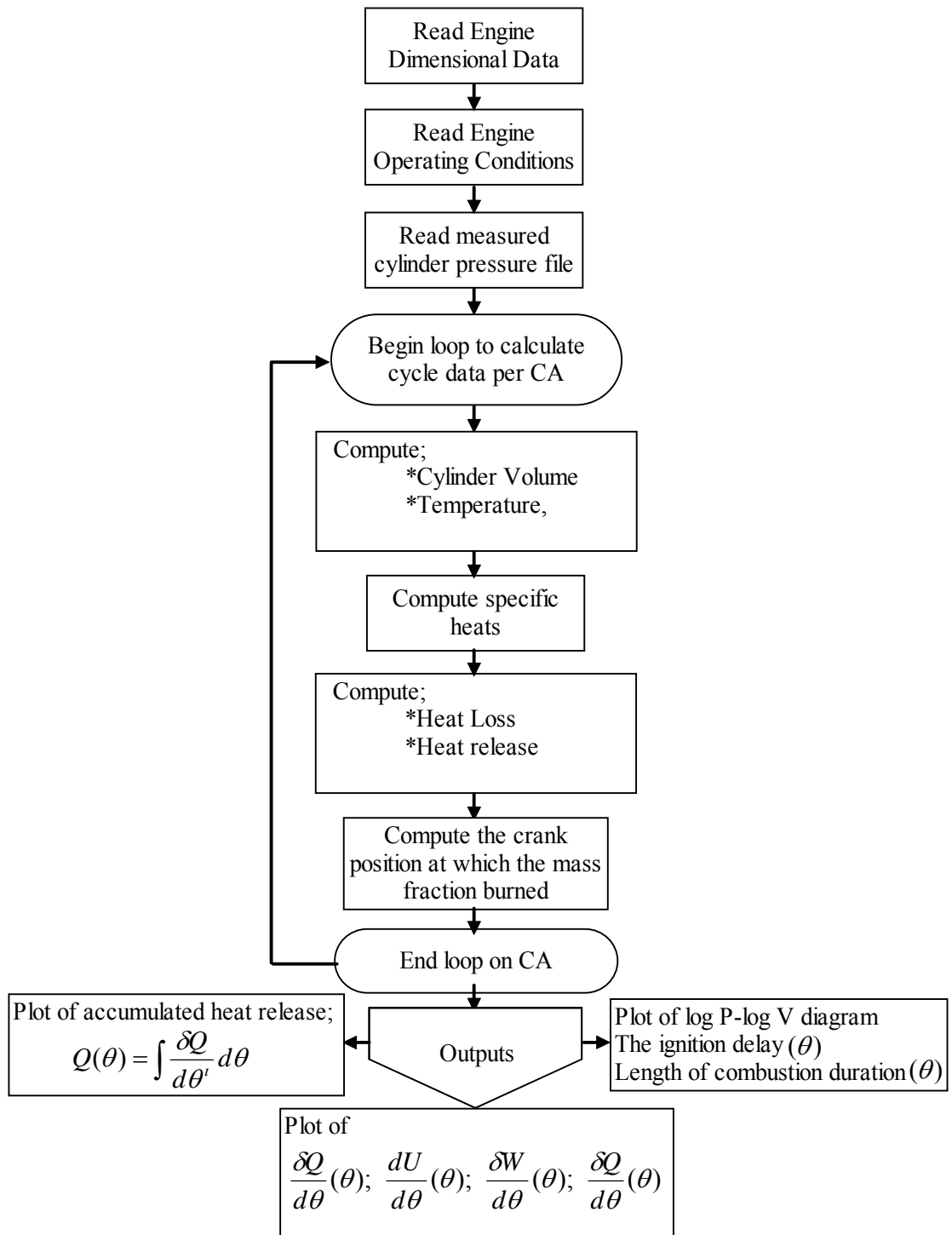
## **APPENDIX 11**

### **PROGRAMS USED IN THESIS**

Different recording and analysis softwares were used in the thesis. Detailed information about computer codes used in this thesis is given in this part. Homemade software was used to receive the data from RS 232 port. This program handled four programs at one time. The flow chart of RS-232 reader program is given in the figure below.

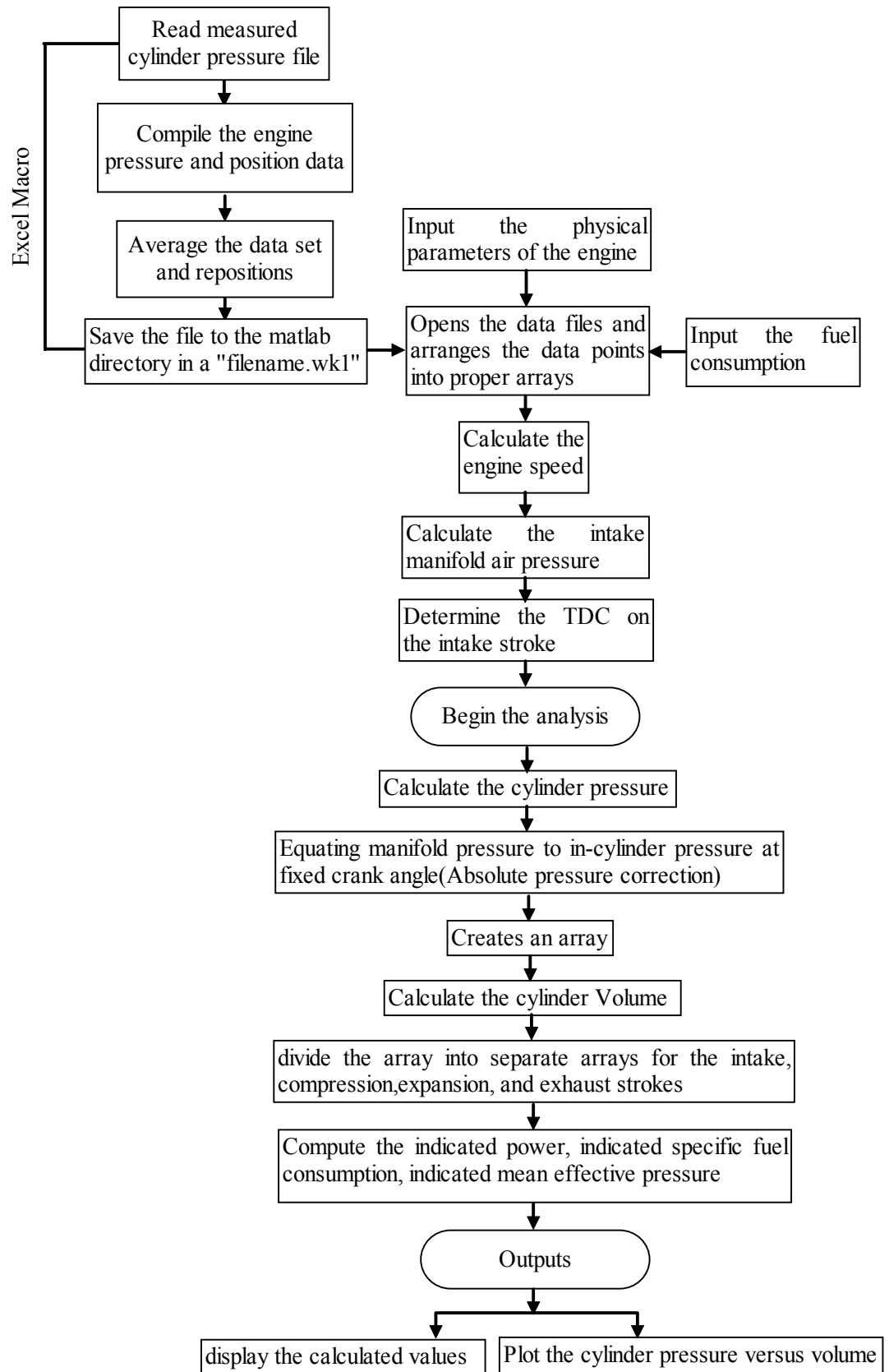


Second homemade program was software for data analysis. This software was used for analyzing the mass fraction burned during combustion. Flow chart of this program is given in the following figure.



Third software was prepared for data analysis. After data has been secured from the engine transducers by data acquisition's software, it was transferred to an excel spreadsheet. These files consist of four columns. These columns are the crank angle, just trash value, cylinder pressure and intake pressure. The flow chart of homemade data analysis software is given in figure below.



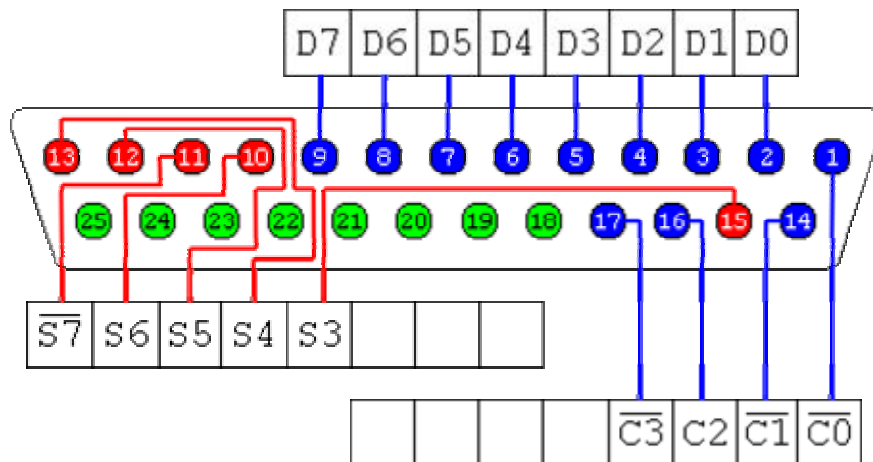


Last program was a Stepping Motor Control Software. Stepper motors provided open-loop, relative motion control. Features that stepper motors provide included:

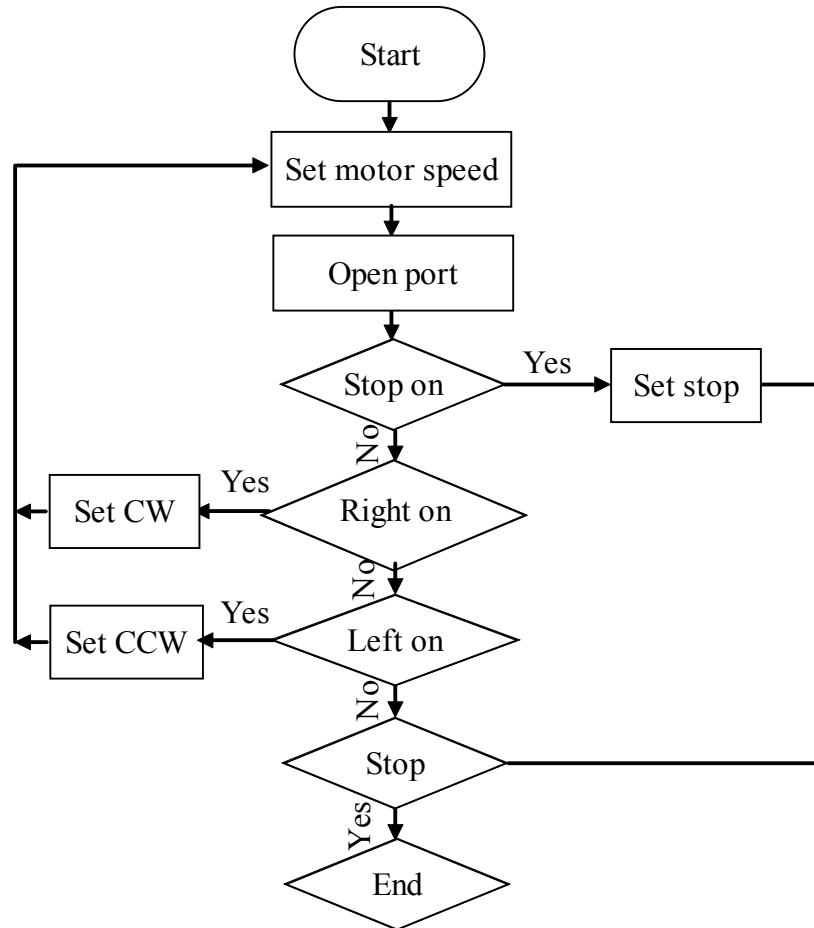
- Excellent rotational accuracy
- Large torque
- Small size
- Well operation over a range of speeds
- Usability for motion or position control

Therefore, stepper motors were mounted on mechanisms given in parts 3.2.13 and 3.2.14. Basic circuits allowed connecting step motors to a personal computer through the parallel port. The original IBM-PC's Parallel Printer Port had a total of 12 digital outputs and 5 digital inputs accessed via 3 consecutive 8-bit ports in the processor's I/O space. The digital interface allows connecting up to six motors to a single PC parallel port.

- 8 output pins accessed via the DATA Port (labeled D0 to D7)
- 5 input pins (one inverted) accessed via the STATUS Port (red pins)
- 4 output pins (three inverted) accessed via the CONTROL Port (labeled C0-C3)
- The remaining 8 pins are grounded (green pins)



This home-made software was used for the controlling the stepper motors. Program could move the stepper motor to any desired position reliably by sending them the proper number of step pulses. The flow chart of the program is given in figure below.



## **PUBLICATIONS**

### **Publication 1**

“Effect of water addition on the exergy balances of an LPG fuelled spark ignition engine” by (Hakan Özcan and Sait Söylemez, 2005a) was published at the International journal of Exergy. We investigated the effect of water addition on the exergy balance of a conventional engine in this paper. The present work is an analytical study depending on experimental measurements.

### **Publication 2**

"Experimental Investigation of Effects of Water Addition on the Exhaust Emissions of a Naturally Aspirated, LPG Fuelled Engine" by (Hakan Özcan and Sait Söylemez, 2005b) was published at the Energy and Fuels. The purpose of this study is to evaluate the effect of water addition on combustion in a conventional SI engine.

### **Publication 3**

"Thermal balance of a LPG fuelled, four stroke SI engine with water addition" by (Hakan Özcan and Sait Söylemez, 2005c) was published at the Energy Conversion and Management. The effect of water injection on spark ignition engine thermal balance and performance has been experimentally investigated in this paper. Different water to fuel ratios by mass were used with variable engine speed ranging from 1000 to 4500 rpm.

#### **Publication 4**

The project report " Experimental investigation of the effect of water injection on the performance of LPG fuelled engine" by (Hakan Ozcan and Sait Söylemez, 2004) investigated the effect of water injection on LPG fueled S.I engine performance, fuel economy, combustion characteristics, and exhaust gas emissions are investigated and compared with no water injection cases experimentally. This report is in Turkish and its code is MF 01.05 in research fund of University of Gaziantep.

## **CURRICULUM VITAE**

The author was born in Zonguldak, in 1973. He has finished the high-school in Kayseri in 1990 and entered the Mechanical Engineering Department of University of Gaziantep in 1992. He got his BS and MS degrees in Mechanical Engineering Department of the University of Gaziantep in 1997 and in 1999. His major interests are alternative sources of energy, advanced methods of thermodynamic analysis and internal combustion engines.

He has been married and has a daughter named as Ecenaz.